Hiding inside the host: Development and application of *Neospora caninum* bradyzoite in vitro culture

Inauguraldissertation

zur

Erlangung der Würde eines Doktors der Philosophie
vorgelegt der
Philosophisch-Naturwissenschaftlichen Fakultät
der Universität Basel

von

Nathalie Vonlaufen

aus
Luzern

Basel, 2003

Genehmigt von der Philosophisch-Naturwissenschaftlichen Fakultät auf Antrag von

Prof. Dr. Stephan Krähenbühl
Prof. Dr. Andrew Hemphill
Prof. Dr. Jürgen Drewe

Basel, den 19. November 2003

Prof. Dr. Marcel Tanner
Dekan

To my parents

Table of contents

Summary

The bradyzoite stage of the apicomplexan parasite *Neospora caninum* represents a hypobiotic, slowly proliferating and tissue cyst forming stage, which can survive in the immunocompetent host for several years. Tissue cysts are orally infectious. In addition, as immunocompetence gets impaired such as in the pregnant cow, bradyzoites transform into the rapidly proliferating and more virulent tachyzoites, which break out of the tissue cysts, cross the placenta and infect the unborn foetus, causing abortion, stillbirth or the birth of weak calves. Thus, the bradyzoite stage is epidemiologically important, since it plays a crucial role in both oral and transplacental transmission.

During the thesis work, an in vitro cultivation model for the generation of bradyzoites containing tissue cysts was developed that allowed to study this parasite stage more closely.

In preliminary studies, different cell lines like Vero cells, fibroblasts and neuroblastoma cells were infected with several *Neospora caninum* isolates and stage conversion was induced using pH-stress, the macrolide antibiotic tylosin and heat stress. However, the number of parasites expressing the bradyzoite-specific antigen BAG1 remained very low. Besides, the host cells tended not to tolerate such culture conditions that rendered a cultivation period over several days impossible.

As an alternative approach to induce stage conversion, organotypic brain slice cultures of rat cortical tissue were used for infection. This cultures provide a three-dimensional array of central nervous tissue with the original complex mixture of neuronal cells. The rationale behind this approach was that cofactors that could contribute to stage conversion were more likely to be provided in such a system than within a single cell. Organotypic brain slice cultures were infected with $2x10^6$ and $2x10^7$ tachyzoites. To some cultures, 100 units of recombinant mouse IFN-γ were added. IFN-γ, a key cytokine in the host immune response to *Neospora caninum* infection has shown to trigger stage conversion in *Toxoplasma gondii* infected macrophages and microglia. However, in none of the

Neospora caninum infected cultures, IFN-γ-treated or untreated cultures, parasites that expressed the bradyzoite marker BAG1 could be detected, neither a cyst wall was found by transmission electron microscopy.

In order to monitor the kinetics of parasite proliferation in this system, a quantitative real-time PCR was developed using a dual fluorescent hybridization probe system and the LightCycler™ instrument for online detection of amplified DNA. Treatment of the infected cultures with IFN-γ resulted in an inhibition of parasite proliferation compared to the untreated cultures. Moreover, smaller pseudocysts were found after IFN-γ-treatment. In addition, neuronal cytoskeletal elements, namely glial acid protein filaments as well as actin microfilament bundles largely colocalised with the pseudocyst periphery.

Although the use of organotypic brain slice cultures did not succeed in stage conversion of *Neospora caninum*, a model was established that can be used to gain more information on the cerebral phase of Neosporosis.

Since inhibitors of the mitochondrial respiratory chain were found to promote stage conversion in *Toxoplasma gondii*, sodium nitroprusside, an exogenous donor of nitric oxide that inhibits the respiratory chain at cytochrome oxidase was tested for stage conversion in *Neospora caninum*. Additionally, long term cultures of murine epidermal keratinocytes were used as host cells, because of their very strong cell-substrate adhesion. Sodium nitroprusside was daily added at a concentration of 70 µM to infected Vero cells, fibroblasts, neuroblastoma cells and keratinocytes for up to 8 days. Keratinocytes were the only host cells to withstand this treatment for a period of at least eight days. In these cultures, sodium nitroprusside strongly inhibited *Neospora caninum* proliferation as assessed by quantitative real-time PCR and induced the expression of BAG1 antigen from day 3 onwards. This data suggests that the inhibition of parasite proliferation is closely linked to the expression of bradyzoite-specific markers. At day 8, around 60% of the parasitophorous vacuoles contained BAG1-positive parasites. Another marker, which was used, was mAbCC2 that is directed against a *Toxoplasma gondii* cyst wall protein. After 8 days, around 60% of all parasitophorous vacuoles exhibited a peripheral labelling with this antibody that indicated the formation of a cyst wall. Inspection by transmission electron

microscopy suggested that the majority of the intracellular compartments occupied by *Neospora* parasites exhibited features that were indicative for tachyzoite-to-bradyzoite stage conversion. Vacuoles contained 1-5 intracellular parasites, featuring electron dense rhoptries, many micronemes that were predominantly located at the anterior end, and large and small dense granules. In addition, amylopectin granules, that are characteristic for the bradyzoite stage, were found. The majority of the parasitophorous vacuoles contained an accumulation of electron dense granular material at the periphery that indicated the formation of a cyst wall, which varied considerably in thickness between 0.1-1 µM.

Although this developed in vitro culture system was efficient in terms of NcBAG1-expression, it was less suitable in order to obtain larger amounts of *Neospora caninum* bradyzoites that are required for biochemical and molecular studies. The separation of bradyzoites from keratinocytes was difficult, due to the fact, that the tissue cysts were surrounded by keratin filament bundles, that hindered the liberation of the parasites. The culture conditions were therefore adapted to Vero cells by decreasing the concentration of sodium nitroprusside to a minimum level of 17 µM, which was tolerated by the less adhesive cell type. The efficiency of tachyzoite-to-bradyzoite conversion was similar to that obtained with 70 µM sodium nitroprusside in keratinocytes as host cells, but resulted in a higher number of NcBAG1-positive individual zoites, due to the increased size of NcBAG1-positive vacuoles. Additionally, the modified system made it now possible to purify bradyzoites out of the host cells. Furthermore, sodium nitroprusside-treatment of infected Vero cells lead to a down regulation of the major tachyzoite surface antigens NcSAG1 and NcSRS2, as assessed by immunofluorescence and immunoblotting. The expression and localisation of dense granule proteins in bradyzoites was also analysed by immunogold transmission electron microscopy and immunofluorescence and showed that the localisation of these proteins shifted towards the periphery of the cysts, compared to tachyzoites where dense granule proteins were found at the anterior and posterior end of the parasites. These results implied an involvement of dense granule proteins in the formation and modification of the cyst wall. In

addition, using purified tachyzoites and bradyzoites, the adhesion and the invasion of these two stages to Vero cells was comparatively assessed and demonstrated that tachyzoites were more invasive than bradyzoites. However, removal of sialic acid by sialidase from the Vero cell surface and parasite surface enhanced the bradyzoite invasion rate from 25% to 46% and 15% to 36% respectively, whereas these treatments had no effect on the tachyzoite invasion rate. Thus, sialic acid plays an important role in the invasion of host cells by bradyzoites.

Zusammenfassung

Das Bradyzoitenstadium des apicomplexen Parasiten *Neospora caninum* ist ein hypobiotisches, langsam proliferierendes und Gewebezysten bildendes Stadium, das im immunkompetenten Wirt mehrere Jahre überleben kann. Die Gewebezysten sind oral infektiös. Während der Trächtigkeit einer Kuh kann es zur Beeinträchtigung der Immunkompetenz kommen, was eine Umwandlung von Bradyzoiten in schnell proliferierende, virulentere Tachyzoiten zur Folge hat. Diese brechen aus der Gewebezyste aus und werden über die Plazenta auf den Foeten übertragen, was zu Abort, Todgeburt oder zur Geburt schwacher Kälber führen kann. Das Bradyzoitenstadium ist epidemiologisch von Bedeutung, da es eine entscheidende Rolle in der oralen und transplazentaren Übertragung spielt.

Während der Doktorarbeit wurde ein *in vitro* Kultivierungsmodell zur Erzeugung von Bradyzoiten entwickelt, das ermöglichte, dieses Parasitenstadium genauer zu studieren.
In Vorversuchen wurden verschiedene Zellinien wie Verozellen, Fibroblasten und Neuroblastomazellen mit unterschiedlichen *Neospora caninum* Isolaten infiziert und die Stadienkonversion wurde unter Anwendung von pH-Stress, dem Makrolid-Antibiotikum Tylosin und Hitzestress induziert. Die Anzahl der Parasiten, die das Bradyzoiten-spezifische Antigen BAG1 exprimierten, blieb jedoch sehr gering. Ausserdem neigten die Wirtszellen dazu, diese Kulturbedingungen nicht zu tolerieren, was eine Kultivierungszeit über mehrere Tage verunmöglichte.
Als eine alternative Methode zur Induktion der Stadienkonversion wurden organotypische Hirnschnittkulturen, die aus dem kortikalen Gewebe von Ratten stammten, zur Infektion verwendet. Diese Kulturen zeichnen sich durch eine dreidimensionale Anordnung des zentralnervösen Gewebes aus, welches das ursprüngliche komplexe Gemisch neuronaler Zellen enthält. Die Idee hinter dieser Methode war, dass Kofaktoren, die zu einer Stadienkonversion beitragen könnten, eher in einem solchem System enthalten sind, als in einer einzelnen

Zelle. Organotypische Hirnschnittkulturen wurden mit $2x10^6$ und $2x10^7$ Tachyzoiten infiziert. Zu einigen Kulturen wurden 100 Einheiten rekombinantes Maus-Interferon-γ hinzugefügt. Interferon-γ ist ein Schlüsselcytokin in der Immunantwort des Wirtes auf *Neospora caninum* Infektionen. Zusätzlich haben Studien gezeigt, dass Interferon-γ eine Stadienkonversion in Makrophagen und Mikroglia, die mit *Toxoplasma gondii* infiziert waren, induzieren konnte. In keiner der mit *Neospora caninum* infizierten Kulturen, die mit Interferon-γ behandelt wurden oder unbehandelt blieben, konnten Parasiten nachgewiesen werden, die den Bradyzoitenmarker BAG1 exprimierten, noch wurde eine Zystenwand unter Anwendung der Transmissionselektronenmikroskopie gefunden.

Um die Kinetik der Parasitenproliferation in diesem System zu ermitteln, wurde eine quantitative „real-time“ PCR entwickelt. Dabei wurde ein zweifach fluoreszierendes Hybridisierungsprobensystem und der LightCycler™ für die Detektion amplifizierter DNA eingesetzt. Verglichen mit unbehandelten Kulturen führte die Behandlung infizierter Kulturen mit Interferon-γ zu einer Hemmung der Parasitenproliferation. Ausserdem wurden generell kleinere Pseudozysten nach Behandlung mit Interferon-γ gefunden. Zusätzlich konnte gezeigt werden, dass Bestandteile des neuronalen Zytoskelettes, wie Filamente des sauren Gliaproteins und Aktinfilamentbündel mit der Peripherie der Pseudozysten kolokalisierten.

Obwohl die Anwendung von organotypischen Hirnschnittkulturen bezüglich der Stadienkonversion von *Neospora caninum* nicht erfolgreich war, wurde ein Modell etabliert, das verwendet werden kann, um mehr Informationen über die zerebrale Phase der Neosporose zu gewinnen.

Da mit Inhibitoren der mitochondrialen Atmungskette gemäss früheren Studien eine Stadienkonversion in *Toxoplasma gondii* induziert werden konnte, wurde der Effekt von Natriumnitroprussid, einem exogenen Stickstoffmonoxiddonor, der die Cytochromoxidase der Atmungskette hemmt, auf die Stadienkonversion von *Neospora caninum* getestet. Zusätzlich wurden Langzeitkulturen von Mauskeratinozyten als Wirtszellen benutzt, die sich durch eine ausgeprägte Zell-Substratadhäsion auszeichnen. Zu infizierten Verozellen, Fibroblasten, Neuroblastomazellen und Keratinozyten wurden täglich 70 µM

Natriumnitroprussid während 8 Tagen zugegeben. Keratinozyten waren die einzigen Wirtszellen, die einer Natriumnitroprussidbehandlung während dieser Zeitspanne standhielten. In diesen Kulturen hemmte Natriumnitroprussid die *Neospora caninum* Proliferation beträchtlich, wie mit quantitativer „real-time“ PCR gezeigt werden konnte und induzierte die Expression des BAG1 Antigens vom dritten Tag an. Diese Ergebnisse weisen darauf hin, dass die Hemmung der Parasitenproliferation eng mit der Expression von Bradyzoiten-spezifischen Markern verbunden ist. Am achten Tag enthielten ungefähr 60% der parasitophoren Vakuolen BAG1-positive Parasiten. Ein weiterer Marker, der verwendet wurde, war der monoklonale CC2 Antikörper, der gegen ein *Toxoplasma gondii* Zystenwandprotein gerichtet ist. Nach 8 Tagen zeigten ungefähr 60% aller parasitophoren Vakuolen eine Anfärbung der Peripherie mit diesem Antikörper auf, was auf die Bildung einer Zystenwand hindeutete. Beobachtungen mit dem Transmissionselektronenmikroskop zeigten, dass die Mehrzahl der intrazellulären Kompartimente, die mit *Neospora caninum* Parasiten besetzt waren, Eigenschaften aufwiesen, die auf eine Konversion von Tachyzoiten zu Bradyzoiten zurückzuführen waren. Die Vakuolen enthielten 1-5 intrazelluläre Parasiten, die aus elektronendichten Rhoptrien, vielen Mikronemen, die vorwiegend am Vorderende des Parasiten zu finden waren und aus grossen und kleinen dichten Granula bestanden. Zusätzlich wurden Amylopektingranula, die kennzeichnend für das Bradyzoitenstadium sind, gefunden. In der Mehrheit der parasitophoren Vakuolen wurde eine Anhäufung von elektronendichtem granulärem Material an der Peripherie gefunden, was auf die Ausbildung einer Zystenwand hindeutete, deren Dicke beträchtlich zwischen 0.1-1 µm variierte.

Obwohl das entwickelte *in vitro* Kultursystem bezüglich der Expression des *Neospora caninum* BAG1 Antigens effizient war, erwies es sich als weniger geeignet, um grössere Mengen an gereinigten *Neospora caninum* Bradyzoiten zu erhalten, die für biochemische und molekulare Studien erforderlich sind. Die Trennung der Bradyzoiten von Keratinozyten erwies sich als schwierig, da die Gewebezysten von Keratinfilamentbündeln umgeben waren, die das Befreien

der Parasiten von der Wirtszelle behinderten. Indem man die Natriumnitroprussidkonzentration auf eine Minimalkonzentration von 17 µM herabsetzte, wurden die Kulturbedingungen Verozellen angepasst. Diese Konzentration wurde vom weniger adhäsiven Zelltypen toleriert. Die Effizienz der Konversion von Bradyzoiten zu Tachyzoiten war vergleichbar mit derjenigen, die mit 70 µM Natriumnitroprussid in Keratinozyten als Wirtszellen erhalten wurde. Die Behandlung führte jedoch zu einer grösseren Anzahl BAG1-positiver individueller Zoiten, was auf eine Grössenzunahme BAG1-positiver Vakuolen zurückzuführen war. Zusätzlich ermöglichte das modifizierte System nun die Reinigung der Bradyzoiten aus den Wirtszellen. Mittels Immunfluoreszenz und Immun-Blotting konnte gezeigt werden, dass die Behandlung von infizierten Verozellen mit Natriumnitroprussid zu einer stark reduzierten Expression der Tachyzoitenhauptoberflächenantigene SAG1 und SRS2 führte. Die Expression und Lokalisation von dichten Granulaproteinen in Bradyzoiten wurde mittels Immungold Transmissionselektronenmikroskopie und Immunfluoreszenz analysiert und zeigte eine Verlagerung dieser Proteine an die Peripherie der Vakuole, wohingegen in Tachyzoiten die dichten Granula am vorderen und hinteren Ende der Parasiten zu finden waren. Diese Erkenntnisse weisen auf eine Beteiligung der dichten Granula am Aufbau und an der Modifikation der Zystenwand hin. Im Weiteren wurde die Adhäsion an und Invasion von gereinigten Tachyzoiten und Bradyzoiten in Verozellen verglichen und es wurde gezeigt, dass Tachyzoiten invasiver waren als Bradyzoiten. Das Entfernen der Sialinsäure durch das Enzym Sialidase von der Verozelloberfläche, beziehungsweise von der Parasitenoberfläche steigerte die Bradyzoiteninvasionsrate von 25% auf 46%, respektive von 15% auf 36%. Diese Behandlung zeigte keinen Effekt auf die Tachyzoiteninvasionsrate. Dies weist auf eine bedeutende Rolle der Sialinsäure bei der Invasion von Bradyzoiten in die Wirtszelle hin.

Abbreviations

ATP	Adenosine-5’-triphosphate
BSA	Bovine serum albumine
cGMP	Cyclic guanosine 5’-monophosphate
CNS	Central nervous system
DBA	Dolichos biflorans agglutinin
EDTA	Ethylendiamine tetraacetic acid
EGF	Epidermal growth factor
EM	Electron microscopy
FCS	Foetal calf serum
FITC	Fluorescein-isothiocyanate
G6PD	Glucose-6-phosphate-dehydrogenase
GFAP	Glial fibrillary acid protein
HFF	Human foreskin fibroblast
HS	Horse serum
Hsp	Heat shock protein
HT_4	Human neuroblastoma cell line
IGTP	Inducibly expressed GTPase
IL	Interleukin
IFN-γ	Interferon-γ
iNOS	Inducible nitric oxide synthase
kDa	Kilo Dalton
mAbCC2	Monoclonal antibody CC2
N. caninum	Neospora caninum
NAD	Nicotinamide-adenine dinucleotide
NADH	Reduced nicotinamide-adenine dinucleotide
NADP	Nicotinamide-adenine dinucleotide phosphate
Nc	Neospora caninum
NcBAG1	Neospora caninum bradyzoite antigen 1
NcGRA	Neospora caninum dense granule protein

NcMIC	Neospora caninum microneme protein
NcSAG1	Neospora caninum surface antigen 1
NcSRS2	Neospora caninum SAG1-related sequence 2
NcSwB1	Neospora caninum swedish bovine1 isolate
NO	Nitric oxide
NOS	Nitric oxide synthase
PBS	Phosphate buffered saline
PCR	Polymerase chain reaction
PDTC	Pyrrolidine dithiocarbamate
SDS	Sodium dodecyl sulphate
SDS-PAGE	Sodium dodecyl sulphate polyacrylamide gel electrophoresis
SNP	Sodium nitroprusside
T. gondii	Toxoplasma gondii
TBS-T	Tris buffered saline with Tween-20
TCA	Tricarboxylic acid cycle
TE	Toxoplasmic encephalitis
TEM	Transmission electron microscopy
Tg	Toxoplasma gondii
TgBAG1	Toxoplasma gondii bradyzoite antigen 1
TgROP2	Toxoplasma gondii rhoptry protein 2
TgSAG1	Toxoplasma gondii surface antigen 1
TgSAG2	Toxoplasma gondii surface antigen 2
Th1	Helper T cell 1
Th2	Helper T cell 2
TNF-α	Tumor necrosis factor-α
Tris	Tris(hydroyxmethyl)-aminomethane
TRITC	Tetramethylrhodamine-isothiocyanate

1. Introduction

1.1 Neospora caninum and Neosporosis

Neospora caninum is an apicomplexan parasite, which is phylogenetically closely related to *Toxoplasma gondii*, but can clearly be distinguished from *Toxoplasma* with regard to its natural host range (Dubey *et al.,* 2002), antigenicity (Howe and Sibley*,* 1999), few ultrastructural features (Hemphill *et al*., 2003; Speer *et al.,* 1999) and differences in its host cell recognition (Naguleswaran *et al.,* 2002).
Infection with *Neospora caninum*, which was first identified in 1988 by Dubey and coworkers in a dog suffering from neurological problems, leads to a disease named Neosporosis. Although this disease affects primarily cattle and dogs, *N. caninum* infection has been shown to occur in a variety of species (Dubey and Lindsay, 1996; Hemphill, 1999). During the last years it became evident, that Neosporosis represents the most important cause of bovine abortions worldwide, and infection with *N. caninum* is therefore regarded as an economically important problem (Dubey, 1999; Trees *et al*., 1999). In Switzerland, approximately 30% of all abortions in cattle are associated with *N. caninum* infection (Sager *et al.,* 2001).

1.2 Life cycle of Neospora caninum

McAllister *et al*. (1998) were the first to show that the dog is a definitive host for *N. caninum*, and this was later confirmed (Lindsay *et al.,* 1999). However, other final hosts cannot be ruled out. Three stages are known in the life cycle of *N. caninum* (Figure 1). Oocysts represent the sexually produced stage, which are generated within canine intestinal tissue and subsequently shed in the environment with the faeces. There, sporulation of oocysts leads to the

production of sporozoites, and sporulated oocysts are orally infectious (McAllister *et al.,* 1998). The sporozoites transform into the rapidly dividing tachyzoites which are present during the acute phase of the infection. Tachyzoites invade any nucleated cell type, including macrophages and lymphocytes, are disseminated throughout the body, and continuous cycles of intracellular proliferation, host cell lysis and reinfection, combined with immunopathological events, can lead to tissue destruction and eventually disease.

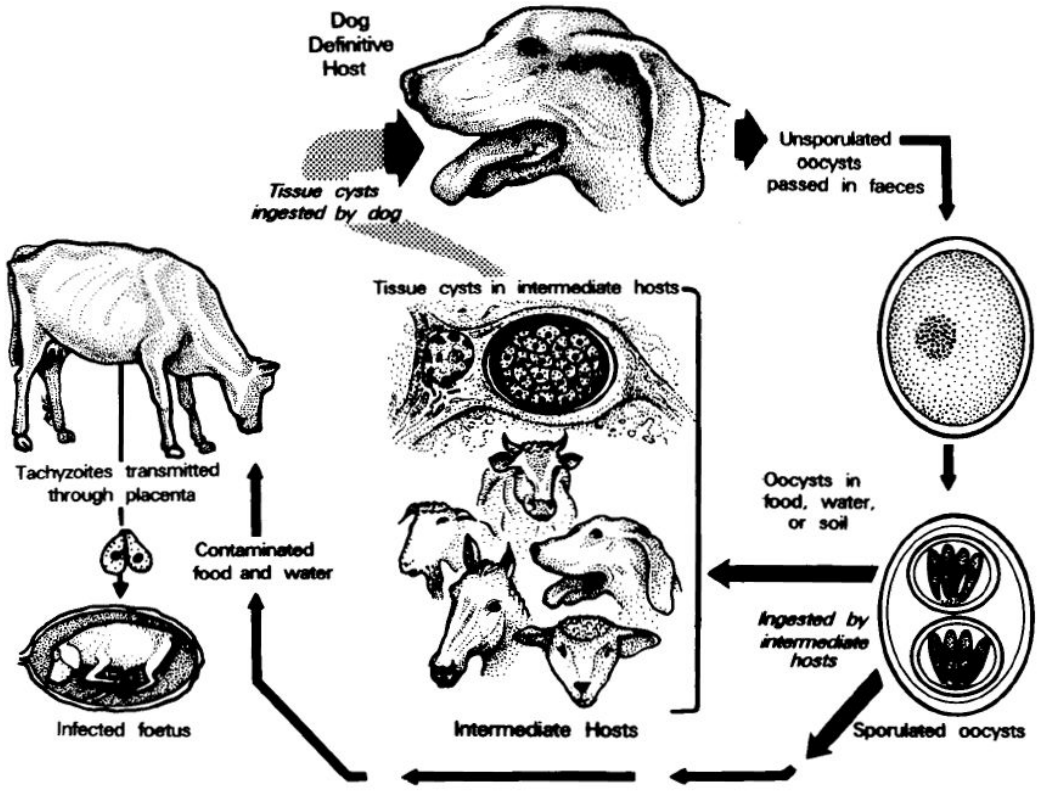

Figure 1: Life cycle of *Neospora caninum* (Dubey 1999).

However, during the normal course of infection, in the immunocompetent host, tachyzoites convert into slowly replicating and tissue cyst forming bradyzoites, and the immune system has been implicated in this development (Buxton *et al.,* 2002; Innes *et al.,* 2002). Tissue cysts containing *N. caninum* bradyzoites can persist in the infected host for several years without causing any clinical signs.

Reactivation of tissue cysts in an immunocompromised situation such as during pregnancy, may lead to bradyzoite-to-tachyzoite reconversion and subsequent infection of the placenta and / or the unborn foetus (Innes *et al.,* 2002; Quinn *et al.,* 2002). Bradyzoites containing tissue cysts are orally infectious. Thus, *N. caninum* tissue cysts are largely responsible for both, horizontal and vertical infection.

1.3 Differentiation of tachyzoites and bradyzoites

1.3.1 Stage specifically expressed antigens

Several antigens have been identified so far in *N. caninum* tachyzoites, using different approaches such as raising monoclonal antibodies or generating polyclonal antisera against the whole parasite, immunoscreening of cDNA expression libraries with sera from infected cattle or subcellular fractionation of parasites and preparation of affinity-purified antibodies. Most of the antigens were found to be localised either on the parasite surface or in secretory organelles, like micronemes, rhoptries and dense granules. Antigens detected so far include two surface antigens NcSAG1 and NcSRS2, the dense granule antigens NcGRA1, NcGRA2, NcGRA6, NcGRA7, a nucleoside-3-phosphate hydrolase, the microneme antigens NcMIC1-4 and NcMIC10 and finally the serine protease Ncp65.

In *N. caninum*, likewise in *T. gondii*, tachyzoites and bradyzoites can be differentiated through detection of stage specific antigen expression and differentially located antigens by immunofluorescence. It was shown by Kasper (1989) that the major *T. gondii* surface antigens TgSAG1 and TgSAG2 were stage specifically expressed in tachyzoites. Similarly, *N. caninum* SAG1 homologue NcSAG1 was observed to be down regulated during tachyzoite-to-bradyzoite stage conversion (Fuchs *et al.,* 1998; Vonlaufen *et al.,* 2002b).

Schares *et al.* (1999) showed by inspection of dog brain tissue harbouring *N. caninum* tissue cysts, that another major 38 kDa surface antigen, now known to be identical to NcSRS2, was also stage specifically expressed in *N. caninum* tachyzoites and not in bradyzoites. In contrast, Fuchs *et al.* (1998) had reported on the expression of NcSRS2 in *N. caninum* tissue cysts generated in mice. Several bradyzoite-specific *T. gondii* antigens have been identified (Bohne *et al.,* 1999; Smith, 1995; Weiss *et al.,* 1992). Among them, the stress response protein TgBAG1 (Bohne *et al.,* 1995), also known as TgBAG5 (Parmley *et al.,* 1995) was found in the cytoplasm of *T. gondii* bradyzoites, and polyclonal antibodies directed against recombinant TgBAG1 were shown to crossreact with bradyzoites of *N. caninum* (McAllister *et al.,* 1996; Tunev *et al.,* 2002; Vonlaufen *et al.,* 2002b; Weiss *et al.,* 1999). Further, the monoclonal antibody mAbCC2, generated against *T. gondii* tissue cysts, was shown to label a 115 kDa *T. gondii* cyst wall protein and a secreted 40 kDa dense granule protein in tachyzoites (Gross *et al.,* 1995). We recently demonstrated that this antibody also crossreacted with *N. caninum* tachyzoites and bradyzoites (Keller *et al.,* 2002; Vonlaufen *et al.,* 2002b). In addition to stage specifically expressed antigens, other *T. gondii* dense granule proteins, which are secreted shortly after invasion and involved in the modification of the parasitophorous vacuole, have been shown to be differentially located in *T. gondii* tachyzoite and bradyzoite cysts (Torpier *et al.,* 1993*).* NcGRA7, formerly designated as Nc-p33 (Hemphill *et al.,* 1998), was found to be localised in the tissue cyst wall (Fuchs *et al.,* 1998). Recently, a mucin domain containing protein was identified in *T. gondii*. The gene, expressing this protein, has been shown to be upregulated in bradyzoites compared to tachyzoites. This finding shows a possible role of mucin in the protection of bradyzoites from degradative enzymes in the gut or a role in the invasion of gut epithelial cells by bradyzoites (Cleary *et al.,* 2002).

1.3.2 Metabolic differences between tachyzoites and bradyzoites of *Toxoplasma gondii* and stage specific enzymes

It is generally assumed, that the fast growing tachyzoite requires more energy than the dormant bradyzoite stage. Tachyzoites utilize the glycolytic pathway as their major energy source. Additionally, mitochondria with a functional tricarboxylic acid cycle (TCA) and a respiratory chain contribute to energy production. Bradyzoites, however, entirely depend on anaerobic ATP generation via glycolysis with the production of lactate. The fact that mitochondrial inhibitors such as antimycin A, myxothiazol and oligomycin promote stage conversion from tachyzoite-to-bradyzoite in vitro, further support the assumption that mitochondrial activity is more important for the tachyzoite stage than for the bradyzoite stage (Bohne *et al.,* 1994; Tomavo and Boothroyd, 1995). Stage specific differences have been reported in the activity of glycolytic enzymes. Lactate dehydrogenase and pyruvate kinase activity was found to be higher in bradyzoites than in tachyzoites (Denton *et al.,* 1996), suggesting, that fermentation of glucose to lactate plays the major role in energy generation in bradyzoites (Figure 2). Furthermore, a high activity of pyrophosphate phosphofructokinase was observed in both stages. This enzyme has shown to be more specific for pyrophosphate than for ATP. This results in an energy outcome of 3 ATP per glucose instead of 2 ATP, showing evidence that *T. gondii* has some adaptation for anaerobic conditions (Denton *et al.,* 1996; Combs *et al.,* 2002). Three isoenzymes, lactate dehydrogenase, glucose-6-phosphate isomerase and enolase have been found to be stage specifically expressed in *T. gondii* at the transcription and protein level (Yang and Parmley, 1997; Dzierszinski *et al.,* 1999 & 2001). Expression of different isoforms might be a way to adjust glycolysis stage specifically. Additionally, glucose-6-phosphate dehydrogenase (G6PD) was found to be down regulated in bradyzoites. G6PD initiates the pentose phosphate pathway, which finally leads to the synthesis of ribose-5-phosphate, an important precursor molecule of DNA and RNA. Down regulation of G6PD shifts the flow of glucose-6-phosphate towards glycolysis or gluconeogenesis / amylopectin synthesis (Cleary *et al.,* 2002).

Bradyzoites contain a large amount of amylopectin granules, a storage form of glucose. In tachyzoites, only few amylopectin granules are found. The explanation for this difference is unknown, but it could reflect the need of an endogenous energy source for long term survival of bradyzoites, which are surrounded by a cyst wall that may be largely impervious to an exogenous source of energy (Coombs *et al.,* 1997).

Holpert *et al.* (2001) have shown that bradyzoites posses a H^+-ATPase, which is a P-type ATPase of plants and lower eukaryotes, that is absent in tachyzoites. H^+-ATPases are located in the plasma membrane and translocate protons across the membrane, generating an electrochemical gradient which drives secondary nutrients and metabolic uptake (Serrano *et al.,* 1988; Morsomme *et al.,* 2000). The functional role of plasma membrane H^+-ATPases in bradyzoites is still unclear. Since the bradyzoite stage is exposed to a sudden pH change while it passes the stomach, it is possible, that P-type ATPases contribute to pH regulation.

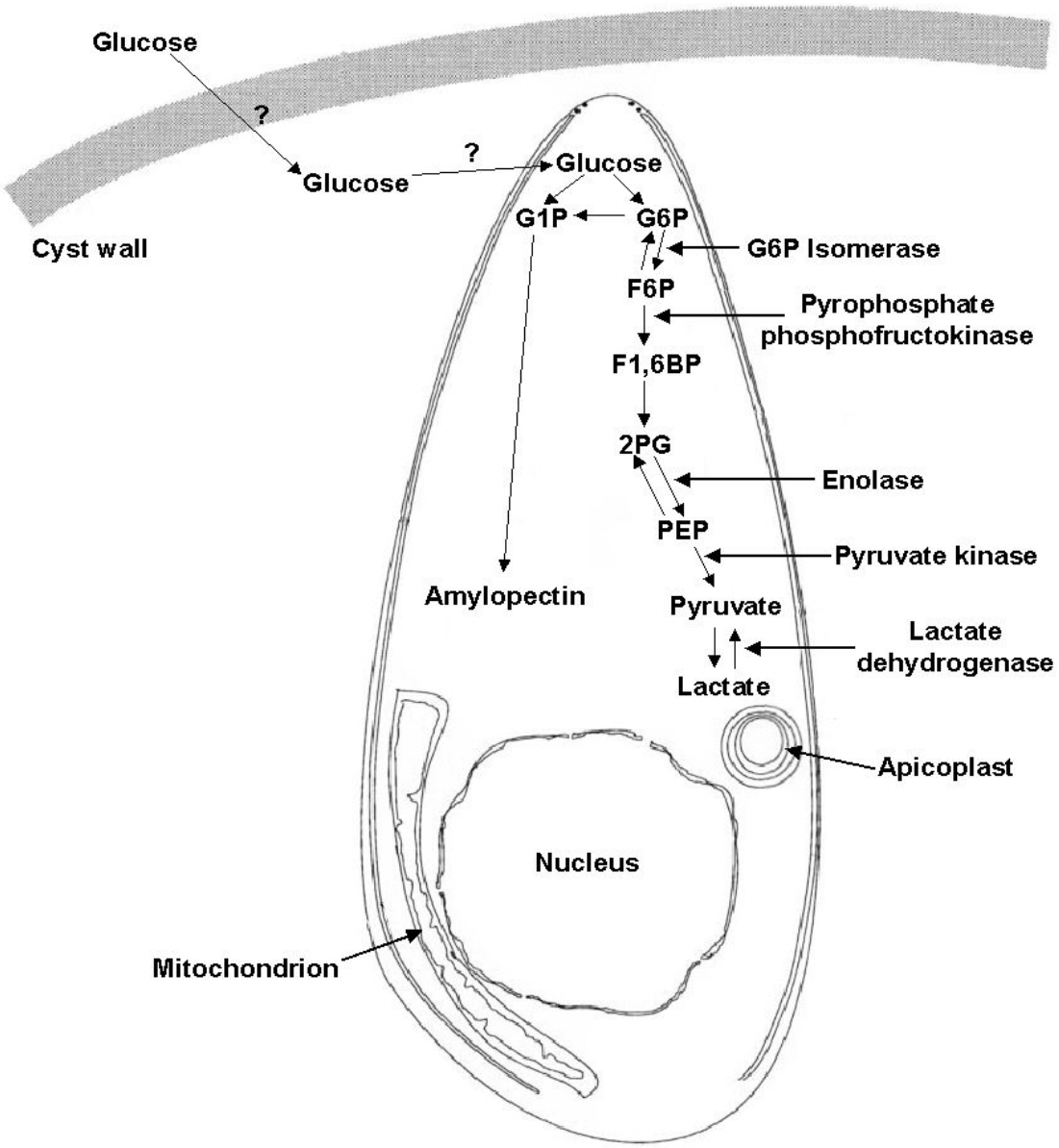

Figure 2: *T. gondii* bradyzoite metabolism. This model predicts that differentiation into the bradyzoite form will be accompanied by the impairment of mitochondrial oxidative phosphorylation and by the synthesis of new sets of metabolic enzymes that will trigger metabolite accumulation and therefore amylopectin synthesis (gluconeogenesis). Only selected steps of both glycolytic pathway and gluconeogenesis are diplayed in order to emphasise those enzymes described in chapter 1.3.2. G1P: glucose-1-phosphate; G6P: glucose-6-phosphate; F6P: fructose-6-phosphate; F1,6BP: fructose-1,6-biphosphate; 2PG: 2-phosphoglycerate; PEP: phosphoenol pyruvate. Adapted from Tomavo (2001).

1.3.3 Ultrastructure of *Neospora caninum* tachyzoites and bradyzoites

Tachyzoites (Figure 3A) are 5-7 µm in lenght and 1-2 µm wide. They contain all the classical features found in apicomplexan parasites. These are a three-layered plasma membrane, an apical complex composed of two apical rings, two polar rings, a conoid and microtubules. Furthermore, they possess secretory organelles like micronemes, rhoptries and dense granules. Micronemes are located at the anterior end of the parasite, whereas rhoptries are arranged along the longitudinal axis of the cell and they are filled with amorphous electron dense material. Dense granules are located at the anterior and posterior end of the parasite (Hemphill *et al.,* 1998). In addition, *N. caninum* tachyzoites like all eukaryotic cells, contain a Golgi complex, rough and smooth endoplasmic reticulum, mitochondria and a nucleus with a nucleolus (Speer and Dubey, 1989; Lindsay *et al*., 1993).

Tissue cysts (Figure 4) of *N.caninum* are primarily found in the brain and are up to 100 µm in diameter. The cyst wall is up to 4 µm thick and consists of a parasitophorous vacuole membrane and a granular layer, where electron dense granules and vesicles are embedded (Jardine *et al*., 1996). The interior of the tissue cyst consists of a less condensed granular matrix, that contains tortous and branched vesicles, small irregular electron dense bodies and lobulated lipid like inclusions (Jardine *et al*., 1996). Bradyzoites (Figure 3B) are approximately 6-8 µm long and 1-2 µm wide and they possess the same organelles that are described for tachyzoites. Additionally, they possess vesicular organelles containing short flat membranous segments and smaller vesicles (Jardine *et al.,* 1996). The nucleus in bradyzoites is subterminally located, whereas in tachyzoites it has a more central position. Further differences are that bradyzoites contain fewer rhoptries and more amylopectin granules than tachyzoites.

Figure 3: Transmission electron microscopy of *N. caninum* tachyzoite (A) and bradyzoite (B). (Speer *et al*., 1999).

Figure 4: Tissue cyst containing bradyzoites. (Speer *et al.*, 1999).

1.4 Host parasite interaction

Since *N. caninum* is an obligatory intracellular parasite, adhesion to and invasion of the host cell are important events for its survival and proliferation. The invasion process starts with a low affinity contact of the parasite with the host cell surface membrane without any consistent orientation and involves immunodominant tachyzoite surface antigens (Hemphill, 1996; Nishikawa *et al.,* 2000). In order to invade the host cell, the parasite reorients itself with its apical tip in contact with the host membrane (Figure 5). This leads to secretion of adhesion proteins from micronemes that form a tight attachment zone between host cell receptor and the actin - myosin cytoskeleton of the parasite, mediating gliding penetration of the parasite into the host cell (Carruthers and Sibley, 1997). Invagination of the host cell plasma membrane is initiated by the

discharge of rhoptry proteins to form a nascent parasitophorous vacuole. After the parasite is fully enclosed by the parasitophorous vacuole membrane, dense granule proteins are released in order to modify the lumen of the vacuole and its membrane.

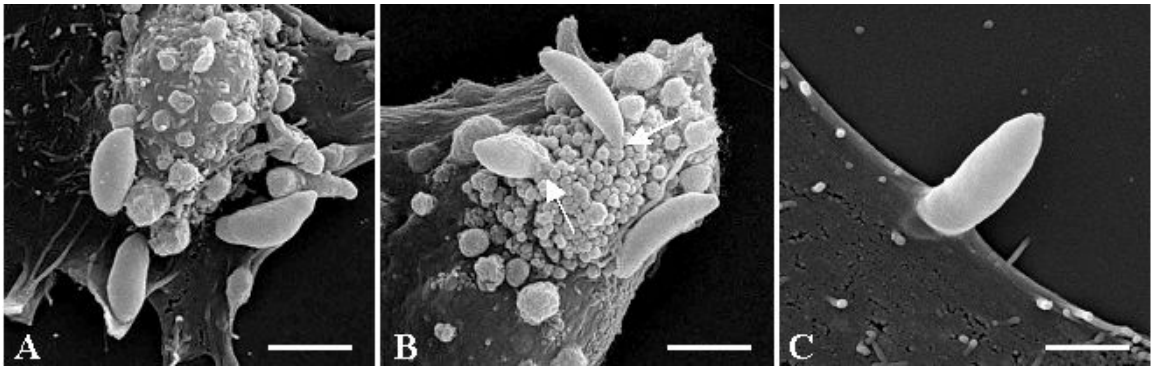

Figure 5: Scanning electron microscopy of adherent and invading *Neospora caninum* in cell culture. (A) Adhesion, (B) Reorientation and (C) Invasion. Arrows in (B) point towards the apical tachyzoite tips. Bar in (A) = 1400 nm, in (B) = 1260 nm, in (C) = 900 nm. Hemphill *et al.* (2003).

In order to gain more information about *N. caninum* proteins that are involved in host cell adhesion and invasion and the corresponding host cell receptors, several experiments were performed. It was shown by Hemphill (1996) and Nishikawa *et al*. (2000) that NcSRS2 and NcSAG1 play a role in the initial low affinity contact between the parasite and the host cell since polyclonal and monoclonal antibodies directed against these antigens inhibited adhesion and invasion of the host cell. Several *N. caninum* microneme proteins identified today possess adhesive domains that could interact with receptors on the surface of target cells. These adhesive motifs include thrombospondin (TSP)-like domain in NcMIC1 (Keller *et al.,* 2002), intergrin- and TSP-type I-like domains in NcMIC2 (Lovett *et al.,* 2000) and epidermal growth factor (EGF)-like domains in NcMIC3 (Sonda *et al.,* 2000). Among them, NcMIC3 is involved in the tight attachment of the parasite to the host cell as demonstrated by in vitro binding assays as well as antibody inhibition experiments (Naguleswaran *et al.,* 2001). Additionally, cell surface proteoglycans, a class of glycoproteins that covers the surface of all mammalian cells, were found to act as possible receptor for *N. caninum*

adhesion to the host cell, through their covalently attached glycosaminoglycan chains. This includes heparin, heparan sulphate, chondroitin sulphate A, B, C and keratin sulphate. It was found that *N. caninum* binds to sulphated glycosaminoglycans with the preference to chondroitin sulphate. The same accounts for the *N. caninum* microneme proteins NcMIC1 and NcMIC3 (Keller *et al.,* 2002; Naguleswaran *et al.,* 2002). *T. gondii* also binds to sulphated glycosaminoglycans, however, it prefers heparin and heparan sulphate as host cell receptor (Ortega-Barria and Boothroyd 1999; Carruthers *et al.,* 2000; Naguleswaran *et al.,* 2002). The significance of proteases in host cell adhesion and invasion was also assessed. It was shown that inhibition of parasite aspartyl proteases reduce the invasive capacity of *N. caninum* whereas inhibition of cysteine proteases significantly increased *N. caninum* invasion. This suggests a negative impact of cysteine proteases on the parasite invasive properties and a functional involvement of aspartyl proteases in host cell entry. The host cell entry of *T. gondii* was not affected by these enzymes. Inhibition of serine proteases, however, affected its entry into the host cell. Contrary to *N. caninum*, treatment of *T. gondii* with inhibitors of metallo-, cysteine- and aspartyl-proteases affected the adhesion of the parasite to the host cell (Naguleswaran *et al.,* 2003).

1.5 Immune response to Toxoplasma gondii and Neospora caninum

The immunological response to *N. caninum* infection has not yet been as well elucidated as in *T. gondii,* probably due to the lack of satisfactory small animal models, contrary to *T. gondii*, where the mouse, a natural host of the parasite, represents the primary mean to study the immune response after *T. gondii* infection. Therefore, most of the data described here originate from studies performed with *T. gondii*. Nevertheless, the mechanism of host protection against *N. caninum* appears to be similar in many aspects to that of *T. gondii*.

Generally, the host immune response to *T. gondii* and other intracellular protozoan parasites is characterized by a Th1 type cell mediated immune response. Activation of antigen presenting cells such as dentritic cells results in the production of IL-12. This in turn activates natural killer cells, $CD4^+$- and $CD8^+$-T cells to produce IFN-γ that stimulates macrophages to produce TNF-α. These two cytokines control parasite proliferation in the infected host. In vitro studies with *T. gondii* have shown that IFN-γ and TNF-α inhibited parasite multiplication in both phagocytic and non phagocytic cells through different mechanisms, depending on the cell type. IFN-γ and TNF-α have shown to stimulate murine macrophages and microglia to produce nitric oxide (NO) by inducible nitric oxide synthase (iNOS) and NO inhibited parasite proliferation (Chao *et al.,* 1993 & 1994). In addition to the antiparasitic activity of NO, IFN-γ and lipopolysaccharide (LPS) induced stage conversion of *T.* gondii in murine macrophages, implying that there are several possible outcomes of exposure of tachyzoites to NO (Bohne *et al.,* 1993). In human gliablastoma cell lines and astrocytes, IFN-γ and TNF-α inhibited parasite proliferation via activation of indolamine-2,3-dioxygenase that leads to degradation of intracellular tryptophan (Däubener *et al.,* 1996). Other mechanisms involved in the control of parasite proliferation are limiting the availability of intracellular iron to the parasite (Dimier *et al.,* 1998) and the production of reactive oxygen intermediates (Murray *et al.,* 1985). Recently, an IFN-γ regulated gene, IGTP was identified that encodes 47-48 kDa proteins that might be involved in the processing and trafficking of immunologically relevant proteins. Halonen *et al*. (2001) have shown that *T. gondii* proliferation in astrocytes from IGTP-deficient mice was not inhibited by IFN-γ compared to that of wild type mice, which demonstrates the role of this gene in the IFN-γ induced inhibition of *T. gondii* in murine astrocytes.

In vivo studies using gene knockout mice, neutralizing antibodies or inhibitors demonstrated the importance of IFN-γ in controlling parasite proliferation and preventing tissue cyst reactivation during both the acute and chronic stage of infection and the significance of TNF-α and iNOS in controlling the chronic infection. The role of IFN-γ in the acute stage of infection was shown by Alexander *et al*. (1997), where IFN-γ and IFN-γ receptor deficient mice could not

survive the early stage of infection. The control of early parasite growth, however, does not seem to be dependent on NO, as mice deficient in iNOS and TNF receptor were able to survive longer than animals deficient in IFN-γ and IFN-γ receptor. In contrast to the acute phase of infection, the treatment of chronically infected mice with the iNOS inhibitor N-monomethyl-L-arginine or anti-TNF-α and anti-IFN-γ monoclonal antibodies resulted in reactivation of the infection and in the development of toxoplasmic encephalitis (TE) (Scharton *et al.,* 1997). These results show that iNOS activated by TNF-α and IFN-γ plays a key role in TE. These findings are interesting with regard to AIDS patients, where reactivation of chronic Toxoplasmosis results in TE. This is associated with a deficiency of $CD4^+$-T cells, which are the major source for IFN-γ. The role of IFN-γ, TNF p55 receptor and iNOS in the expression of bradyzoite antigen BAG5 and cyst formation was further analysed and revealed, that the induction of BAG5 expression and cyst formation seems to be dependent on IFN-γ but independent on TNF p55 receptor and iNOS functions (Silva *et al.,* 2002).
Since proinflammatory mediators can be detrimental to the host, their effect needs to be counterbalanced by the simultaneous induction of regulatory cytokines such as IL-10 and IL-4 in order to limit host pathology. Mice deficient in IL-4 and IL-10 have shown an increased mortality during the acute phase of infection (Gazzinelli *et al.,* 1996; Suzuki *et al.,* 1996).

Experiments performed in mice infected with *N. caninum* demonstrated that the immune response to *N. caninum* like in *T. gondii* is dominated by Th1-cytokines with IFN-γ and IL-12 as the major mediator during acute infection. Mice depleted of IL-12 or IFN-γ were unable to survive the infection with *N. caninum* (Khan *et al.,* 1997; Bazler *et al.,* 1999; Dubey *et al.,* 1998). Using in vitro cultures of murine macrophages, it was demonstrated, that IFN-γ inhibited *N. caninum* proliferation via NO generation, as it was earlier described for *T. gondii*. Additionally, a dose dependent growth inhibition was observed (Tanaka *et al.,* 2000). In this context, it is noteworthy to mention that infection of murine fibroblasts with *N. caninum* and treatment with IFN-γ induced apoptosis in the host cell that was associated with DNA fragmentation and increased caspase 3

and 8 activity, whereas *T. gondii* protected fibroblasts from cell death (Nishikawa *et al.,* 2002). Beside cellular immune response, humoral immune response seems also to play a crucial role in the protection against *N. caninum* infection, since antibody knock out mice (μMT mice) succumbed to the infection (Eperon *et al.,* 1998).

Studies performed in naturally and experimentally infected cattle suggest, that similar to mice, the Th1 response plays a major role in the protection against *N. caninum* infection (Lunden *et al.,* 1998). Cattle generally show few clinical signs following an infection with *N. caninum*. Problems, however, arise during pregnancy, when changes in the cytokine profile at the maternal-foetal interface occur and influence the outcome of pregnancy (Innes *et al.,* 2002). Early in gestation, the mother is able to mount an effective Th1 response to *N. caninum* infection that can lead to abortion of the foetus. At mid gestation, a Th2-cytokine environment dominates the maternal-foetal interface. IL-10 is known to down regulate the production of IFN-γ, which might triggers recrudescence of the chronic infection and facilitates parasite invasion and infection of the foetus. This can result in the death of the foetus or in the birth of a live, congenitally infected calf, which might shows clinical signs at birth. In late gestation, the mother gives birth to healthy, but congenitally infected calves. Therefore, it is important to prevent congenital transmission by the way of developing novel vaccines.

1.6 Mode of action of nitric oxide

In eukaryotic cells, nitric oxide (NO) is mainly produced by the enzyme nitric oxide synthase (NOS). Three isoforms of this enzyme are known. These are nNOS (neuronal NOS), iNOS (inducible NOS) and eNOS (endothelial NOS). These enzymes use arginine, NADPH and oxygen as substrates and produce citrulline, NADP and NO. The major physiological action of NO is the relaxation of smooth muscle, neurotransmission, inhibition of platelet aggregation and regulation of cell respiration that are mediated by NO binding to the haem iron of

guadenylate cyclase (Denninger *et al.,* 1999) and cytochrome oxidase (Brown, 2001). During the inflammatory process of the cell, iNOS expression is induced by cytokines such as IFN-γ and TNF-α that lead to the production of high levels of NO. Cell damage and even cell death can occur that is mediated through different mechanisms. NO and its derivatives peroxynitrate, nitrogen dioxide and nitrosothiol can bind to enzymes of the respiratory chain specially to cytochrome oxidase leading to inhibition of respiration and causing cytotoxicity in those cells that are unable to survive only on glycolytic ATP production. Furthermore, NO can affect DNA synthesis through inactivation of the ribonucleotide reductase enzyme and DNA damage. DNA damage leads to expression of the tumour suppressor gene p53 that arrests the cell cycle to allow additional time for DNA repair. However, if the repair process fails, it triggers apoptosis. The effect of NO on cells, however, ultimately depends on many complex conditions, such as the rate of NO production, its diffusion rate, the concentration of potential reactants such as superoxide and oxygen in the cells, the presence of enzymes such as catalase and superoxide dismutase which decompose H_2O_2 and superoxide respectively, the level of antioxidants such as glutathione and finally the distance between generator cells and target cells (Burney *et al*., 1997). Furthermore, it has to be taken into consideration that different cell types exhibit different sensitivity to NO.

Besides its role as a physiological and pathological regulator on the host cell, NO also exerts an antiparasitic effect. It was shown by Shaw *et al*. (2002) that NO inhibited cysteine proteases in *T. gondii* that lead to inhibition of parasite replication. Other mechanisms described to be involved in the antiparasitic effect of NO are the inhibition of ribonucleotide reductase, the inhibition of enzymes of the respiratory chain like cytochrome oxidase and NADH dehydrogenase, the blocking of enzymes of the TCA cycle like aconitase and finally the inhibition of aldolase, an enzyme of the glycolytic pathway.

As already described, NO can induce stage conversion in *T. gondii* in vitro (Bohne *et al.,* 1994). In our study, we used sodium nitroprusside (Figure 6) as a NO donor to induce stage conversion in *N. caninum* at a concentration that did

not have a negative impact on the host cell but on the same time could support stage conversion.

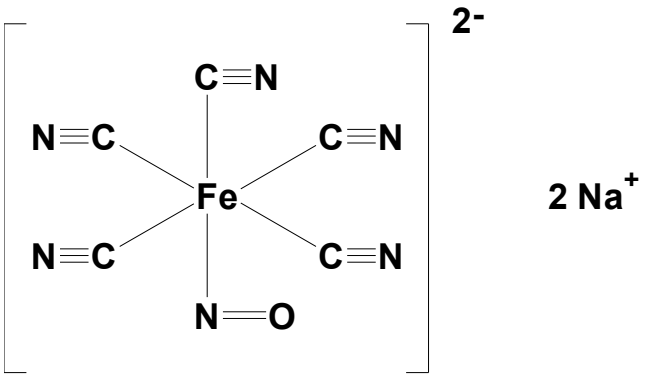

Figure 6: Sodium nitroprusside.

1.7 In vitro cultivation systems of Neospora caninum

1.7.1 In vitro cultivation of *Neospora caninum* tachyzoites

In vitro cultivation of *N. caninum* tachyzoites could be achieved in a wide range of cell types, including both primary cells and established cell lines. In vitro cultures of tachyzoites were used to develop tools for immuno- and molecular diagnosis such as the enzyme-linked immunosorbent assay (ELISA), the indirect fluorescent antibody technique (IFAT) and the polymerase chain reaction (PCR). Furthermore, in vitro generated tachyzoites were used to assess the susceptibility to a wide range of chemotherapeutical agents (Lindsay *et al.,* 1994) and to study the biology, especially the host parasite interaction during host cell invasion (Hemphill *et al.,* 2003). In vitro tissue cultures has also enabled genetic manipulation of the parasite in order to study proteins involved in host cell adhesion and invasion and it has been shown that *Toxoplasma* proteins are expressed, sorted and targeted properly in *Neospora* (Howe and Sibley*,* 1997).

1.7.2 Organotypic culture system of rat brain cortical tissue slices

This in vitro culture technique was initially developed by Stoppini *et al.* (1991) to study the physiology of neuronal tissue in vitro. The main feature of these slice cultures is to maintain a well preserved three-dimensional organization of the tissue, while simplifying the in vivo situation by excluding blood derived elements of the host defence, such as $CD4^+$- and $CD8^+$-T cells, natural killer cells, macrophages, neutrophils, antibodies and complement. In contrast to in vivo experiments, this model enables manipulations to be carried out in a controlled environment under defined conditions, with a direct access to a complex network of host cells such as astrocytes, microglia and neurons. The principle of this culture system is to maintain nervous tissue on a porous and transparent membrane at the interface between the culture medium and the atmosphere. By capillarity, the culture medium crosses the membrane and covers the slices by a thin film of medium. In these conditions, the explants do not dry out and remain well oxygenated. They can be kept in culture for several weeks.

1.7.3 In vitro cultivation model systems for the induction of bradyzoites

For the generation of *N. caninum* tissue cysts, animal models were developed. Tissue cysts could be produced in the brain of immunocompromised mice that were parenterally inoculated with tachyzoites (McGuire *et al.,* 1997a) and they were found as early as 17 days post inoculation. In addition, a method for the separation and cryopreservation of *N. caninum* tissue cysts from mouse brain was worked out (McGuire *et al.,* 1997b). However, the number of cysts produced in mice remains low compared to the avirulent strains of *T. gondii*, where the mouse represents a natural host of the parasite. A recent study carried out by Gondim *et al*. (2002) showed that dogs shed fewer oocysts when fed with mouse

brain tissue containing *N. caninum* tissue cysts than the one fed with bovine tissue. This suggests that mice are an inefficient model for the production of tissue cysts. Another approach to generate tissue cysts is the use of gerbils where larger number of tissue cysts could be obtained (Gondim *et al.,* 2001).

However, it would be a great advantage to have an in vitro cultivation model to study the molecular basis of stage conversion and to produce large amounts of bradyzoites required for scientific studies. For this purpose, several protocols were developed for *T. gondii* to generate bradyzoites in vitro.

Tachyzoite-to-bradyzoite conversion in *T. gondii* could be induced by applying external stress to various types of infected cells. It was shown that modulation of the culture conditions such as altering the pH, increasing the temperature, chemical stress (Soete *et al*., 1994) and the use of mitochondrial inhibitors (Bohne *et al.,* 1994) lead to stage conversion and cyst formation. In murine macrophages, IFN-γ induced stage conversion of *T. gondii* by a mechanism related to NO release. Identical results were obtained by the use of sodium nitroprusside as a source of exogenous NO (Bohne *et al.,* 1993 and 1994). More recently, it was shown that increased cyclic nucleotide levels in the host or parasite also seems to be linked to stage conversion (Kirkmann *et al*., 2001). Contrary to *T. gondii*, *N. caninum* tissue cysts have been difficult to obtain in vitro. Protocols developed for *T. gondii*, based on increasing the pH of the medium and treatment of infected human fibroblasts with tylosin over a period of 4 days, have yielded relatively few parasites undergoing stage conversion, showing, that the efficiency in the differentiation process in vitro is rather low compared to *Toxoplasma* (Weiss *et al.,* 1999).

1.8 Aim of this work

The major aim of this work was to develop a workable in vitro cultivation model for the efficient generation of *N. caninum* tissue cysts harbouring the bradyzoite stage. Once established, some practical applications of this model should be demonstrated. This includes the analysis of bradyzoite-specific antigen expression that could contribute to the immunodiagnosis of Neosporosis in chronically infected animals, investigations on the ultrastructure of in vitro generated *N. caninum* tissue cysts and finally studies on the biology of the bradyzoite stage with regard to adhesion and invasion of the host cell should be performed.

2. Material and Methods

2.1 Application of a real-time fluorescent PCR for the quantitative assessment of Neospora caninum infections in organotypic slice cultures

If not otherwise stated, all reagents and tissue culture media were purchased from Gibco-BRL.

2.1.1 Vero cell culture

Cultures of Vero cells were maintained in 20ml of RPMI-1640 medium supplemented with 7% foetal calf serum (FCS), 2 mM glutamine, 50 U/ml penicillin, and 50 µg/ml streptomycin at 37˚C / 5% CO_2 in T-75 tissue culture flasks. Cultures were trypsinised at least once a week.

2.1.2 Maintenance and purification of parasites

Neospora caninum tachyzoites of the Swedish isolate NcSwB1 (Stenlund *et al*., 1997) were maintained in Vero cell monolayers at 37˚C / 5% CO_2 in RPMI-medium containing 2 mM glutamine, 50 U/ml penicillin, 50 µg/ml streptomycin, and 5% Ig-free horse serum (HS). Parasites were harvested from their feeder cell cultures by passage through PD-10™ column filled with Sephadex G25M (Pharmacia) as previously described (Hemphill *et al*., 1996). The eluted purified parasites were centrifuged at 4˚C and were resuspended in cold RPMI-medium and used for infection.

2.1.3 Infection of organotypic rat brain slice cultures

Organotypic slice explants of rat brain cortex were prepared essentially as described by Stoppini *et al.* (1991). The tissue samples corresponding to serial slices were allowed to recover from explantation trauma for 1 week before infection was initiated. For infection, slice cultures were overlaid with 10^6 freshly isolated and purified NcSwB1 tachyzoites in 300 µl of RPMI-1640 culture medium without serum for 1h at 37ºC / 5% CO_2, followed by two washes in RPMI-1640. Control cultures were treated identically without parasites. The infected slices were then further maintained at 37ºC for 1-5 days prior to analysis.

2.1.4 Immunohistochemistry

For immunohistochemical monitoring of parasite proliferation, tissue slices were fixed overnight in 5ml of 4% paraformaldehyde in PBS, pH 7.2, at 4ºC, placed into 18% sucrose in PBS for 24h, cut at 10-20 µm intervals on a cryostat (Cryocut 1800, Leica Instruments, Nussloch, Germany) and mounted onto poly-L-lysine coated slides. Unspecific binding sites were blocked by incubation of slices in PBS / 3% BSA / 50 mM glycine, pH 7.2, for 2h at 24ºC. Tachyzoites were visualised by applying a polyclonal rabbit anti-*N. caninum* antiserum and a goat anti-rabbit IgG conjugated to FITC (Sigma) as previously described (Hemphill *et al*., 1996). Specimens were subsequently stained with a monoclonal antibody directed against glial fibrillary acid protein (GFAP; Chemicon International Inc.) and a goat anti-mouse IgG conjugated to Texas red (Sigma). They were then embedded in a mixture of glycerol / gelvatol containing 1.4-diazobicyclo[2.2.2] octan (Merck) as an anti-fading reagent, and were inspected on a Nikon Eclipse E800 digital confocal fluorescence microscope. Processing of images was performed using the Openlab 2.07 software (Improvision, Heidelberg, Germany).

2.1.5 Processing of DNA samples and LightCycler™-based quantitative PCR

DNA was extracted from entire brain slices by using the DNAeasy™ Kit (Qiagen, Basel, Switzerland) according to the standard protocol suitable for tissue samples. DNA was eluted in 100 µl AE buffer (elution buffer from the kit) and subsequently boiled for 5 min. For quantitative PCR forward primer Np21plus and reverse primer Np6plus were used. These primers had been designed to amplify a 337-bp sequence of the Nc5 region of *N. caninum* (Müller *et al*., 1996). Detection of DNA amplification products through fluorescence resonance energy transfer on the LightCycler™ Instrument (Roche Diagnostics, Basel, Switzerland) was achieved by hybridization of Nc5-specific 5‘-LC-Red 640-labelled Np 5LC (5‘-TCCCTCGGTTCACCCGTTCACACAC-3‘) detection probe and 3‘-fluorescein labelled Np 3FL (5‘-CACGTATCCCACCTCTCACCGCTACCA-3‘) anchor probe (TIB MOLBIOL, Berlin, Germany). The resonance energy transfer was over a 3-base gap between the two probes. PCR amplification was performed with 1 µl of 1:5 diluted sample DNA (see also below) using the LightCycler™ DNA Master Hybridization Probes Kit (Roche Diagnostics, Basel, Switzerland) in a standard reaction supplemented with $MgCl_2$ to a final concentration of 3 mM containing 0.5 µM of each primer plus 0.3 µM of each probe. After denaturation of DNA for 30s at 95°C, amplification was done in 50 cycles (5 cycles including denaturation: [95°C, 1 s], annealing: [63°C, 5 s], extension: [72°C, 20 s], plus 10 cycles including denaturation: [95°C, 1s], “touch-down“ annealing: [63°C to 53°C, temperature reduction: 1°C per cycle], 5 s; extension: [72°C, 20 s], plus 35 cycles including denaturation: [95°C, 1 s], annealing: [53°C, 5 s] and extension: [72°C, 20 s]; ramp rates in all cycle steps were 20°C/s) with 1 µl of 1:5 diluted DNA samples (see above). Fluorescence was measured at the end of each annealing phase in the “single“ mode with the channel setting F2/1. Fluorescence signals from the amplification products were quantitatively assessed by applying the standard software (version 3.5.3) of the LightCycler™ Instrument. Quantification of PCR products was achieved by plotting the fluorescence signals versus the cycle numbers at which the signals crossed the

baseline (see Figure 8A). Adjustment of the baseline was performed by using the “minimize error“ mode. Positive samples were identified by a fluorescence signal, which accumulated to values above the baseline within 50 cycles of reaction. As external standards, samples containing DNA equivalents from 100, 10 and 1 parasite(s) were included. Linearity among the standard reactions was reflected by the correlation coefficient, which was calculated by computer program to be 1. Lack of PCR-inhibitory effects as well as overall comparability of the different standard and sample reactions was evidenced by demonstrating the quasi-identity of the slopes from the amplification plots (monitoring amplification rates) at the baseline crossing points (see Figure 8A). Furthermore, reproducibility of the test system was demonstrated by proving an overall low variation within three independent runs of the standard reactions representing 100 (interassay coefficient of variation, 7.8%), 10 (13.3%), and 1 (17.2%) parasite(s), respectively.

2.2 Infection of organotypic slice cultures from rat central nervous tissue with Neospora caninum

If not otherwise stated, all reagents and tissue culture media were purchased from Gibco-BRL.

2.2.1 Vero cell culture

Vero cells were cultivated as described in 2.1.1.

2.2.2 Maintenance and purification of parasites

Neospora caninum tachyzoites of the Swedish isolate NcSwB1 were maintained in Vero cell monolayers and purified as described in 2.1.2.

2.2.3 Organotypic culture of rat brain cortical tissue slices and infection with *Neospora caninum* tachyzoites

Organotypic slice explants of rat brain cortex were prepared essentially by a modification of the procedure described for hippocampal tissue by Stoppini *et al.* (1991; 2000). The slices were allowed to recover from explantation trauma and to mature for 1 week before infection was initiated. For infection, cultures were overlaid with 2 x 10^6 or 2 x 10^7 freshly isolated and purified NcSwB1 tachyzoites in 300 µl of culture medium without serum for 1h at 37ºC / 5% CO_2, followed by two washes in medium. Control cultures were treated identically without

parasites. The infected slices were then further cultured at 37ºC for 1-7 days prior to analysis. In some experiments, infected slice cultures were cultured in the presence of 100 U/ml of recombinant mouse IFN-γ (Genzyme).

2.2.4 Lightmicroscopy and immunohistochemistry

At the appropriate time points, the brain slices were carefully removed from the filter, and were fixed overnight in 5ml of 4% paraformaldehyde in PBS, pH 7.2, at 4ºC. They were then placed into 18% sucrose in PBS for 24h, were subsequently cut at 10-20 µm intervals on a cryostat (Cryocut 1800, Leica Instruments) and mounted onto poly-L-lysine coated slides. They were stored at -20ºC for a maximum of 1 week prior to use.

Primary antibodies for the detection of parasites were the mAb NcmAb-4 directed against the major tachyzoite antigen NcSAG1 (Björkman and Hemphill, 1998), and an affinity-purified rabbit anti-NcSRS2 antibody (Hemphill *et al*., 1997). For the visualisation of cytoskeletal elements within the host neuronal tissue, the following reagents were used: Intermediate filaments were detected using a mAb directed against glial fibrilary acid protein (GFAP; Chemicon International Inc.). For the detection of tubulin, immunolabelling was carried out employing the mAb5-1-2 directed against α-tubulin (Sigma-Aldrich). Bound antibodies were visualised employing the appropriate TRITC- or FITC-conjugated secondary antibodies (Sigma). Actin microfilaments were demonstrated by staining with rhodamin-conjugated phalloidin (Sigma).

For staining of frozen sections, specimens were washed in PBS, and non-specific binding sites were blocked by incubation in blocking buffer (PBS / 3% BSA / 50 mM glycine) for 2h at room temperature. Incubations with primary antibodies were performed in dilution buffer (PBS / 0.3% BSA) for 45 min, followed by three washes in PBS, 5 min each. Secondary antibodies were used at a 1:100 dilution in dilution buffer for 30 min, followed by three washes in PBS, 15 min each. In case of double immunofluorescence labelling, all four layers

were applied sequentially. Finally, nuclei were fluorescently stained with the DNA-specific dye Hoechst 22358, (1 µg/ml in PBS), according to Fuchs *et al*. (1998). Specimens were subsequently embedded in a mixture of glycerol / gelvatol containing 1.4-diazobicyclo[2.2.2]octan (Merck) as an anti-fading reagent. The preparations were viewed on a Leitz Laborlux S fluorescence microscope for black and white photography. For colour micrographs, specimens were inspected on a Nikon Eclipse E800 digital confocal fluorescence microscope. Processing of images was performed using the Openlab 2.0.7 software (Improvision).

2.2.5 Transmission electron microscopy (TEM)

Tissue slices were fixed in 100 mM sodium phosphate buffer, pH 7.2, containing 2.5% glutaraldehyde and 0.25% tannic acid for 4h at room temperature (Hemphill and Croft, 1997), followed by postfixation in 1% OsO_4 for 4h at 4ºC. Subsequently specimens were washed in water and were prestained in 1% uranyl acetate in water for 1h at 4ºC, followed by extensive washing in water. Tissue slices were then dehydrated in a graded series of ethanol, and were embedded in Epon 820 resin. The resin was polymerised at 65ºC over a period of 48h. Ultrathin sections were cut on a Reichert and Jung ultramicrotome and were loaded onto 300 mesh copper grids (Plano GmbH). Staining with uranyl acetate and lead citrate was performed as described (Hemphill and Croft, 1997). Finally, grids were viewed on a Hitachi H-600 transmission electron microscope operating at 100 kV.

2.2.6 Processing of DNA samples and LightCycler™-based quantitative PCR

PCR-quantification of parasite proliferation within infected slice cultures maintained in the presence or absence of IFN-γ was performed according to Müller *et al.,* (2002) as described in 2.1.5.

2.3 Exogenous nitric oxide triggers Neospora caninum tachyzoite-to-bradyzoite stage conversion in keratinocytes

Unless otherwise stated, all tissue culture reagents and biochemicals were purchased from Sigma (St. Louis, MO)

2.3.1 Vero cells, human foreskin fibroblast (HFF) and human neuroblastoma (HT4) cell cultures

Vero cells, HFF, and neuroblastoma cells were maintained in RPMI-1640 medium (Gibco-BRL) supplemented with 10% FCS, 2 mM glutamine, 50 U penicillin / ml, and 50 µg of streptomycin / ml at 37°C with 5% CO_2 in tissue culture flasks. Cultures were trypsinised at least once a week.

2.3.2 Murine epidermal keratinocyte cell cultures

Cultures of murine epidermal keratinocytes (obtained from CELLn-TEC, Berne, Switzerland) were maintained in defined keratinocyte-SFM medium plus supplement (Gibco-BRL) at 37°C / 5% CO_2 in tissue culture flasks. The medium was supplemented with 10 ng/ml EGF (Bioconcept / Perotech), 10^{-10} M cholera toxin (Sigma) and 1x antibiotic-antimycotic (100 U/ml penicillin, 100 mg/ml streptomycin, 250 ng/ml amphotericin). This culture medium contains 0.07 mM calcium, a concentration reported to support the proliferation of mouse and human keratinocytes cultures (Hennings *et al.,* 1980; Jensen *et al.,* 1990). At confluency, cells were trypsinised (0.25% / 0.125% trypsin-EDTA) (Bioconcept /

Amimed), and seeded at 3 x 10^4 cells / cm^2 in new culture flasks (Caldelari *et al*., 2001).

2.3.3 Maintenance and purification of *Neospora caninum* and *Toxoplasma gondii* tachyzoites

Neospora caninum tachyzoites of the Liverpool isolate (Nc-Liverpool) (Barber *et al.,* 1995), Swedish isolate (NcSwB1) (Stenlund *et al.,* 1997) and Nc-1 isolate (Dubey *et al*., 1988) were maintained in Vero cell monolayers at 37°C / 5% CO_2 in RPMI-1640 medium containing 2 mM glutamine, 50 U penicillin / ml, 50 µg of streptomycin / ml, and 5% Ig-free HS (Hemphill *et al*., 1996). *T. gondii* tachyzoites (RH and ME-49, respectively) were cultured under identical conditions, except that horse serum was replaced by FCS. Parasites were harvested from their host cell cultures by passage through PD-10™ column filled with Sephadex G25M (Pharmacia) as previously described (Hemphill, 1996). The purified tachyzoites were centrifuged at 4°C, were resuspended in supplemented keratinocyte-SFM medium (see 2.3.2), counted in a Neubauer chamber, and were immediately used for infection experiments.

2.3.4 Infection of murine epidermal keratinocytes and induction of stage conversion

Monolayers of keratinocytes were grown to 80-90% confluency, either directly in 24 well tissue culture plates, on poly-L-lysine (100 µg/ml) coated glass coverslips in 24 well tissue culture plates, or in T25 tissue culture flasks. Prior to infection, the medium was removed, and cells were overlaid with 1ml (for 24 wells) or 10ml (for tissue culture flasks) of supplemented keratinocyte-SFM medium containing 70 µM sodium nitroprusside (SNP) (stock solution 10 mg/ml in distilled water)

and 10^5/ml of either *N. caninum* (Nc-Liverpool, NcSwB1 and Nc-1, respectively) or *T. gondii* tachyzoites (RH, ME-49, respectively). Control cultures contained no SNP. The infected monolayers were cultured at 37°C / 5% CO_2 for 1 to 8 days. SNP was added daily to the cultures. After 4 days, the medium was replaced with fresh medium with or without SNP, respectively. The specimen were inspected daily by phase contrast microscopy.

2.3.5 Monitoring of *Neospora caninum* proliferation in murine epidermal keratinocytes by quantitative Neospora-specific real-time PCR

For quantification of parasite proliferation, keratinocytes were grown in 24 well culture plates and were infected with 10^5 freshly isolated and purified Nc-Liverpool tachyzoites. To some cultures, 70 µM SNP was added at the time of infection. After 1, 2, 3 and 4 days, DNA was extracted from infected cell monolayers using the DNAeasy™ Kit (Qiagen) according to the standard protocol suitable for cultured animal cells provided by the manufacturers. DNA was eluted in 100 µl AE buffer and subsequently boiled for 5 minutes. Quantitative PCR amplification was performed on a LightCycler™ (Roche) with 4 µl of 1:400 diluted sample DNA, according to the protocol described by Müller *et al*. (2002) as described in 2.1.5. As external standards, samples containing *Neospora* DNA equivalent to 10, 5 and 1 tachyzoite(s) were included.

2.3.6 Immuno- and lectin-fluorescence labelling of infected cultures

At days 4 and 8 post infection, coverslips were rinsed 3 times in PBS and placed into fixation buffer (3% paraformaldehyde in PBS) for 30 min. Subsequently, the cells were permeabilised in PBS containing 0.2% Triton-X-100 for 30 min, washed in PBS, and were incubated in blocking solution (PBS / 3% BSA) over night at 4°C. The following primary antibodies were diluted in PBS / 0.3% BSA: (i) NcmAb-4, a mAb directed against the immunodominant tachyzoite surface antigen NcSAG1 (Björkman and Hemphill, 1998) was used at 1 µg/ml; (ii) a polyclonal rabbit anti-*N. caninum* tachyzoite hyperimmune serum (Hemphill *et al*., 1996), diluted at 1:500; (iii) a polyclonal antiserum directed against TgBAG1 that crossreacted with *N. caninum* bradyzoites and cysts in vivo (McAllister *et al*., 1996), diluted at 1:250; (iv) mAbCC2, a rat mAb directed against a *T. gondii* cyst wall protein (Gross *et al.,* 1995), diluted at 1:100. Incubations with primary antibodies were performed for 1h, followed by three washes in PBS, 5 min each. Bound antibodies were detected by incubation of coverslips with the appropriate TRITC- or FITC-conjugated secondary antibodies diluted at 1:100 in PBS / 0.3% BSA for 30 min. For double-fluorescence staining, antibodies were always applied sequentially, one layer at a time. Lectin staining was performed using biotinylated *Dolichos biflorans* agglutinin (DBA), exhibiting a high affinity for N-acteylgalactosamine residues, at a dilution of 1:200. As secondary antibody, anti-biotin-FITC conjugate, diluted 1:100 in PBS / 0.3% BSA was applied. Finally, the preparations were washed in PBS three times for 5 minutes, incubated in the fluorescent dye Hoechst 33258 (1 µg/ml in PBS) for 2 minutes, rinsed again in PBS and mounted in Fluoprep (BioMerieux S.A.). All specimens were viewed on a Nikon Eclipse E 800 digital confocal fluorescence microscope. Processing of images was performed using the Openlab 2.0.7 software (Improvision).

2.3.7 Transmission electron microscopy (TEM)

Keratinocytes were grown in a 25cm^2 culture flask. They were infected with 10^6 freshly isolated and purified tachyzoites of the Nc-Liverpool isolate. 70 µM SNP was added at the time of infection, control cultures received no SNP. Infected monolayers were cultured as described above (see 2.3.4). After 8 days cells were washed in PBS, and were fixed in 100 mM sodium phosphate buffer, pH 7.2, containing 2.5% glutaraldehyde. They were then removed from the culture flask using a rubber policeman, and were maintained in the primary fixation buffer for 3h at room temperature. Subsequently, the specimens were washed in PBS. The preparations were post-fixed in 2% OsO_4 in 100 mM sodium phosphate buffer pH 7.2 for 2h, washed 4 times in water and were prestained in 1% uranyl acetate in water for 30 minutes. Specimens were then dehydrated using a graded series of ethanol (50-70-90-100%) and were embedded in Epon 820 resin as described (Hemphill and Croft, 1997). The resin was polymerised at 65°C over a period of 24h. Ultrathin sections were cut on a Reichert and Jung ultramicrotome and were loaded onto 300 mesh copper grids (Plano GmbH). Staining with uranyl acetate and lead citrate was performed as described (Hemphill and Croft, 1997). Finally, grids were viewed on a Phillips 600 transmission electron microscope operating at 60kV.

2.4 In vitro induction of Neospora caninum bradyzoites in Vero cells reveals differential antigen expression, localisation, and host cell recognition of tachyzoites and bradyzoites

2.4.1 Cell cultures

Vero cells were cultivated as described in 2.1.1. Murine epidermal keratinocytes were cultivated as described in 2.3.2.

2.4.2 Maintenance and purification of *Neospora caninum* tachyzoites

Neospora caninum tachyzoites of the Liverpool isolate (Nc-Liverpool) (Barber *et al*., 1995) were maintained and purified as described in 2.3.3.

2.4.3 Monitoring of *Neospora caninum* proliferation in infected host cell monolayers by quantitative real-time PCR

In order to asses the influence of different concentrations of SNP on parasite proliferation, murine epidermal keratinocytes were grown in 24 well culture plates, and infected with 10^5 freshly isolated and purified Nc-Liverpool tachyzoites, as described by Vonlaufen *et al*. (2002b). Different concentrations of SNP (up to 70 µM) were added at the time of infection. Control cultures received no SNP. After 2, 4, 6 and 8 days, DNA was extracted from infected cell monolayers using the DNAeasy™ Kit (Qiagen). DNA was eluted in 100 µl AE buffer and subsequently boiled for 5 minutes. Quantitative PCR amplification

was performed on a LightCycler™ (Roche) with 4 µl of 1:400 diluted sample DNA, according to the protocol described by Müller *et al*. (2002) as described in 2.1.5. As external standards samples containing *Nesopora* DNA equivalent to 100, 10 and 1 parasite(s) were included.

2.4.4 Induction of *Neospora caninum* tachyzoite-to-bradyzoite stage conversion in Vero cells and purification of parasites

To induce tachyzoite-to-bradyzoite stage conversion in Vero cells, the previous protocol for the bradyzoite culture in murine epidermal keratinocytes (Vonlaufen *et al*., 2002b) was modified. Vero cell confluent monolayers were grown on poly-L-lysine (100 µg/ml) coated glass coverslips in 24 well tissue culture plates or in T75 or T175 tissue culture flasks. Prior to infection, the medium was removed and cells were overlaid with 1ml / well (24 well) or 20ml or 60ml (T75 and T175 tissue culture flasks, respectively) of RPMI-medium containing 10% FCS and freshly purified 1 x 10^5 tachyzoites / cm^2. To induce stage conversion, 17 µM SNP was added at the time of infection. Infected cultures were maintained at 37° C / 5% CO_2, and inspected microscopically daily. Each day, the medium was replaced with fresh medium, containing 17 µM SNP. Control cultures contained no SNP. The SNP-stressed cultures were grown for 8 days; control cultures were cultured for 2 days.

SNP-treated *N. caninum* parasites were harvested from Vero cell cultures after 8 days of cultivation and isolated according to the previously described protocol for tachyzoites (Hemphill *et al*., 1996) with some modifications. Briefly, SNP-treated cultures were trypsinised, and were repeatedly passed through a 25G needle. Following centrifugation at 600 x g at 4°C for 10 min, the pellet was resuspended in cold RPMI-1640 and washed twice by centrifugation at 600 x g. Under these conditions, cellular debris remained largely in the supernatant, while intact parasites were recovered in the pellet fraction. The final pellet was resuspended in 2ml of cold RPMI-1640, and parasites were purified by passage through PD-

10™ columns. The purified parasites were centrifuged at 4ºC at 600 x g and pellets were stored at -80ºC for further analysis, or parasites were immediately fixed and used for immunofluorescence labelling as described below.

2.4.5 Immunofluorescence labelling of isolated parasites and infected Vero cell cultures

All manipulations were done at room temperature. Either isolated parasites were fixed in 3% paraformaldehyde in PBS and were allowed to settle down onto poly-L-lysine coated glass coverslips for 30 min, or SNP-treated and untreated infected Vero cell cultures grown on poly-L-lysine coated coverslips were fixed in 3% paraformaldehyde in PBS for 30 min. Following fixation, specimens were permeabilised in 0.2% Triton-X-100 in PBS for 30 minutes, washed in PBS, and unspecific binding sites were blocked in 3% BSA in PBS overnight at 4ºC. The following primary antibodies were diluted in 0.3% BSA in PBS: (i) NcmAb-4 directed against NcSAG1 (Björkman and Hemphill, 1998) was used at 1 µg/ml; (ii) mAb5.2.15, cell culture supernatant, directed against NcSRS2 (Schares *et al*., 1999) undiluted; (iii) polyclonal rabbit anti-*N. caninum* tachyzoite hyperimmune serum (Hemphill *et al*., 1996) 1:500; (iv) polyclonal rabbit antiserum directed against TgBAG1 (McAllister *et al*., 1996) 1:250; (v) mAbCC2, raised against a *T. gondii* cyst wall antigen (Gross *et al*., 1995) 1:100; (vi) polyclonal rabbit antibody against NcGRA7 (Lally *et al*., 1997) 1:50; (vii) polyclonal mouse serum against NcGRA1 (Atkinson *et al*., 2001) 1:50; (viii) polyclonal mouse serum against NcGRA2 (Ellis *et al*., 2000) 1:50. Incubation with primary antibodies was performed for 1h, followed by 3 washes in PBS, 5 min each. The bound primary antibodies were detected by incubation with the appropriate rhodamin- or FITC-conjugated secondary antibodies diluted 1:100 in 0.3% BSA in PBS for 30 min. For double-fluorescence staining, antibodies were always applied sequentially, one layer at a time. Finally, the preparations were washed in PBS (3 x 5 min), and were incubated in the fluorescent dye Hoechst 33258 (1 µg/ml in PBS) for 2

min, rinsed again in water and mounted in Fluoprep (BioMerieux S.A.). All specimens were viewed on a Nikon Eclipse E 800 digital confocal fluorescence microscope. Processing of images was performed using the Openlab 2.0.7 software (Improvision).

2.4.6 Transmission electron microscopy and immunogold transmission electron microscopy

For conventional TEM of *N. caninum* bradyzoite cultures, infected monolayers were fixed, dehydrated, embedded in Epon 820 resin, and further processed as previously described for infected murine epidermal keratinocytes (Vonlaufen *et al*., 2002b), as described in 2.3.7.

For immunogold transmission electron microscopy, bradyzoite-infected Vero cell cultures were fixed in PBS containing 3% paraformaldehyde for 30 min at 24˚C. The preparations were washed three times in PBS, and were removed from the surface of the tissue culture flask using a rubber policeman. They were kept in PBS / 50 mM glycine for 1h at 4˚C, and were washed extensively in PBS by several rounds of centrifugation. Specimens were then dehydrated using a graded series of ethanol (50-70-90-100%) at -20˚C, 5 min each, and were embedded in LR-White resin at -15˚C, with four changes of fresh resin over a period of three days. The resin was polymerized at 58˚C for 24h. Sections were cut using a Reichert & Jung ultramicrotome, and were picked up onto 200 mesh formvar-carbon-coated nickel grids (PLANO GmbH, Marburg, Germany). Loaded grids were stored at 4˚C for a maximum of 48h prior to use.

Prior to labelling of LR-White sections, electron microscopy (EM) grids were incubated in EM blocking buffer (PBS / 0.5% BSA / 50 mM glycine) for 1h at room temperature. All subsequent steps were also performed at room temperature. Sections were rinsed in PBS, and incubated with either monoclonal or polyclonal antibodies diluted as for immunofluorescence in EM blocking buffer (see above) for 1h. Following washing in 5 changes of PBS, 2 min each, EM

grids were incubated with goat anti-mouse- or goat anti-rabbit-IgG conjugated to 10 nm gold particles (Amersham), at a dilution of 1:5 in PBS / 0.5% BSA for 45 min. After 6 washes in PBS, 5 min each, the specimens were shortly rinsed in distilled water, and were air-dried. Finally, grids were stained with lead citrate and uranyl acetate, and were subsequently viewed on a Phillips 300 transmission electron microscope operating at 60 kV.

2.4.7 SDS-PAGE and immunoblotting

Protein extracts, corresponding to identical numbers of purified *N. caninum* tachyzoites and bradyzoites, were separated by SDS-PAGE under reducing conditions, and were electrophoretically transferred onto a nitrocellulose membrane as previously described (Sonda *et al*., 2000). Non specific binding sites were blocked in 3% BSA in TBS-T (20 mM Tris, 150 mM NaCl, 0.3% Tween 20, pH 7.4) for 2h at room temperature. Polyclonal anti-BAG1 antibody (1:2000), NcmAb-4 (1:2000), mAb5.2.15 (1:1) and anti *Neospora* hyperimmune serum (1:1000) were diluted in TBS-Tween / 0.3% BSA, and were applied overnight at 4°C. Bound antibodies were visualised using appropriate alkaline phosphatase conjugates (Promega, Zürich, Switzerland).

2.4.8 Pyrrolidine dithiocarbamate (PDTC)-PCR-based quantification of host cell interactions of bradyzoites and tachyzoites

Adhesion to and invasion of Vero cells by *N. caninum* tachyzoites and bradyzoites was investigated using the PDTC-PCR adhesion / invasion assay according to Naguleswaran *et al*. (2003). Briefly, Vero cell monolayers were grown to confluency in 96 well flat bottom tissue culture plates (Sarstedt Inc., Nümbrecht, Germany). 1 x 10^5 parasites (either freshly purified tachyzoites or bradyzoites) resuspended in 100 µl of RPMI-1640 were added to the monolayers. They were allowed to invade for 30 min at 37°C / 5% CO_2. In some experiments, monolayers were treated with 50 mU/ml neuraminidase (*Vibrio cholerae*) at 37°C for 2h prior to parasite incubation. Alternatively, tachyzoites and bradyzoites were pretreated with 50 mU/ml neuraminidase at 37°C for 30 min prior to letting them interact with host cells. Unbound parasites were removed by washing in RPMI-1640, and infected monolayers were incubated with RPMI-1640 containing 100 µM PDTC, 0.2 µM $CuSO_4$ and the respective parasite specific hyperimmune serum (1:200) for 2h at 37°C. This killed and permeabilised extracellular parasites but left intracellular ones unharmed (Naguleswaran *et al*., 2003). In parallel, control incubations in RPMI-1640 were performed. Subsequently, the wells were washed once with RPMI-1640, and RPMI-1640 containing 1 mg/ml DNaseI was added and the preparations were incubated for 1h at 37ºC. Finally, all wells were washed with RPMI-1640 containing 1 mM EDTA to inhibit DNaseI-activity, and the cellular material was taken up in 100 µl of lysis buffer (DNAeasy™ Kit, Qiagen). The specimens were transferred to Eppendorf tubes, and heated for 5 min at 95°C. DNA was purified by using the DNAeasy™ Kit (Qiagen) according to the manufacturers instructions. Parasite numbers were determined by real-time PCR using the LightCycler™ Instrument as described by Müller *et al.,* (2002) in 2.1.5.

3. Results and Discussion

3.1 Application of a real-time fluorescent PCR for quantitative assessment of Neospora caninum *infections in organotypic slice cultures*

Two sets of 10 serial rat brain slices were incubated in the presence of 10^6 *N. caninum* tachyzoites per set. Between days 1 and 5 post inoculation, samples were investigated for infection intensities by examination of slices either through immunohistochemistry (Figure 7) or quantitative PCR (Figure 8). In addition, an uninfected control sample (representing day 0) was analysed by each technique. Semiquantitative immunohistological evaluation revealed a progressive increase of the intracellular parasite numbers (Figure 7). These results were largely confirmed by PCR on a quantitative level. For quantitative PCR-based determination of parasite numbers at the different time points post inoculation, corresponding data from the DNA amplification plots were compared to the standard plots representing DNA equivalents from approximately 100, 10 and 1 parasite(s) (Figure 8A). By assessing parasite numbers as means (plus standard deviations) from values determined in three independent PCR runs, infection intensities were revealed to continuously increase to a number of approximately 48‘000 parasites per slice at day 5 post inoculation (Figure 8B).

Taken together, the present results showed that inoculation of organotypic rat brain slice cultures with an appropriate number (approximately 10^6) of *N. caninum* tachyzoites results in continuous parasite growth over a period of at least 5 days. The investigation revealed that the proliferation rate can precisely be monitored by using the highly sensitive Nc5-PCR (Müller *et al*., 1996) for quantitative detection of accumulating parasites. In contrast, immunofluorescence detection of parasites allows only a semi-quantitative assessment of parasite proliferation.

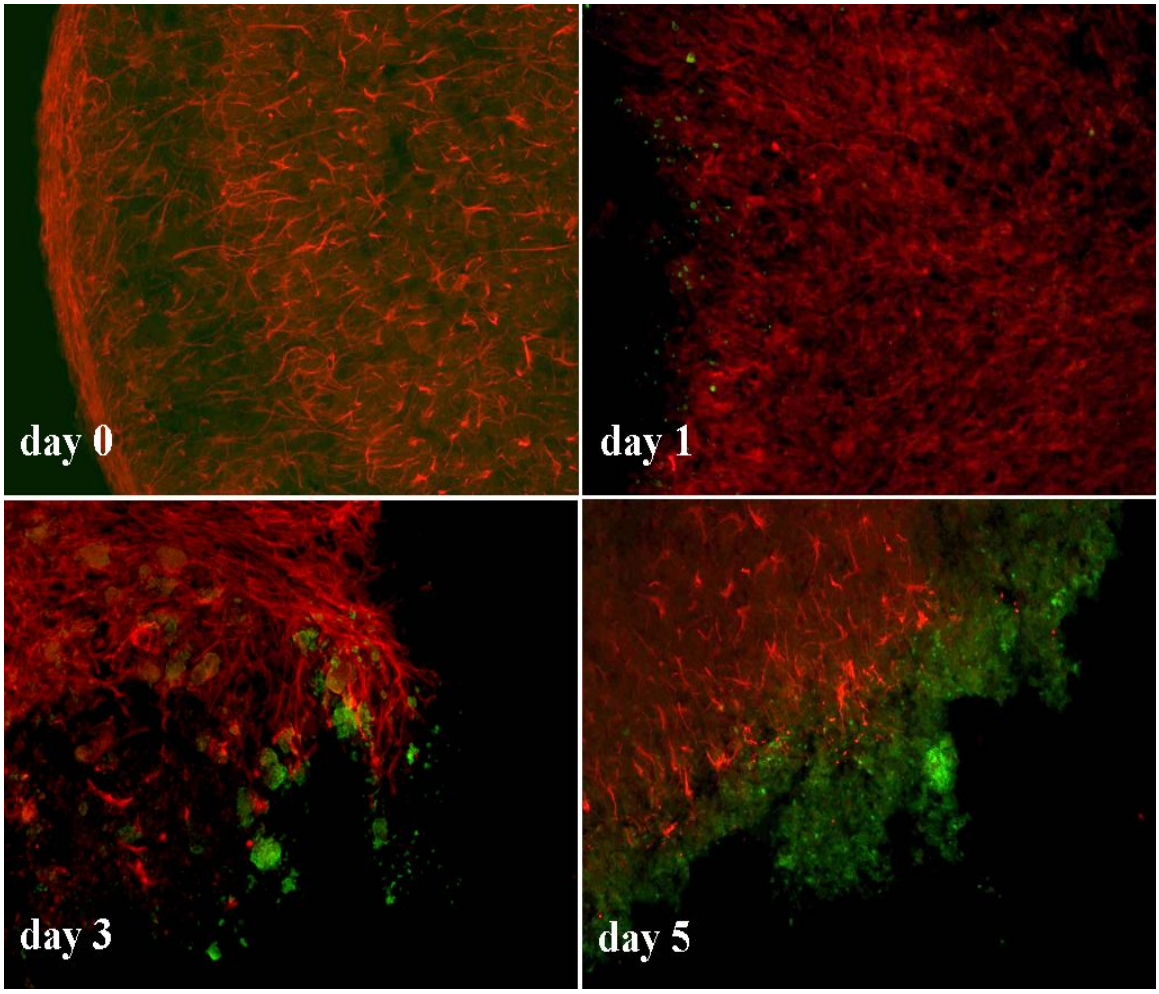

Figure 7: Monitoring of parasite proliferation following infection of organotypic cultures with 10^6 *N. caninum* tachyzoites (days 1 to 5). Parasites were detected by immunolabelling using a polyclonal anti-*N. caninum* antiserum followed by detection with a fluorescein isothiocyanat-conjugated anti-rabbit antibody. The brain tissue was counterstained employing a monoclonal antibody directed against GFAP followed by staining with an anti-mouse-Texas red conjugate.

The excellent operating characteristics make the quantitative PCR assay a versatile tool to study, *ex vivo* and under experimentally controlled conditions, a large variety of biological parameters relevant during the cerebral phase of a *N. caninum* infection. Accordingly, PCR-based parasite quantification of organotypic brain tissue samples may become an important experimental model for the generation of novel information on those processes that cause neuronal pathogenicity in bovine and canine Neosporosis. In addition, PCR-based quantification of *Neospora caninum* can be applied to determine infection

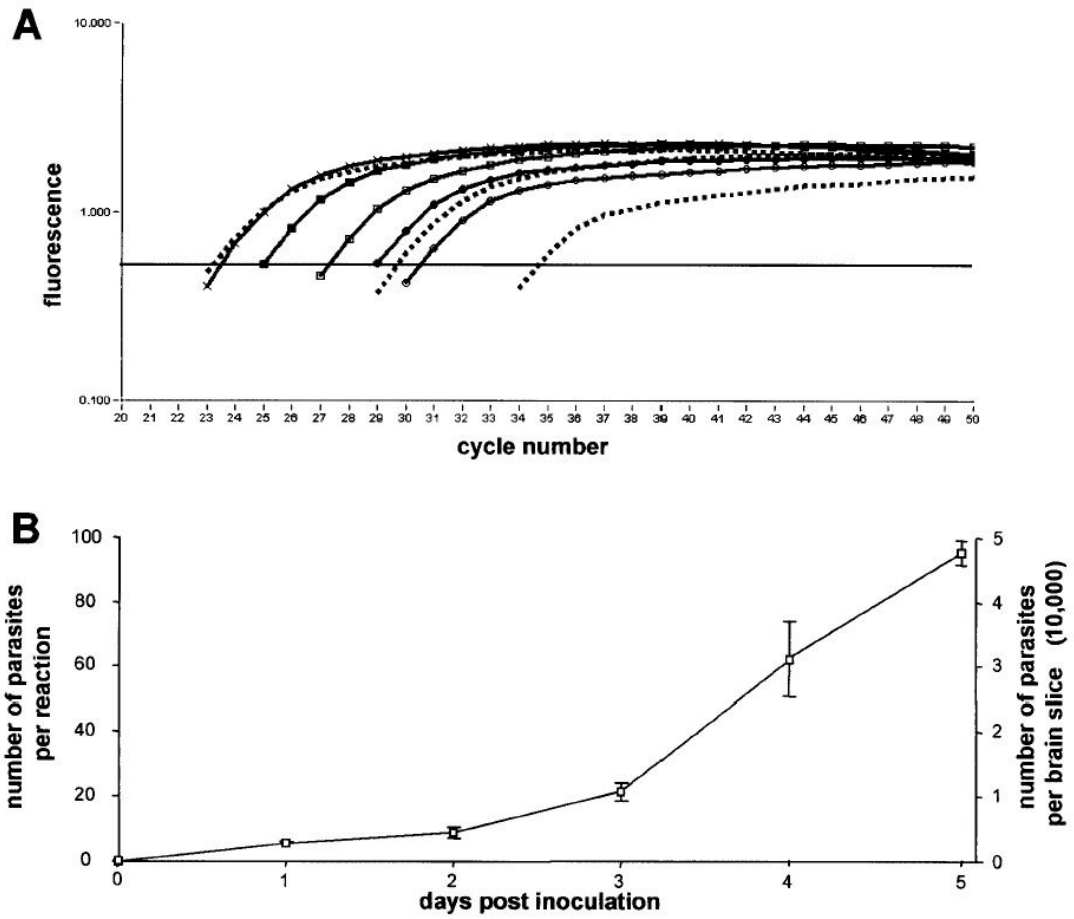

Figure 8: LightCycler™-PCR for quantitative assessment of *N. caninum* in organotypic rat brain tissue samples. (A) Typical example from three independent PCR runs including amplification plots representing standard reactions (dotted lines) for 100 (left), 10 (middle) and 1 parasite (right), or reactions representing samples taken at days 1 (open circles), 2 (closed circles), 3 (open squares), 4 (closed squares), and 5 (crosses) post inoculation with 10^6 parasites. Quantification of PCR products was achieved by plotting the fluorescence signals versus the cycle numbers at which the signals crossed the baseline (indicated as horizontal lines) and standards (dotted curves) were used for calculation of the parasite numbers within the samples. (B) Parasite growth kinetics, expressed as mean values plus standard deviations from three independent determinations. Values are given as parasite numbers detected in the various reactions (left scale). The extrapolated numbers of parasites corresponding to the entire section of brain slice are indicated on the right.

intensities in tissues and body fluids originating from both experimentally and naturally infected samples, and thus is useful for epidemiological and clinical studies, as well as for research applications, such as the assessment of the efficacy of treatment and / or vaccination strategies to be developed in the future.

3.2 Infection of organotypic slice cultures from rat central nervous tissue with Neospora caninum

3.2.1 Results

3.2.1.1 Maintenance of Neospora caninum tachyzoites in organotypic slice cultures from rat cortical brain tissue

Organotypic rat cortical central nervous system (CNS) tissue was maintained for 1 week prior to infection with 10^6 freshly isolated *N. caninum* tachyzoites in order to determine whether these cultures would sustain the growth and proliferation of *N. caninum*. The distribution of tachyzoites following infection was monitored on frozen sections by immunofluorescence using monoclonal and polyclonal antibodies directed against NcSAG1 and NcSRS2, respectively. NcSAG1 and NcSRS2 represent the immunodominant surface antigens of *N. caninum* tachyzoites (Hemphill, 1999). In brain tissue slices fixed at day 1 following infection, we found single tachyzoites or groups of few parasites which had invaded the tissue (Figure 9). The overall number of tachyzoites was low, not more than approximately 40-60 parasites per tissue slice, and tachyzoites were scattered along the periphery of the tissue sections. On day 2, a slightly increased number of parasites could be seen. At 3 days following infection, larger groups of tachyzoites were visible, some already spreading and infecting neighbouring cells, but mostly still preferentially located at the periphery of the sections (Figure 9). Electron microscopy of infected cultures fixed and processed at days 2-3 following infection (Figure 10A-C) revealed that tachyzoites were located, and proliferating within classical parasitophorous vacuoles. The lumen of the vacuole was filled with a parasitophorous vacuole tubular network. Pseudocysts containing between 4 and 10 tachyzoites were detected, in all cases surrounded by a parasitophorous vacuole membrane. In no case a cyst wall was visible. Around days 4-5, the number of parasites was increasing

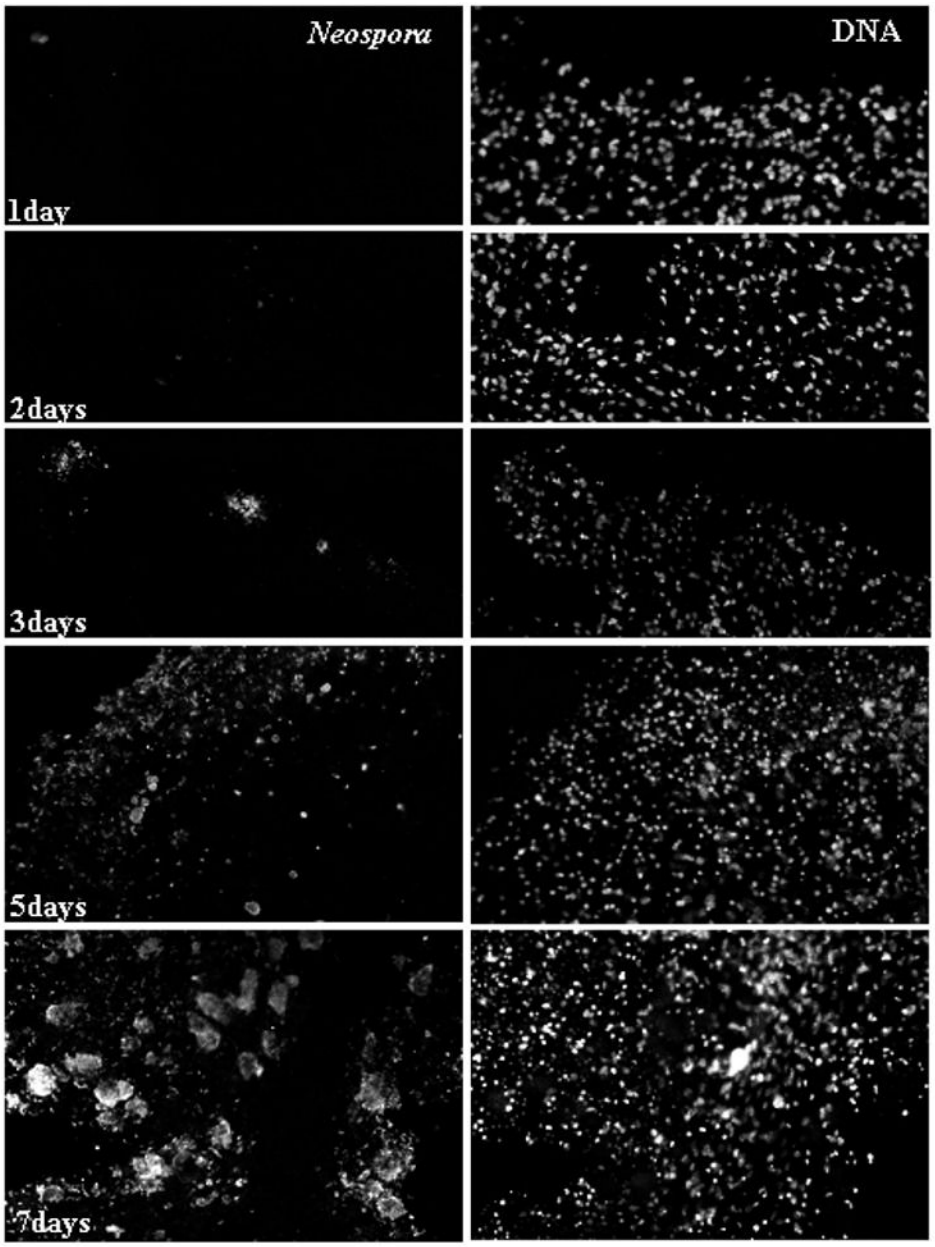

Figure 9: Time course of infection of organotypic cultures of rat cortex with 2 x 10^6 *N. caninum* tachyzoites. Parasites were immunolabelled with a mAb directed against NcSAG1 and FITC-conjugated secondary antibodies (left), and the nuclei were stained with the fluorescent dye Hoechst 22348 (right). Note the massive proliferation between days 3 and 7.

Next Page:

Figure 10: TEM of infected organotypic cultures. Fixation and processing for TEM was carried out at day 2 (A, B), day 3 (C), and at day 4 (D) following infection with 2 x 10^6 *N. caninum* tachyzoites. Arrows point towards the parasitophorous vacuole membrane; no cyst wall is formed. tn = parasitophorous vacuole tubular network. (A) Bar = 790 nm; (B) Bar = 600 nm; (C) Bar = 990 nm; (D) Bar = 680 nm.

Figure 10:

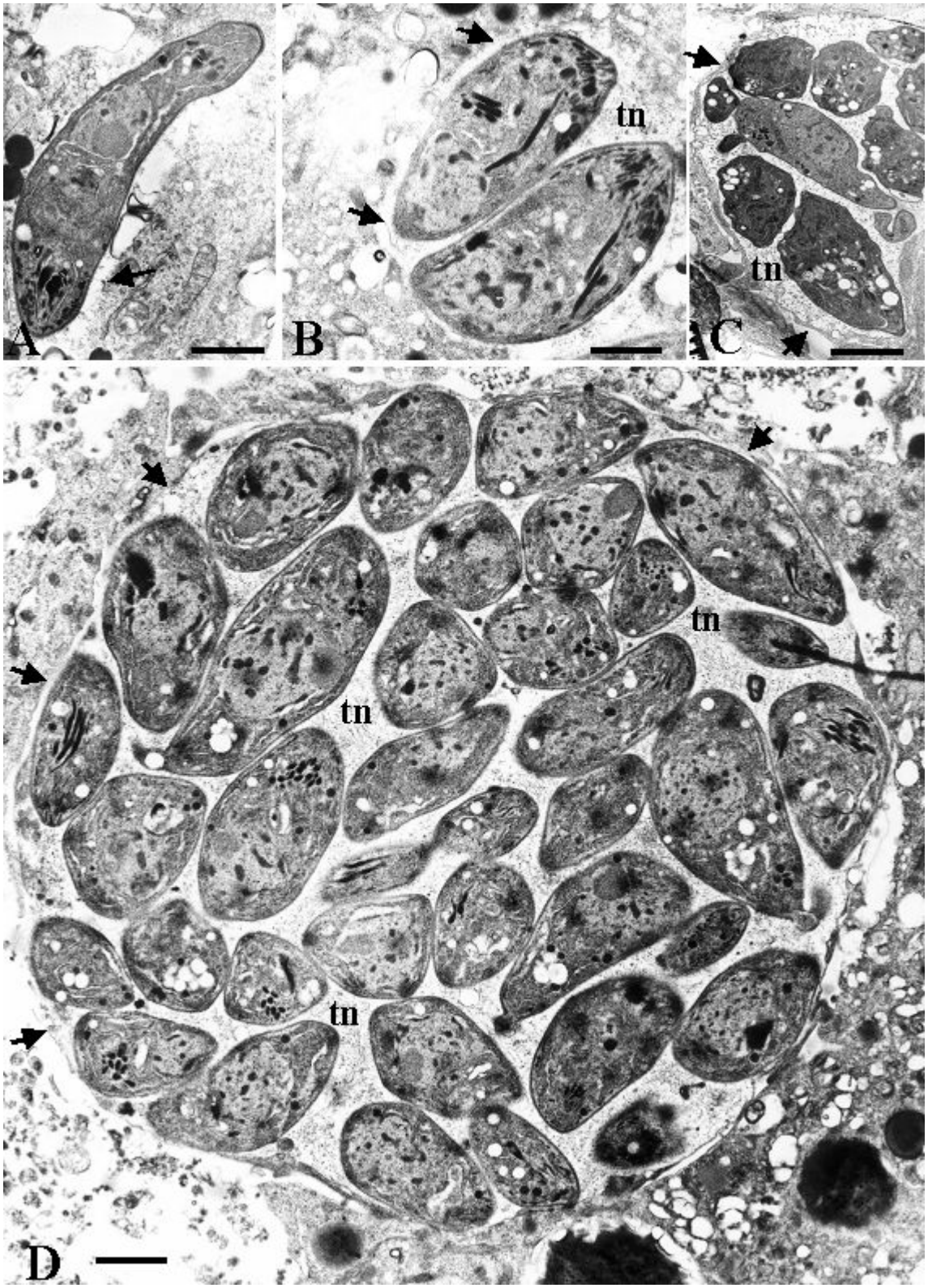

dramatically as assessed by immunofluorescence (Figure 9) and by quantitative PCR-assay (Figure 13). Many of the pseudocysts had collapsed, liberating tachyzoites, which readily had entered neighbouring cells. The distribution of parasites has moved from the periphery towards the interior of the section, reflecting the development of tachyzoites and the spread to adjacent regions of the tissue. In this phase, larger pseudocysts similar to the one shown in Figure 10D could be seen. At day 7, all areas of the tissue were heavily infected with tachyzoites, and large pseudocysts containing hundreds of tachyzoites were visible (Figure 9). TEM revealed that these events resulted not only in the deterioration of the overall morphological and structural organisation of the infected host tissue, but that the massive proliferation of parasites also resulted in a large number of necrotic tachyzoites due to the lack of viable host cells (data not shown). Similar observations were made when organotypic brain slice cultures were infected with 2 x 10^7 tachyzoites, except that the time frame between initial invasion and complete colonialization of the tissue slices was reduced to 3-4 day (data not shown). Taken together, organotypic slice cultures of rat cortical brain tissue constituted a favourable environment for the maintenance and proliferation of *N. caninum* tachyzoites.

3.2.1.2 Neuronal cytoskeleton and Neospora caninum infection

The interaction between neuronal cytoskeletal elements of organotypic cortical tissue slices and *N. caninum* tachyzoites were investigated by immunofluorescence. These interactions appeared most evident with regard to the intermediate filaments formed by glial fibrillary acid protein (GFAP), which at the same time serves as a marker for astrocytes. In uninfected control cultures, anti-GFAP immunolabelling revealed the highly organised, three-dimensional structure of GFAP-containing filaments. Double staining of GFAP and *N. caninum* in infected cultures showed that the overall structure of the intermediate filament network was heavily distorted in regions of massive tachyzoite

proliferation, starting at about day 4 to 5 following infection with 2 x 10^6 parasites (data not shown). In areas where tachyzoites were still located intracellularly,

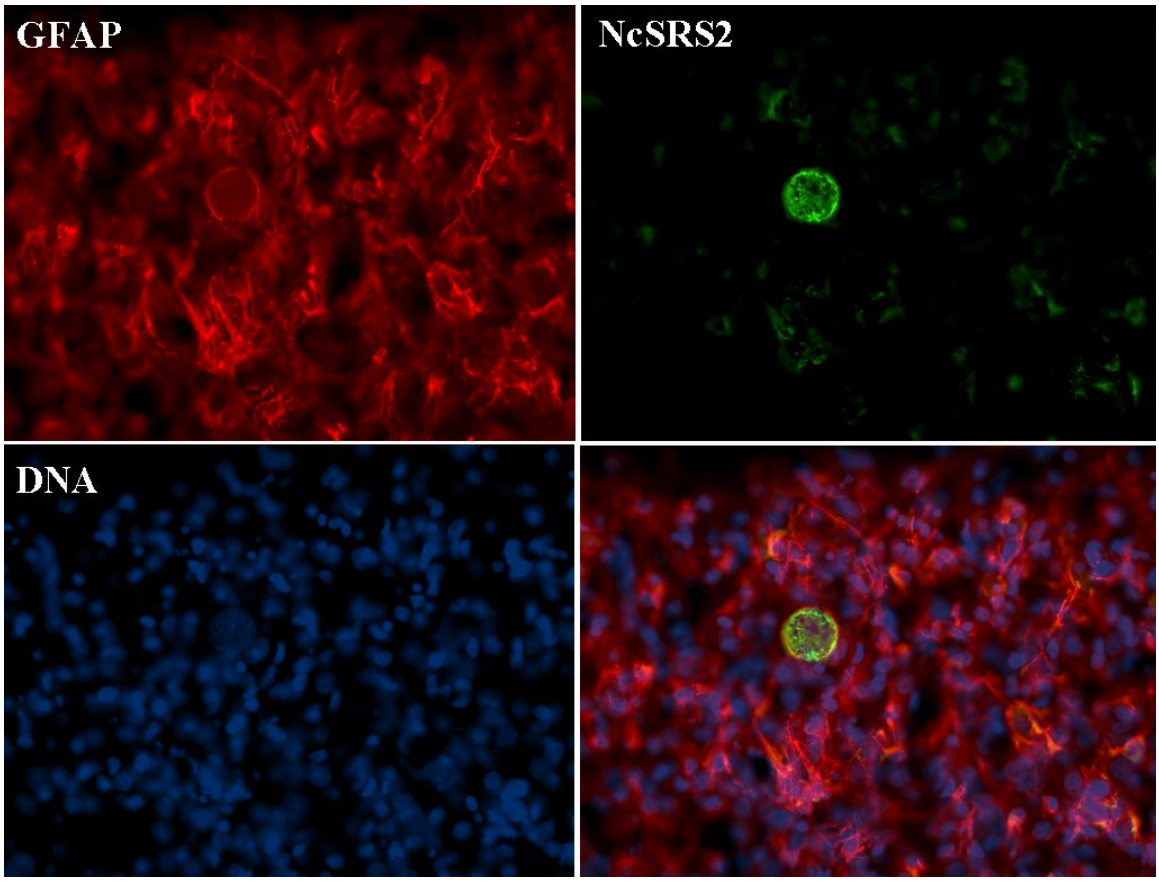

Figure 11: GFAP and pseudocysts. Immunofluorescence staining of GFAP labelling (red), NcSRS2 staining (green) indicative for *N. caninum* tachyzoites, DNA-labelling (blue), and the overlay. Note the close colocalisation of peripheral GFAP filaments with the pseudocyst periphery.

enclosed in a large pseudocyst, the glial filaments were in close juxtapositon to the pseudocyst membrane, indicating that an association between the parasite pseudocyst membrane and astrocyte-derived intermediate filaments is maintained (Figure 11). In contrast, double staining with anti-tubulin antibodies did not reveal any association of microtubules with *N. caninum* (data not shown).

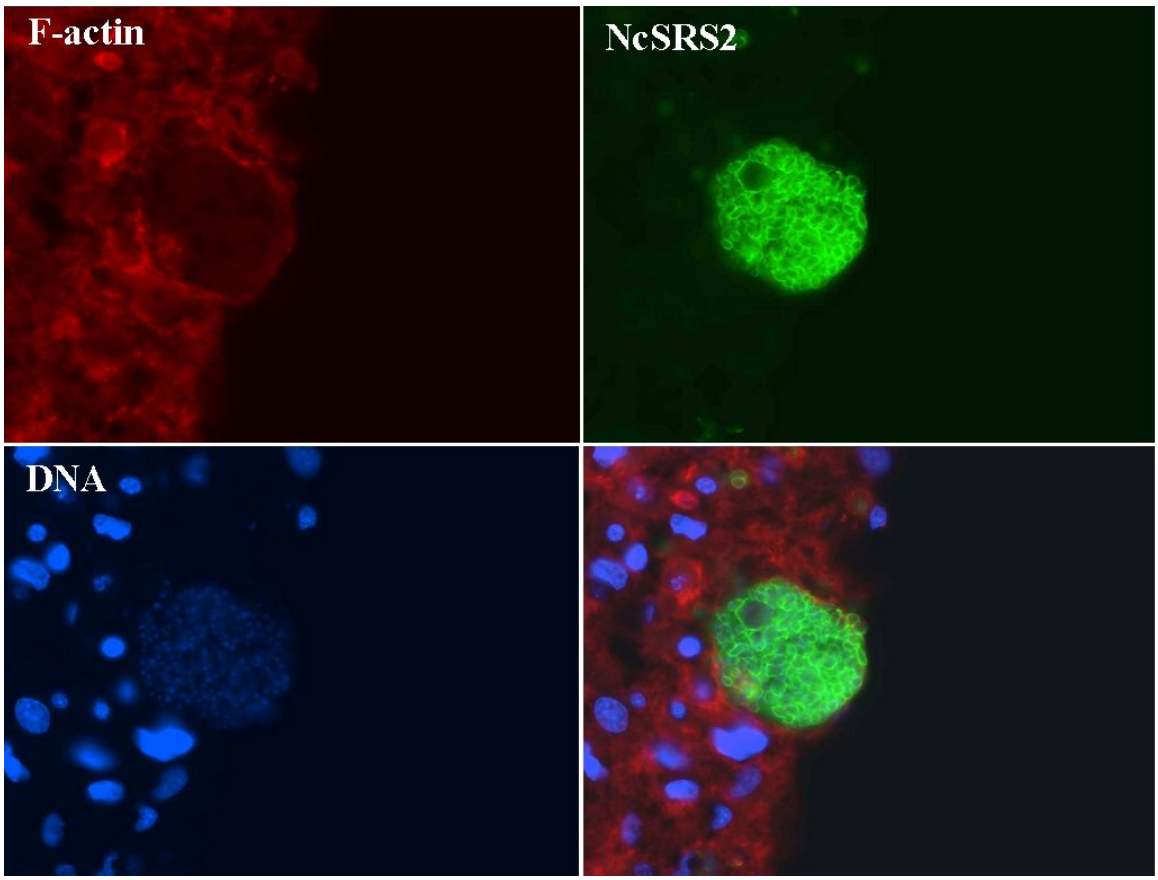

Figure 12: Actin microfilaments and *N. caninum* pseudocysts. Fluorescence staining of actin microfilaments using phalloidin-rhodamin (F-actin, red), corresponding staining for *N. caninum* tachyzoites using anti-NcSRS2 antibodies (green), DNA labelling (blue) and overlay. Note the close association and overcoating of pseudocysts with actin microfilament bundles.

The third class of cytoskeletal filaments, actin microfilaments, were visualised with phalloidin-TRITC labelling. While individual actin microfilaments were not easily discernable in uninfected areas of the tissue (data not shown), we identified a close association between actin microfilament bundles and the periphery of pseudocysts, with microfilaments forming an enveloping layer around the entire pseudocyst, largely colocalising with the actual pseudocyst membrane (Figure 12).

3.2.1.3 Modulation of Neospora caninum-infected organotypic cultures with IFN-γ

Infected slice cultures were maintained in the presence of 100 units of recombinant mouse IFN-γ for a time period of up to 5 days, with IFN-γ-treatment starting immediately after infection has taken place. The effect of IFN-γ-treatment with regard to parasite proliferation was comparatively assessed with untreated cultures using quantitative PCR. This assay allows the determination of infection intensities by using a dual fluorescent hybridization probe system and the LightCycler™ Instrument for online detection of amplified DNA. Quantitative PCR (Müller *et al*., 2002) revealed that after a cultivation period of 5 days the number of tachyzoites was two-fold lower in IFN-γ-treated cultures compared to untreated cultures (Figure 13A). However, during the first 3 days of culture, proliferation was not affected by the presence of IFN-γ, and the inhibitory effect became manifest only from day 4 onwards. In organotypic cultures treated with IFN-γ, the size of the few pseudocysts which were detected was consistently small, containing only few tachyzoites, even after 5 days of culture (Figure 13B). Larger pseudocysts were never observed. More frequently, parasitophorous vacuoles, containing remnants of tachyzoites which apparently became non-viable after they had entered their host cells, could be seen (Figure 13C).

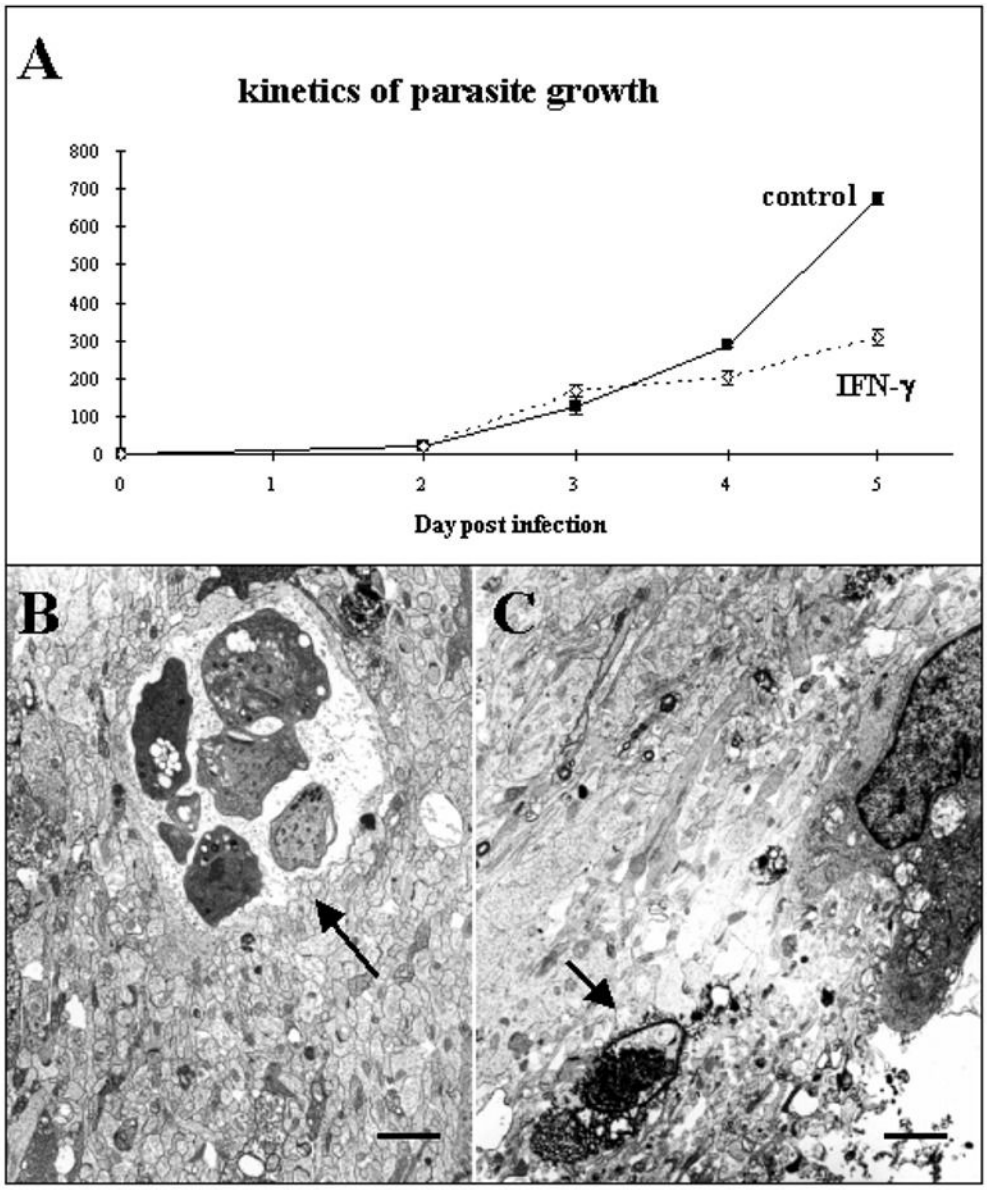

Figure 13: Effect of IFN-γ on parasite proliferation in organotypic cultures from rat CNS. (A) Quantitative PCR, showing the number of *N. caninum* parasites detected during the PCR reaction plotted against days post infection. Note the diminished proliferation of tachyzoites from day 3 onwards. (B) Pseudocyst of IFN-γ-treated tissue at day 5 following infection. Note that the number of tachyzoites is low, bar = 800 nm. (C) Non-viable necrotic tachyzoite located intracellularly within a parasitophorous vacuole, bar = 630 nm.

3.2.2 Discussion

Neosporosis is generally a mild, asymptomatic disease that begins with an acute phase in which tachyzoites invade their host cells, divide rapidly, form pseudocysts which rupture, and relased tachyzoites infect neighbouring cells. This process triggers an efficient immune response in the host, and is followed by the formation of intracellular tissue cysts containing the bradyzoite stage of the parasite, surrounded by a cyst wall, eventually leading to chronic infection. The current evidence suggests that during chronic infection *N. caninum* is sequestered into immuno-privileged sites such as the CNS. There, tissue cysts harbouring the bradyzoite stage of the parasite may be the source of successive waves of parasitaemia which, for instance during pregnancy, are responsible for foetal infection. The invasion of the CNS by *N. caninum* tachyzoites, and the subsequent damage to it, eventually gives rise to frequent abortion in cattle or causes neurological manifestations as they have been observed in infected calves and dogs (Dubey and Lindsay, 1996; Hemphill, 1999). Thus, an in vitro model which can be used to study the proliferation, ultrastructural characteristics, development, and the interactions of *N. caninum* within the context of a three-dimensionally organised neuronal tissue, and which at the same time can be modulated and influenced under controlled conditions, is needed to gain more information on the cerebral phase of Neosporosis. Organotypic cultures of rat CNS tissue were therefore infected with cell culture derived parasites in order to assess the suitability of this system.

In the initial phase of development following infection with 2 x 10^6 parasites, meaning during the first 48h post infection, invasion of peripheral host cells was evident, but proliferation of tachyzoites was not notably observed, neither by immunofluorescence (see Figure 9), nor by quantitative PCR (see Figure 13), indicating that the parasites had to adjust to the altered culture conditions (such as changes in culture medium and different host cell types). During later timepoints (days 3-5), proliferation of tachyzoites took place rapidly, resulting in the transient formation of pseudocysts with ultrastructural characteristics similar to pseudocysts observed in natural infections (Dubey and Lindsay, 1996).

Collapse of these pseudocysts and host cell lysis was associated with progressive invasion of the entire tissue slices. Consequently, this resulted in almost complete breakdown of the structural integrity of the tissue, with fatal consequences also for the parasites by days 5-7.

Immunofluorescence staining, employing a GFAP-specific mAb which serves as a marker for astrocytes, was carried out. It has been shown earlier that the predominant population within these organotypic culture slices were in fact astrocytes (Stoppini *et al*., 1991). First, we found that the formation of pseudocysts was accompanied by profound changes in GFAP-filament distribution, in that glial filaments were observed in close juxtaposition to the cytoplasmic side of the pseudocyst membrane (see Figure 11). This was true for virtually all pseudocysts observed, thus pseudocyst formation (and thus parasite proliferation) took place predominantly in astrocytes.

Our observations concerning the close interaction of intermediate filaments with pseudocysts are in agreement with previous studies, which reported the association and overcoating of parasitophorous vacuoles with vimentin-type intermediate filaments in Vero cells infected with *T. gondii* tachyzoites (Halonen and Weidner, 1994). Halonen *et al*. (1998) had also shown that host cell intermediate filaments were associated with the cytoplasmic side of *T. gondii* tissue cyst (harbouring bradyzoites) within in vitro cultured murine astrocytes. Layers of glial filaments had also been observed around young *T. gondii* tissue cysts developing in astrocytes of human brain (Powell *et al*., 1978). However, our study suggests that an additional class of cytoskeletal filaments is in close contact with the pseudocyst membrane. Actin microfilaments, visualised by phalloidin-TRITC staining, were consistently found closely associated with the pseudocysts periphery (see Figure 12). These findings are suggestive, but by no means a definitive proof, for a physical link between actin filaments and the pseudocyst membrane. Whether these microfilaments at the pseudocyst periphery originate from the parasite or from the host is not yet clear, but the lack of staining in the cyst interior suggests that they originate from the host cells. It is also not clear whether these microfilament bundles specifically colocalise with the pseudocyst periphery, or whether they are just simply forced towards the

host cell periphery by the growing pseudocyst. In contrast to Sims *et al*. (1988), which earlier described a microtubular-intermediate filament layer present on the cytoplasmic side of mature *Toxoplasma* cysts in neurons in murine brain, we could not detect any evidence for microtubule-based filamentous overcoating around pseudocyts in *N. caninum* infected organotypic slice cultures (data not shown). The functional significance of this microfilament- and GFAP-filament-overcoating of *N. caninum* pseudocysts is not understood, but this type of cytoskeletal alteration could be an important factor mediating physical stability of pseudocysts, and could also account for the exclusion of host cell organelles from the vacuoles. For instance, by overcoating with host cell cytoskeletal elements lysosomes could be prevented from fusing with the parasitophorous vacuole membrane (Halonen *et al*., 1998).

Astrocytes appear to be efficiently invaded within these organotypic cultures. Astrocytes play a central role in brain energy metabolism, and they contain the principal stock of glycogen of the brain (Swanson and Choi, 1993; Swanson, 1992). Therefore, invasion of astrocytes could be of advantage for *N. caninum* with regard to its energy metabolism. In addition, IFN-γ inhibits *T. gondii* tachyzoite proliferation in astrocytes via mechanisms independent of nitric oxide, tryptophan starvation or iron deprivation (Halonen *et al*., 1998; Halonen and Weiss, 2000). Also for *T. gondii*, astrocytes have been shown to support tachyzoite-to-bradyzoite conversion, and thus tissue cyst formation, upon stimulation with IFN-γ and TNF-α (Fagard *et al*., 1999). Thus, invasion of astrocytes enhances the parasite's prospects for intracellular survival in case of an inflammatory response on part of the host. Another argument which is in favour of preferential invasion of astrocytes is the fact that it has been shown earlier that in vitro cultured rat hippocampus neurons were about 20 times less efficiently infected by *T. gondii* tachyzoites compared to astrocytes (Creuzet *et al*., 1998). This was attributed to the small size of neurons, the possible absence of cell surface receptors required for entry, the mitotic status of the host cell, and / or the release of cytokines (Fagard *et al*., 1999).

Since IFN-γ is a key cytokine in the host immune response to *N. caninum* infection (Kahn *et al*., 1997), and for *T. gondii* has shown to trigger the

conversion from tachyzoites into bradyzoites (Fagard *et al*., 1999), we investigated the effects of IFN-γ-treatment on the proliferation and development of *N. caninum* within these organotypic cultures. As evidenced by quantitative PCR (see Figure 13), parasites proliferated in both, IFN-γ-treated and untreated cultures, with equal efficiency until day 3 post infection. Thereafter, IFN-γ exhibited a profound inhibitory effect with regard to the proliferation of tachyzoites. This diminished proliferation was also noted by immunofluorescence (data not shown), and by TEM. At day 5, only small pseudocysts containing few tachyzoites were visible in IFN-γ-treated infected cultures, and many necrotic parasites were found which had invaded their host cell but were apparently killed intracellularly (see Figure 13B, C). The mechanisms which resulted in this proliferation inhibitory effect or in the intracellular killing of parasites are unknown and will be investigated in the future using the organotypic tissue culture model for *N. caninum* infection.

3.3 Exogenous nitric oxide triggers Neospora caninum tachyzoite-to-bradyzoite stage conversion in keratinocytes

3.3.1 Results

3.3.1.1 Exogenous NO inhibits parasite proliferation in murine epidermal keratinocytes

To investigate whether the addition of exogenous NO to cell cultures induces stage conversion from tachyzoites to bradyzoites, and thus slows down the proliferation *of N. caninum* in vitro, either Vero cells, HFF, HT4 cells or murine epidermal keratinocytes were infected with *N. caninum* tachyzoites of the Nc-1-, NcSwB1-, and the Nc-Liverpool isolate, respectively. The NO donor sodium nitroprusside was added to the culture medium at a final concentration of 70 µM at the time of infection. Preliminary results showed that all host cell types were readily infected with all *Neospora* isolates, but murine epidermal keratinocytes were the only host cell type which remained largely intact following the SNP-treatment for 4 days, while Vero cells, HFF and HT4 cells exhibited severe signs of structural disintegration, resulting in cell death (data not shown). Thus, murine epidermal keratinocytes were used in all subsequent experiments.

The effect of SNP-treatment of infected murine epidermal keratinocytes on the proliferation of Nc-Liverpool within the time span of 4 days was measured by quantitative *Neospora*-specific real-time PCR employing the LightCycler™ Instrument. As shown in Figure 14, during the first 24h of culture, parasite proliferation was not notably affected by the presence of sodium nitroprusside. From day 2 onwards, an inhibitory effect on parasite proliferation became evident in the treated cultures compared to the untreated cultures. At day 3, SNP had severely inhibited parasite proliferation, while in untreated keratinocyte cultures *N. caninum* tachyzoites divided normally. At day 4, the number of parasites was approximately 5 times higher in untreated monolayers compared to SNP-treated cells.

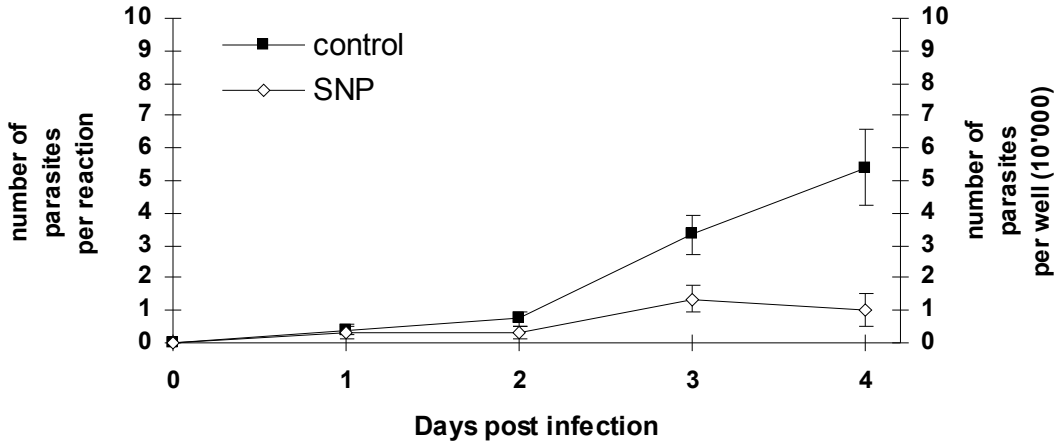

Figure 14: Proliferation of *Neospora caninum* in murine epidermal keratinocytes as assessed by quantitative *Neospora*-specific real-time PCR. Confluent keratinocyte monolayers were inoculated with 10^5 *N. caninum* tachyzoites, and were cultured in the presence (SNP) or absence (control) of 70 µM sodium nitroprusside (SNP) for 1-4 days, respectively. Note the distinctly inhibited parasite proliferation in sodium nitroprusside-treated cultures.

3.3.1.2 Exogenous NO induces the expression of bradyzoite-specific markers in Neospora caninum infected keratinocytes

After different timepoints of SNP-treatment of murine epidermal keratinocytes infected with the Nc-Liverpool isolate, the expression of the stage specific marker BAG1 was analysed by immunofluorescence microscopy, and respective results are shown in Figure 15 and Figure 16. No BAG1-expression could be detected prior to day 3 (data not shown), thus day 4 p.i. was chosen as the first timepoint of analysis. Expression of BAG1 was quantified by determining the percentage of BAG1-positive parasitophorous vacuoles in 10 randomly chosen microscopic fields. After 4 days, 35% of all vacuoles were found to contain BAG1-positive parasites, and after 8 days of culture, 60% exhibited BAG1-expression (Figure 15). Similar experiments were performed using Nc-1 and NcSwB1 isolates, however, for these two isolates the maximum percentage of BAG1-positive parasitophorous vacuoles after 8 days of SNP-treatment was consistently

between 1 and 3% only (data not shown). Surprisingly, infection of murine epidermal keratinocytes with *T. gondii* RH and *T. gondii* ME-49 and cultivation in the presence of SNP did neither result in markedly reduced proliferation nor in expression of BAG1 in both *Toxoplasma* strains (data not shown).

In most BAG1-positive parasitophorous vacuoles in Nc-Liverpool infected keratinocytes, all parasites within a given vacuole reacted with BAG1. However, occasionally, parasitophorous vacuoles were observed which contained both, BAG1-positive and BAG1-negative parasites (Figure 16A-C). Although it was possible that within a single host cell more than one parasitophorous vacuole was present, the vacuoles within this single host cell were always entirely BAG1-positive or negative (data not shown). BAG1-positive parasitophorous vacuoles were generally smaller and contained less parasites than BAG1 negative ones. This became more evident after 8 days of in vitro culture (Figure 16D-F). Also after 8 days, those parasitophorous vacuoles expressing BAG1 showed a strongly diminished expression of the tachyzoite marker antigen NcSAG1 (Figure 16D-F). In the untreated control cultures, consistently less than 5% of the parasitophorous vacuoles contained BAG1-positive parasites after 4 days, and after 8 days, large portions of the monolayer were destroyed due to extensive tachyzoite proliferation (data not shwon).

The mAbCC2 is directed against a *T. gondii* cyst wall antigen (Gross *et al*., 1995), and we had found earlier that this mAb crossreacts with the cyst wall of *N. caninum* tissue cysts in the CNS of experimentally infected mice (Keller *et al*., 2002). The expression and distribution of the *Neospora* antigen crossreacting with mAbCC2 (which we named NcCC2) was also analysed by immunofluorescence after 4 and 8 days of culture in the presence of SNP (Figure 17). After 4 days of SNP-treatment of infected keratinocyte monolayers, a majority of Nc-Liverpool containing parasitophorous vacuoles (over 80%) exhibited either only very little expression of this antigen, or NcCC2 was found to be localised in the lumen of the parasitophorous vacuoles (Figure 17A). Only a small fraction of all vacuoles (< 2%) exhibited staining at the vacuolar periphery (data not shown). The situation was different after 8 days of SNP-treatment (Figure 17B-D), with a much larger portion of parasitophorous vacuoles

exhibiting distinct peripheral staining with the mAbCC2. Quantification by counting 10 randomly chosen microscopic fields showed that after 8 days of SNP-treatment, 85% of all parasitophorous vacuoles tested positive for the mAbCC2, with 60% of vacuoles exhibiting peripheral labelling, and 25% showing intravacuolar staining (Figure 18). In untreated cultures, mAbCC2-immunoreactive vacuoles were found in approximately 10% of all parasitophorous vacuoles, however, immunolabelling was never associated with the periphery of the vacuoles (not shown). In SNP-treated cultures, peripheral, thus cyst wall-associated staining was generally found in small parasitophorous vacuoles, containing up to seven parasites, and intravacuolar staining was observed in larger parasitophorous vacuoles (Figure 17A, B). Often, vacuoles containing only one or two parasites were also found to exhibit peripheral NcCC2 expression (Figure 17B).

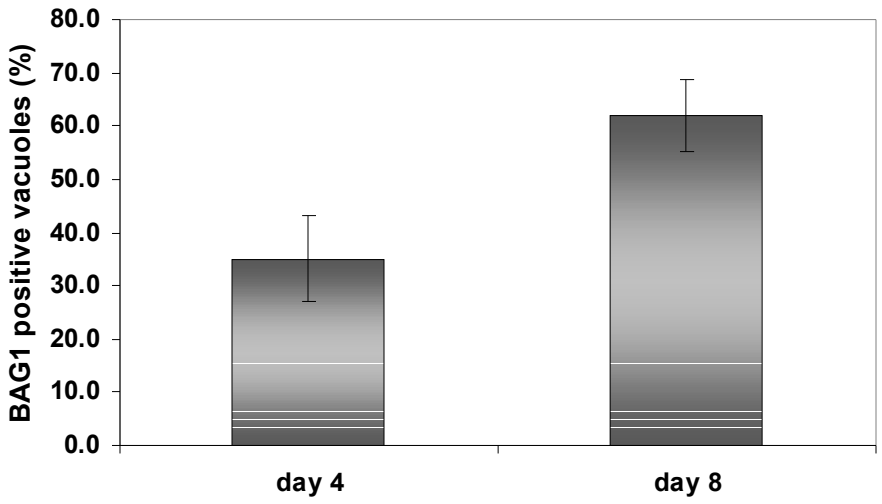

Figure 15: Quantification of bradyzoite antigen 1-expression as assessed by immunofluorescence staining. Monolayers were infected with *N. caninum* tachyzoites and cultured in the presence of sodium nitroprusside, and fixed and processed for bradyzoite antigen-immunofluorescence after 4 and 8 days of culture. The percentage of bradyzoite antigen 1-expressing parasitophorous vacuoles was determined by counting bradyzoite antigen 1-positive vacuoles in 10 randomly chosen fields in the fluorescence microscopy. Note the distinct increase in bradyzoite antigen 1-positive parasitophorous vacuoles at 8 days.

When similar experiments were performed with the NcSwB1 isolate, less than 5% of the parasitophorous vacuoles exhibited staining of the cyst wall following SNP-treatment, and most of the vacuoles showed intravacuolar labelling or were mAbCC2 negative (data not shown). In virtually all cases, peripheral mAbCC2-staining in parasitophorous vacuoles containing Nc-Liverpool cultured in SNP-treated murine epidermal keratinocytes was accompanied by the expression of

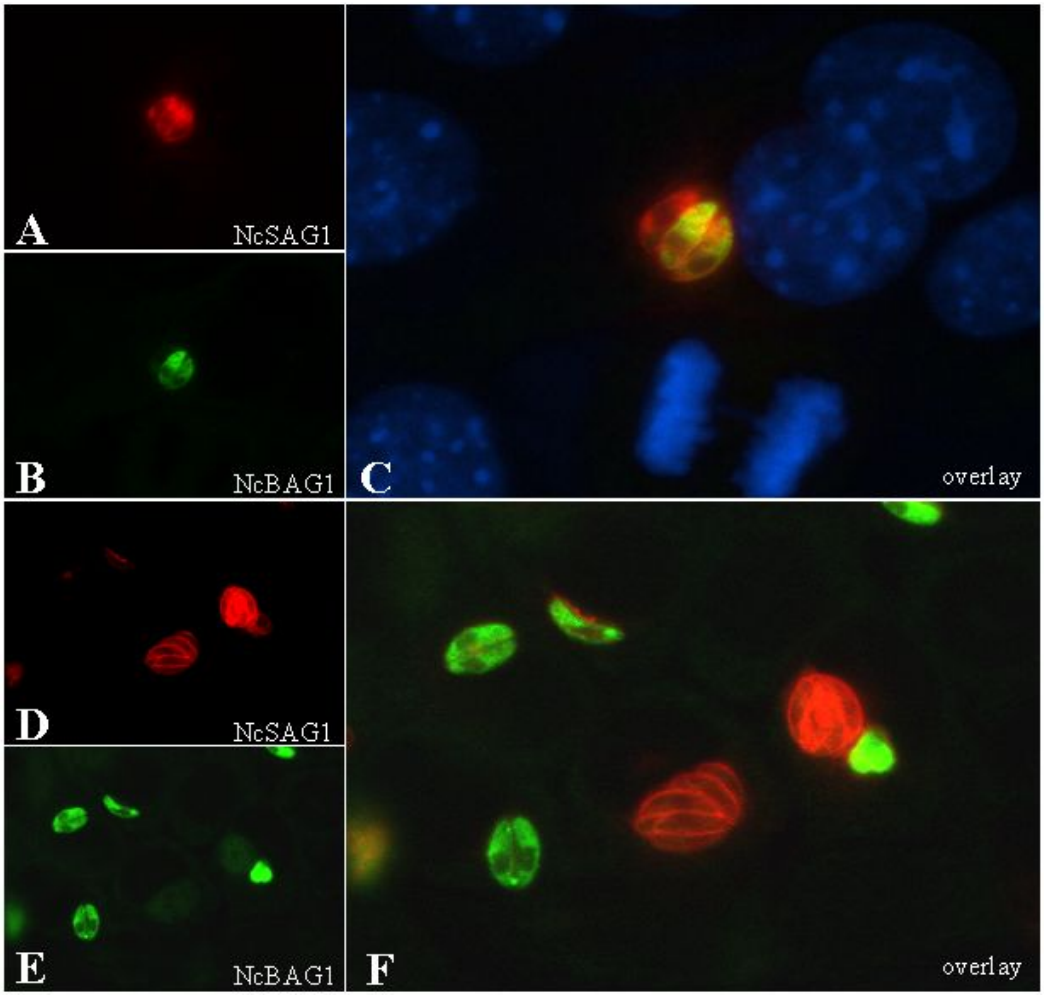

Figure 16: Bradyzoite antigen 1/NcSAG1 double immunofluorescence performed on *Neospora caninum*-infected murine epidermal keratinocytes treated with sodium nitroprusside for 4 days (A-C) and 8 days (D-F), respectively. The overlay in (C) demonstrates the occurrence of asynchronous bradyzoite antigen1-expression within a single parasitophorous vacuole. (D-F) Bradyzoite antigen 1-expression is accompanied by strongly reduced expression of the tachyzoite marker NcSAG1 after 8 days of sodium nitroprusside-treatment.

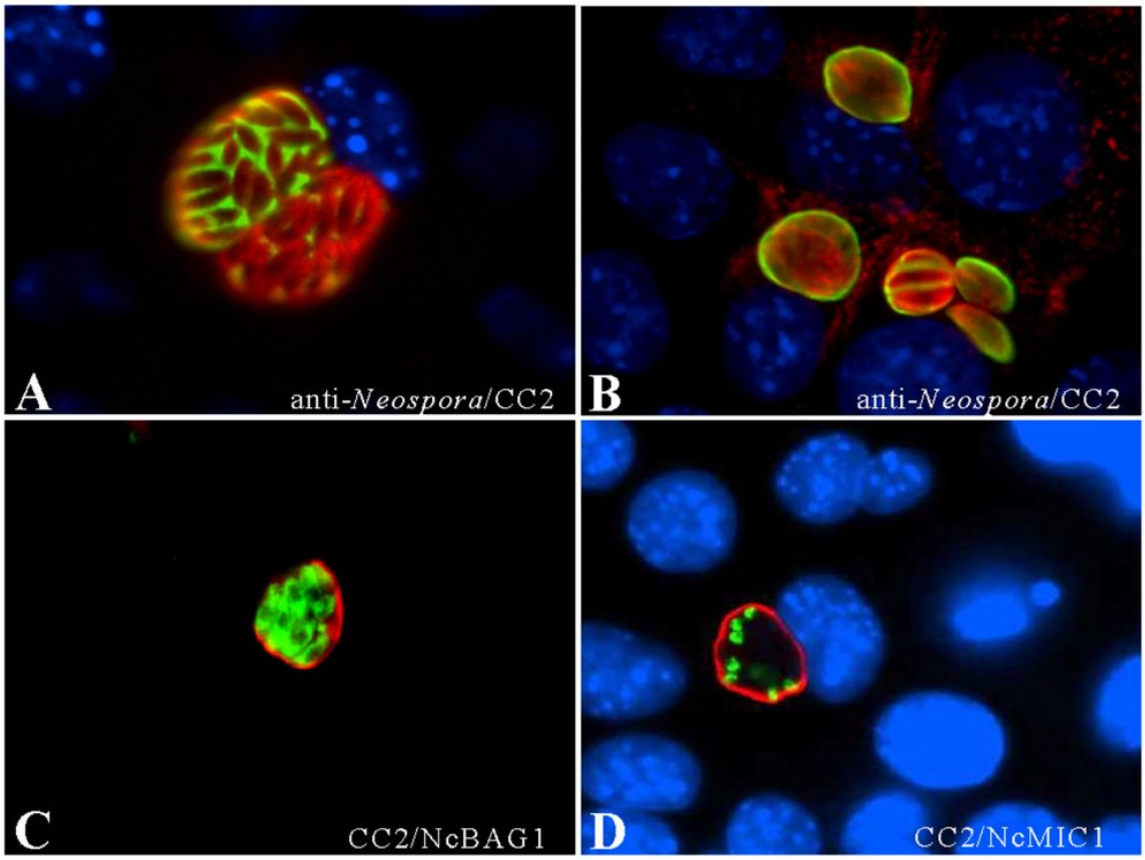

Figure 17: Expression of NcCC2 cyst wall antigen after 4 days (A) and 8 days (B-D) of sodium nitroprusside-treatment. (A, B) mAbCC2/anti-*Neospora* double immunofluorescence performed after 4 days (A) and 8 days (B) of sodium nitroprusside-treatment. Note the intravacuolar labelling with mAbCC2 (green) after 4 days (A), and the distinct staining of the periphery after 8 days of sodium nitroprusside-treatment (B). (C, D) Indicate that all parasitophorous vacuoles expressing peripheral NcCC2 (red) also express bradyzoite antigen 1 (C) as well as the microneme antigen NcMIC1 (D).

BAG1 (Figure 17C), whereas parasitophorous vacuoles that exhibited intravacuolar mAbCC2 labelling, did not express the BAG1 antigen (data not shown). The microneme protein NcMIC1 (Keller *et al.*, 2002) could be detected at the apical end of parasites undergoing SNP-treatment for 8 days (Figure 17D). Staining of parasitophorous vacuoles with the lectin Dolichos biflorans agglutinin (DBA) was also found to occur exclusively in vacuoles containing BAG1-positive parasites (Figure 19A-C), albeit only in about 10% of BAG1-positive vacuoles. We found that, similar to mAbCC2, after 8 days of SNP-treatment, DBA labelled exclusively the vacuole periphery, and strictly colocalised with mAbCC2 staining (Figure 19D-F).

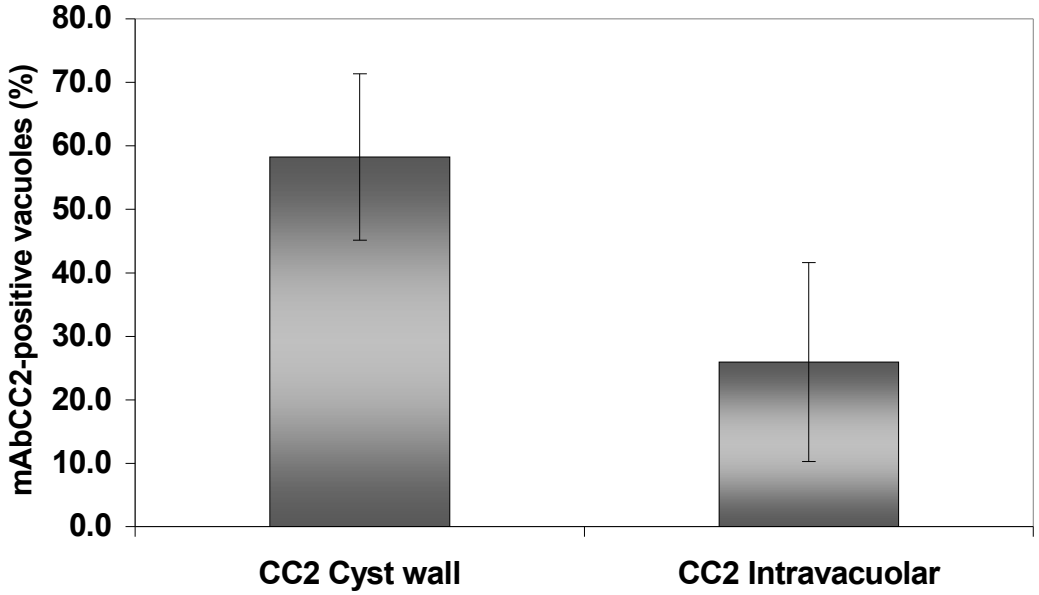

Figure 18: Quantification of intravacuolar and peripheral labelling of parasitophorous vacuoles with mAbCC2 in *Neospora caninum*-infected murine epidermal keratinocytes treated with 70 µM sodium nitroprusside for 8 days. Note that almost 60% of parasitophorous vacuoles exhibit staining at the periphery of the parasitophorous vacuoles.

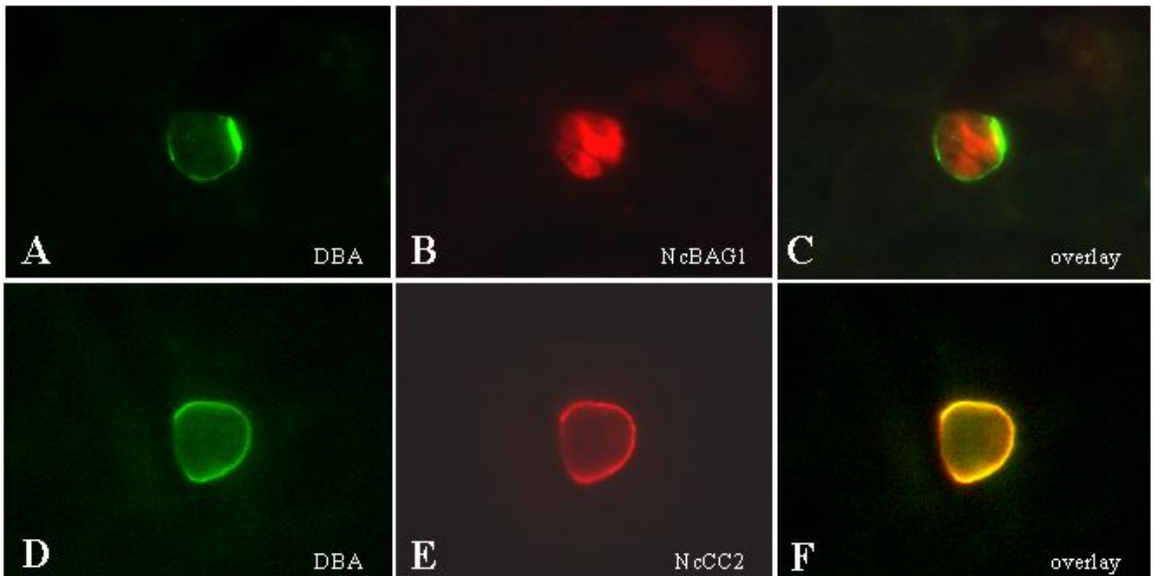

Figure 19: Expression of Dolichos biflorans agglutinin-binding sites in the periphery of parasitophorous vacuoles of *Neospora caninum* infected keratinocytes after 8 days of sodium nitroprusside-treatment. Note that all Dolichos biflorans agglutinin-positive vacuoles also express bradyzoite antigen 1 (A-C), and all Dolichos biflorans agglutinin colocalises with mAbCC2 labelling (D-F).

3.3.1.3 Treatment of Neospora caninum infected murine epidermal keratinocytes with sodium nitroprusside induces the formation of a cyst wall-like structure

Nc-Liverpool infected and SNP-treated murine epidermal keratinocytes were inspected by TEM (Figure 20, Figure 21). Parasitophorous vacuoles containing one to five intracellular parasites were found, the majority of which contained electron dense accumulations of granular material located at their periphery, forming a cyst wall-like structure (Figure 20A, Figure 21A). The parasitophorous vacuole membrane (PVM) was always located distally to this cyst wall (Figure 20C, D, Figure 21C). In contrast, the parasitophorous vacuoles of *N. caninum* tachyzoites generated in these cells in the absence of SNP lacked this peripheral electron dense layer, and the vacuole was always delineated by the parasitophorous vacuole membrane only (Figure 20B). The irregularly shaped cyst wall-like structures generated in SNP-treated keratinocytes surrounded the entire lumen of the parasitophorous vacuole. They were composed of condensed electron dense granules, few vesicles, and variied considerably in thickness (0.1-1 µm). The matrix of these in vitro generated tissue cysts were filled with similar, but less condensed granular material that also contained vesiculated structures and flat membranous segments (Figure 21B, C). Bradyzoites found within these cysts contained electron-dense rhoptries, many micronemes predominantly located at the anterior end, and large and small dense granules. Amylopectin granules were also found (Figure 20, Figure 21). In addition, vesiculated organelles filled with irregularly arranged membrane segments were observed (Figure 20A, Figure 21C). Taken together, TEM strongly suggested that in vitro *N. caninum* tissue cyst formation has been initiated in these SNP-treated murine epidermal keratinocytes.

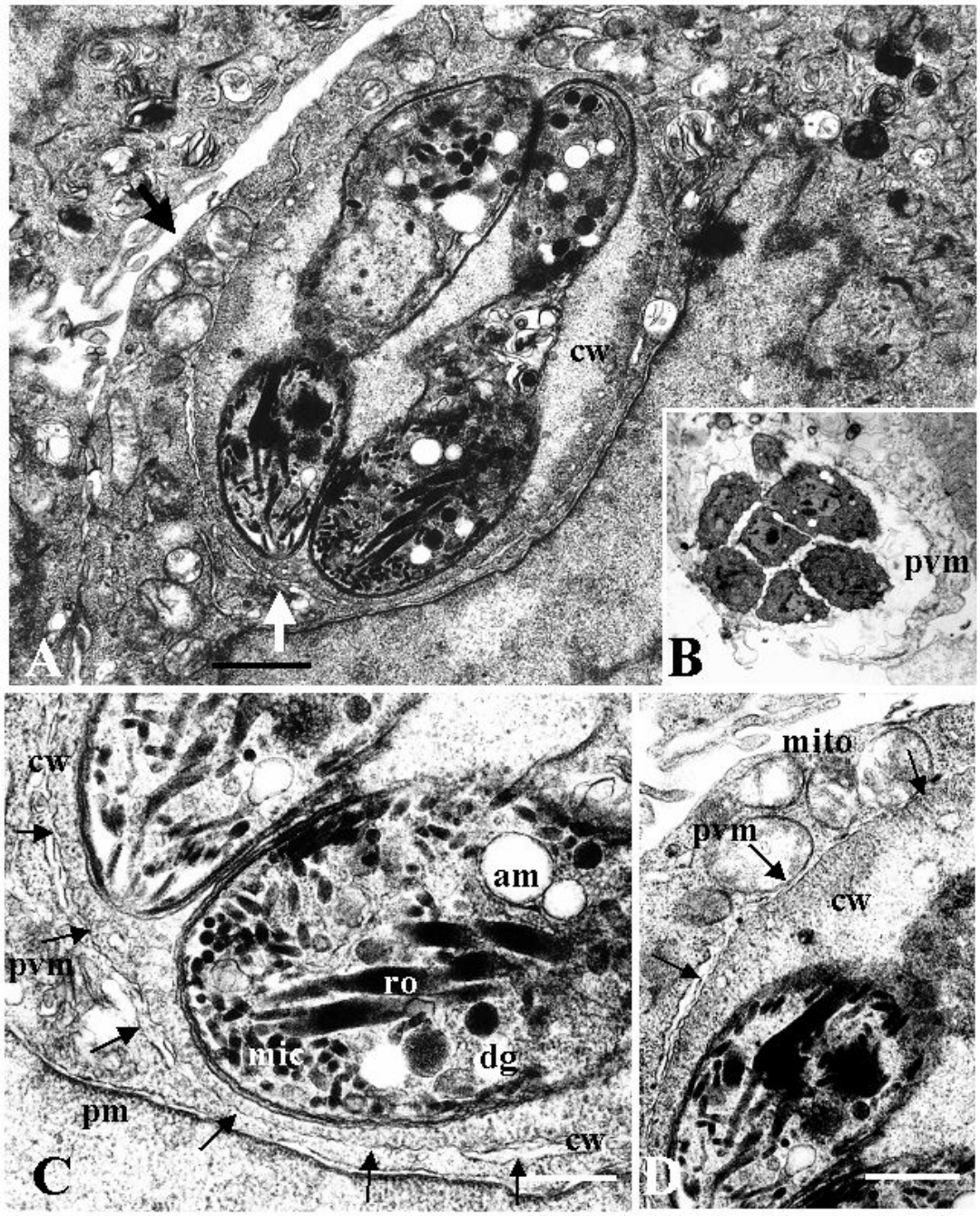

Figure 20: Transmission electron microscopy of a *Neospora caninum* tissue cyst obtained after 8 days of sodium nitroprusside-treatment (A, C, D), and a parasitophorous vacuole containing *Neospora caninum* tachyzoites from untreated cultures (B). In (A) a tissue cyst is shown, with peripherally accumulated electron dense material forming a cyst wall. (B) Shows, as a comparison, a parasitophorous vacuole in untreated cells which is delineated only by a parasitophorous vacuole membrane (pvm). (C) and (D) are higher magnification views of the areas in (A) pointed out with the white bold arrow (for C) and the black bold arrow (for D). Micronemes (mic), rhoptries (ro), dense granules (dg) and amylopectin granules (am) are visible. The vacuolar membrane (pvm) is marked with thin arrows, and is localised distally to the cyst wall (cw). Tissue cysts are closely associated with host cell mitochondria (mito). pm = host cell plasma membrane. Bar in (A) = 0.9 µm, in (B) = 2.3 µm, in (C) = 0.4 µm, in (D) = 0.6 µm.

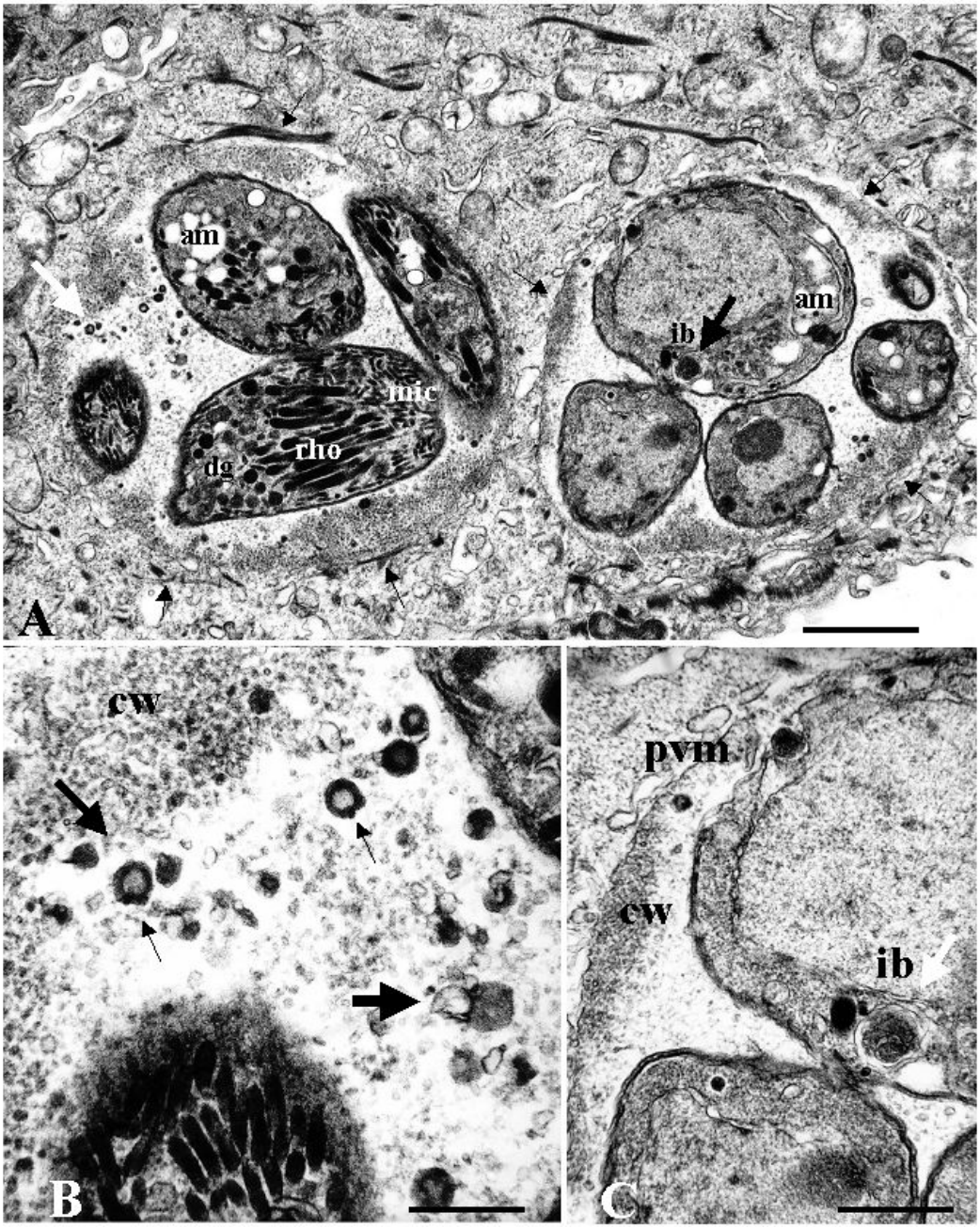

Figure 21: A murine epidermal keratinocyte containing two distinct *Neospora caninum* tissue cysts after 8 days of sodium nitroprusside-treatment. (A) Shows an overview. The periphery of the vacuoles is indicated with small arrows, and the thickness of the cyst wall varies within a cyst, and between cysts. Micronemes (mic), rhoptries (rho), dense granules (dg) and amylopectin granules (am) are visible. (B) and (C) are higher magnification views onto the areas pointed out with the white bold arrow (for B) and the black bold arrow (for C). Note that the matrix of the parasitophorous vacuole contains granules of similar ultrastructure, but in a less condensed form, compared to the granular material building up the cyst wall (cw). Also visible within the matrix are small vesiculated lipid particles (small arrows in B), and flat lipid-like membranous segments (large horizontal arrow). Note in (C) the presence of vesiculated, inclusion body-like organelles (ib), filled with irregularly arranged membrane segments. Bar in (A) = 0.75 µm, in (B) = 0.2 µm, in (C) = 0.35 µm.

3.3.2 Discussion

In this study, we report on a novel cell culture system which allows an efficient induction of *N. caninum* tachyzoite-to-bradyzoite stage conversion. This cell culture system is based on the Nc-Liverpool isolate (Barber *et al*., 1995), the use of murine epidermal keratinocytes (Caldelari *et al*., 2000) as host cells, and continuous treatment of infected cells with 70 µM SNP. Under these conditions, we monitored parasite proliferation by quantitative PCR, studied the induction of bradyzoites specific markers (BAG1, NcCC2, DBA) within infected monolayers, and we present electron microscopic evidence which strongly suggests that tissue cysts with a defined cyst wall are being formed in vitro under the culture conditions described herein.

Preliminary studies employing Vero cells, HFF and HT4 have demonstrated, that the number of parasites expressing the bradyzoite antigen BAG1 was relatively low under conditions where pH stress, treatment with tylosin, SNP-treatment or increased temperature stress were used. Besides, these treatments had a negative impact on the structural integrity of the host cells, finally resulting in the destruction of the cell monolayers after 4-6 days, and rendering these systems largely unsuitable for a longer culture period (data not shown). In contrast, we found that the primary cultures of murine epidermal keratinocytes used in this study are able to withstand the SNP-treatment for a period of at least 8 days, due to the strong adhesive properties of these epithelial cells to the substrate.

SNP releases NO that reacts with the iron sulphur centres of several proteins involved in the electron transport of the respiratory chain and with the haem iron of cytochrome oxidase. This results in a decrease of ATP formation and in a diminished binding of oxygen to cytochrome oxidase (Cooper, 1999). The adaptation of the parasites to a decreased energy production and to an anaerobic environment may trigger the differentiation process, and thus results in the formation of the slowly dividing bradyzoites which consume less energy. It was demonstrated for *T. gondii*, that stage conversion also occurred in host cells lacking mitochondrial functions, indicating, that it is the parasite mitochondrium

which mediates this effect (Bohne *et al.,* 1994), and most likely the same accounts for *N. caninum* in this culture system.

SNP-treatment strongly inhibited *N. caninum* proliferation, and induced the expression of BAG1 antigen from day 3 onwards, as demonstrated by immunofluorescence using a polyclonal antiserum directed against TgBAG1 (McAllister *et al*., 1996). By quantitative PCR, significantly decreased parasite growth in SNP-treated cultures was also observed on day 3 (see Figure 14) and thus inhibition of proliferation seems to be associated with BAG1-expression. This also indicates that reduced parasite replication is linked to stage conversion, and is confirmed by the fact that high levels of BAG1-expression were generally found in smaller vacuoles (see Figure 16). The findings, that NO-induced stress can also result in DNA damage and repair and will delay the entry of a cell into mitosis (Nasmyth, 1996), may be another explanation for the reduced rate of parasite replication after SNP-treatment.

In untreated infected murine epidermal keratinocytes, BAG1-expression occurred only in a very low number of parasites, indicating that spontaneous stage conversion in vitro is a rather rare event.

The percentage of BAG1-positive vacuoles steadily increased during the observed culture period of 8 days (see Figure 15). We also observed heterogenous parasite populations in some vacuoles, where all individuals reacted with the anti NcSAG1 antibody, but not all parasites reacted with anti-BAG1 antibody. Similar findings had been obtained earlier with *T. gondii* (Bohne *et al.,* 1993), suggesting, that conversion from tachyzoites to bradyzoites is an asynchronous process. However, the observation that after 8 days, most BAG1-positive parasites did not express the major tachyzoite surface antigen NcSAG1 anymore, suggested that a dramatic change in surface antigen pattern was taking place. Upon immunohistochemical staining of *N. caninum* tissue cysts generated in mice by the method of McGuire *et al.* (1997), it was found that NcSAG1 is stage-specifically expressed in tachyzoites (Fuchs *et al*., 1998). BAG1 in *T. gondii* was found to be homologous to small heat shock proteins of plants (Bohne *et al.,* 1995). The expression of heat shock proteins e.g. Hsp30/BAG1, is related to the stress induced by SNP and is associated with

bradyzoite differentiation. Thus, the BAG1-positive and NcSAG1-negative parasites found after 8 days of SNP-treatment can be designated as bradyzoites or at least bradyzoite-like organisms.

The mAbCC2 was originally generated against *T. gondii* tissue cysts, and was shown to recognise a 115 kDa cyst wall associated protein in *T. gondii* bradyzoites, and a 40 kDa dense granule protein in *T. gondii* tachyzoites which is secreted into the lumen of the parasitophorous vacuole (Gross *et al.,* 1995). The relationship between these two proteins in the two different stages has not been clarified to date, but it was shown by Sahm *et al.* (1997) that the mAbCC2 labelled the periphery of the parasitophorous vacuole of single *T. gondii* bradyzoites, suggesting, that some parasites already secrete this protein as soon as they enter the host cell (Sahm *et al.,* 1997). The same was found in our study for *N. caninum* (see Figure 17).

Similar to the situation in *T. gondii*, mAbCC2 labelling could be found at two distinct locations in SNP-treated *N. caninum* parasitophorous vacuoles. After eight days of treatment, the majority of parasitophorous vacuoles (60%) exhibited distinct peripheral, presumably cyst wall-associated staining, while only 25% of all parasitophorous vacuoles showed intravacuolar labelling, and 15% of parasitophorous vacuoles remained unlabelled. Apparently the parasites exhibiting no mAbCC2 reactivity and those which exhibited intravacuolar labelling were not affected by exogenous NO, since they occupied larger vacuoles (indicative of a faster replication rate), and they did not express detectable amounts of BAG1. In contrast, all parasites showing cyst wall-associated mAbCC2 labelling were found in smaller parasitophorous vacuoles (indicative of a slower replication rate), and all expressed BAG1 (see Figure 17). These findings also suggest that in *N. caninum* BAG1-expression is linked to the differentiation process from tachyzoites to cyst wall forming bradyzoites in vitro. It was previously shown in *T. gondii* that inhibition of heat shock protein synthesis by quercetin suppressed the induction of bradyzoite formation in vitro (Weiss *et al.,* 1998), implying an involvement of heat shock protein e.g. Hsp30/BAG1 in stage conversion. However, in another in vitro study, Bohne *et al.* (1998) revealed, that a BAG1-deficient mutant of *T. gondii* was still capable of stage

conversion and expression of bradyzoite antigens including the 115 kDa protein recognised by mAbCC2. Zhang *et al.* (1999) showed that disruption of the gene coding for BAG1 was associated with a change in cyst development in vivo, although cyst formation in vivo was not inhibited in this study either. Thus, the role of Hsp30/BAG1 in stage conversion remains to be elucidated.

The lectin DBA represents a marker which has been shown earlier by Weiss *et al*. (1999) to be indicative for the formation of *N. caninum* tissue cysts in vitro. We found that, after 8 days of SNP-treatment, DBA-binding could be detected in the periphery of only a limited number (10%) of all vacuoles, all of which expressed BAG1 as well. In no case, a BAG1-negative parasitophorous vacuole exhibited binding to DBA. Thus, DBA binding sites are most likely expressed at a relatively late stage of tissue cyst formation, compared to BAG1 and NcCC2. In addition, the binding site for DBA in SNP-treated *N. caninum* tissue cysts largely colocalised with mAbCC2 labelling, and this may indicate, that DBA could bind to the NcCC2 antigen itself, implying, that CC2 is probably a glycoprotein. These results are interesting in the light of the findings in *T. gondii*, which demonstrated the binding of DBA to CST1, a 116 kDa tissue cyst wall-associated antigen (Zhang *et al.,* 2001) which could well be identical to the mAbCC2-reactive 115 kDa antigen originally described by Gross *et al*. (1995).

Further information was obtained by TEM (see Figure 20 and Figure 21). We found that the majority of intracellular compartments occupied by *Neospora* parasites exhibited features, which indicate that parasites are undergoing bradyzoite stage conversion. In addition, our observations suggest, that the formation of a tissue cyst wall takes place in vitro. However, at present we do not know how mature and biologically functional these in vitro generated tissue cysts and bradyzoites really are. For instance, the microneme protein NcMIC1, previously shown to be not expressed in mature tissue cysts of mouse brain tissue (Keller *et al*., 2002) is still expressed in these in vitro generated tissue cysts despite of clear peripheral mAbCC2 labelling (see Figure 17). In addition, the fact that only a fraction of BAG1-positive parasitophorous vacuoles also exhibited peripheral DBA staining, indicates that many of these in vitro generated cysts are not yet fully mature. Besides this, TEM showed that in certain regions

the cyst wall was still very thin, suggesting, that cyst wall formation has not been accomplished yet and the development of fully mature cysts may requires a longer cultivation period than 8 days. This would be consistent with in vivo observations in mice, where *N. caninum* tissue cysts were not found earlier than 3 weeks after infection (Lindsay and Dubey, 1989). Current studies are directed towards the development of a longer term culture system based on the murine epidermal keratinocyte host cells used in this study.

The in vitro model for generating *N. caninum* tissue cysts presented herein only applies for the Nc-Liverpool isolate. Stage conversion is highly inefficient when other isolates such as Nc-1 or NcSwB1, the least virulent *N. caninum* isolate (Atkinson *et al.,* 1999) are used. This is in agreement with earlier findings and other in vitro systems for *N. caninum* bradyzoite culture (Weiss *et al*., 1999), and confirms the genetic and biological diversity among *N. caninum* isolates (Schock *et al*., 2001). It is somewhat surprising that this in vitro model was found to be completely inefficient also for bradyzoite formation of *T. gondii* where the less virulent strains such as ME-49 are more suitable for the in vitro production of tissue cysts than virulent ones such as RH (Mc Hugh *et al.,* 1994; Gross *et al.,* 1996; Boothroyd *et al.,* 1997). However, we found that SNP-treatment of murine epidermal keratinocytes infected with either *T. gondii* ME-49 or *T. gondii* RH did not induce BAG1-expression, nor peripheral mAbCC2 labelling, nor did it result in a marked reduction of *T. gondii* proliferation within these keratinocytes (data not shown). This could be explained by the observation, that prolonged passage of *T. gondii* or other apicomplexa in vitro can lead to a loss of ability to differentiate into other stages (Frenkel *et al.,* 1976). However, it could also indicate that *T. gondii* and *N. caninum* require intrinsically different stimuli for the induction of stage conversion and tachyzoite-to-bradyzoite differentiation. This could in turn have strong implications with regard to the epidemiology of these two closely related species.

3.4 In vitro induction of Neospora caninum bradyzoites in Vero cells reveals differential antigen expression, localisation, and host cell recognition of tachyzoites and bradyzoites

3.4.1 Results

3.4.1.1 Reduction of sodium nitroprusside concentration during in vitro culture of infected host cell monolayers influences parasite proliferation but not NcBAG1-expression

We have previously demonstrated that addition of 70 µM SNP to *N. caninum* infected murine epidermal keratinocyte host cells at the time point of infection, followed by culture of several days, had a profound inhibitory effect on parasite proliferation, and was leading to tachyzoite-to-bradyzoite stage conversion in about 60% of the parasitophorous vacuoles (Vonlaufen *et al*., 2002b). In this study, we tested a range of concentrations (up to 70 µM) of SNP, and assessed parasite proliferation by quantitative real-time PCR. Figure 22A shows results obtained with 70 µM and 17 µM SNP, as well as the growth curve of untreated cultures. After 2 days of SNP-treatment, no difference in parasite proliferation was visible in 17 µM SNP-treated cultures compared to the cultures treated with 70 µM SNP. However, after 4 and 8 days, 2.5-fold higher parasite numbers were detected in the 17 µM SNP-treated cultures compared to the ones grown in the presence of 70 µM SNP. Eight days treatment of parasites with 70 µM SNP resulted in a nearly completely abolished parasite proliferation, whereas in the 17 µM-treated cultures still a slight increase in parasite numbers was observed, but proliferation was still severely inhibited compared to untreated cultures (Figure 22A). In parallel, corresponding infected cultures were investigated by immunofluorescence. In terms of number of vacuoles exhibiting NcBAG1-expression, there was no difference observed between cultures treated with 17 or 70 µM SNP, with approximately 60% of parasitophorous vacuoles containing

NcBAG1-expressing parasites after 8 days of treatment. We also found that the absolute number of NcBAG1-positive, individual zoites increased, due to the

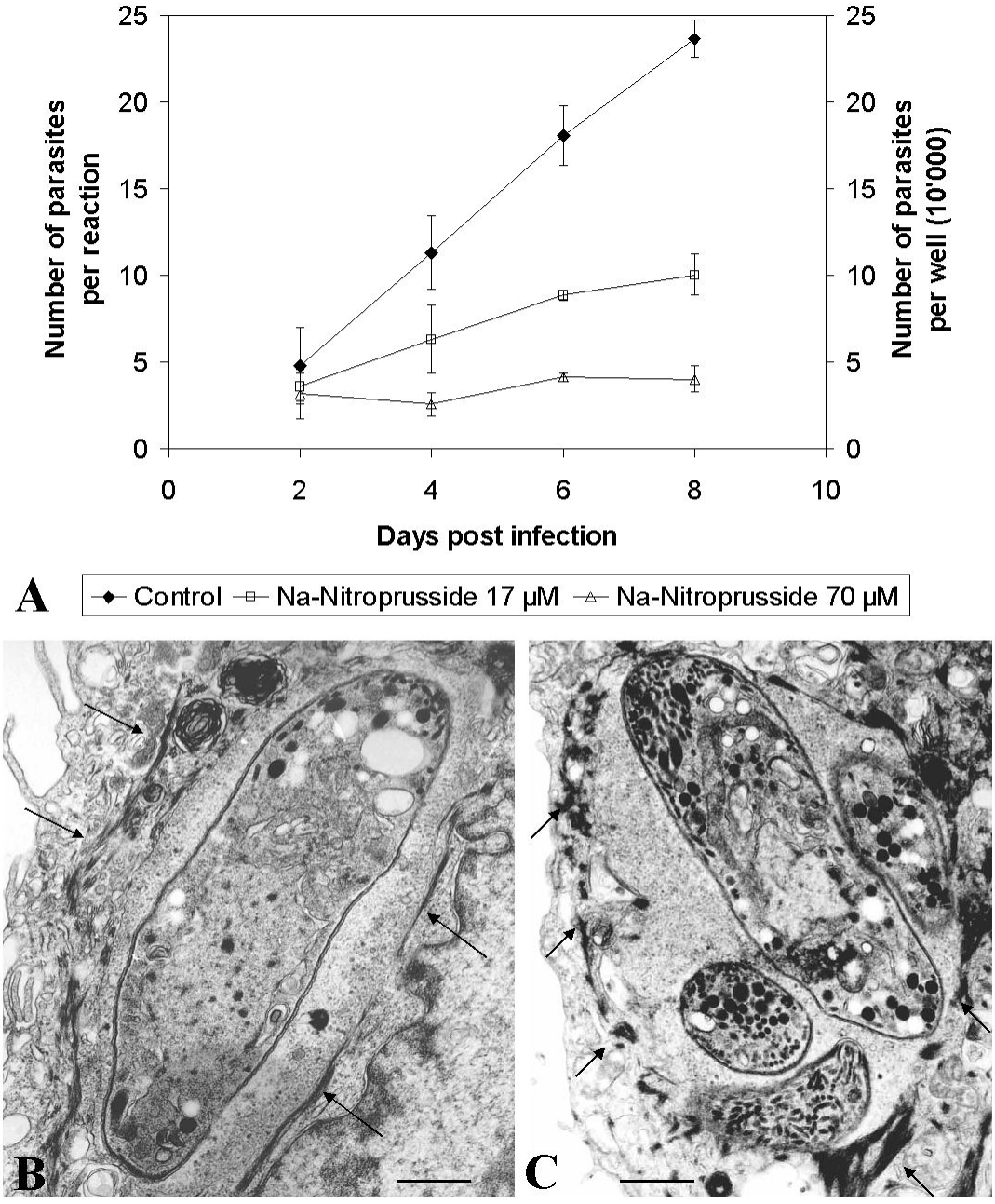

Figure 22: Proliferation and stage conversion of *N. caninum* in murine epidermal keratinocytes. (A) Illustrates parasite proliferation either in the absence, or in the presence of 17 and 70 µM sodium nitroprusside as assessed by quantitative real-time PCR. Data are displayed as means ± standard deviation. (B, C) TEM of *N. caninum* bradyzoites cultured in the presence of 70 µM (B) and 17 µM (C) sodium nitroprusside. Note the presence of keratin filament bundles surrounding the cysts (arrows). Bars in (B) = 0.40 µm, (C) 0.48 µm.

larger size of the vacuoles in those cultures treated with 17 µM SNP (data not shown).

Attempts to purify *N. caninum* out of SNP-treated murine epidermal keratinocyte monolayer cultures consistently failed. The reasons for this are seen by TEM in Figure 22B and C, which show that infected keratinocytes contain thick keratin-filament bundles which surround the parasitophorous vacuoles. This cytoskeletal cage rendered parasites inaccessible for any isolation or purification attempts.

3.4.1.2 Exogenous NO induces stage conversion of Nc-Liverpool in Vero cells

Preliminary studies showed that the application of 20-70 µM SNP to Nc-Liverpool-infected Vero cells resulted in detachment of the monolayer latest at day 4 of culture (data not shown). The findings on keratinocytes described above prompted us to decrease the SNP-concentration to a level, which could be sustained by Vero cell monolayers. Therefore, 17 µM SNP was added daily to infected Vero cells for a period of 8 days, and this did not significantly impair the integrity of the monolayer as assessed by light microscopy. Immunofluorescence labelling of infected and SNP-treated Vero cells revealed, that the expression of the bradyzoite-specific NcBAG1-antigen (Figure 23) as well as peripheral labelling of parasitophorous vacuoles with the mAbCC2 (Figure 23G-I) was as efficient as in keratinocytes. In addition, intracellular parasites expressing NcBAG1 consistently exhibited a reduced staining with antibodies directed against NcSAG1 and NcSRS2 (Figure 23A-F).

TEM (Figure 23J) demonstrated that *N. caninum* bradyzoites generated in 17 µM SNP-treated Vero cells were located in a parasitophorous vacuole, and were surrounded by a peripheral accumulation of electron-dense material which resembles a cyst wall. The vacuole was not notably surrounded by any cytoskeletal elements, but by mitochondria instead.

Compared to murine epidermal keratinocytes, where keratin filament bundles represented the major obstacle for the parasite purification, Nc-Liverpool parasites could be readily purified from the feeder cells (Figure 23K, L). The yield per T175 flask was typically around 3-5 x 10^6 parasites. Immunofluorescence labelling of purified parasites revealed that a major portion (50-80%) exhibited staining with anti-NcBAG1 antibodies, thus this purified population was heavily enriched in parasites undergoing stage conversion.

Purified *N. caninum* parasites were used to assess the differences in protein expression of tachyzoites (grown in the absence of SNP) and bradyzoites (grown in the presence of 17 µM SNP). Silver staining of SDS-PAGE separated extracts revealed partially distinct banding patterns for bradyzoite and tachyzoite extracts (Figure 24). Immunoblotting confirmed the down regulation of tachyzoite antigen expression, and more specifically of NcSAG1- and NcSRS2-expression in bradyzoites, and the induction of NcBAG1-expression (Figure 24).

3.4.1.3 Differential localisation of Neospora caninum dense granule antigens in tachyzoite and bradyzoite-infected Vero cells

Besides the reduced expression of the immunodominant surface antigens NcSAG1 and NcSRS2 in *N. caninum* parasites expressing NcBAG1 (Figure 23, Figure 24), we also investigated the expression and localisation of several dense granule proteins in in vitro generated *N. caninum* tachyzoites and bradyzoites (Figure 25). Tachyzoites and bradyzoites were cultured for 2 and 8 days respectively in Vero cell monolayers grown in tissue culture flasks. The staining pattern in tachyzoites for NcGRA1, NcGRA2 and NcGRA7 was virtually identical for all three antigens, as exemplified in Figure 25A-C for NcGRA1. Granular type immunolabelling was found predominantly within the parasite cytoplasm at the anterior and posterior end of the tachyzoites. In contrast, the in vitro generated *N. caninum* bradyzoites exhibited staining for NcGRA1 (Figure 25D-F) and NcGRA7

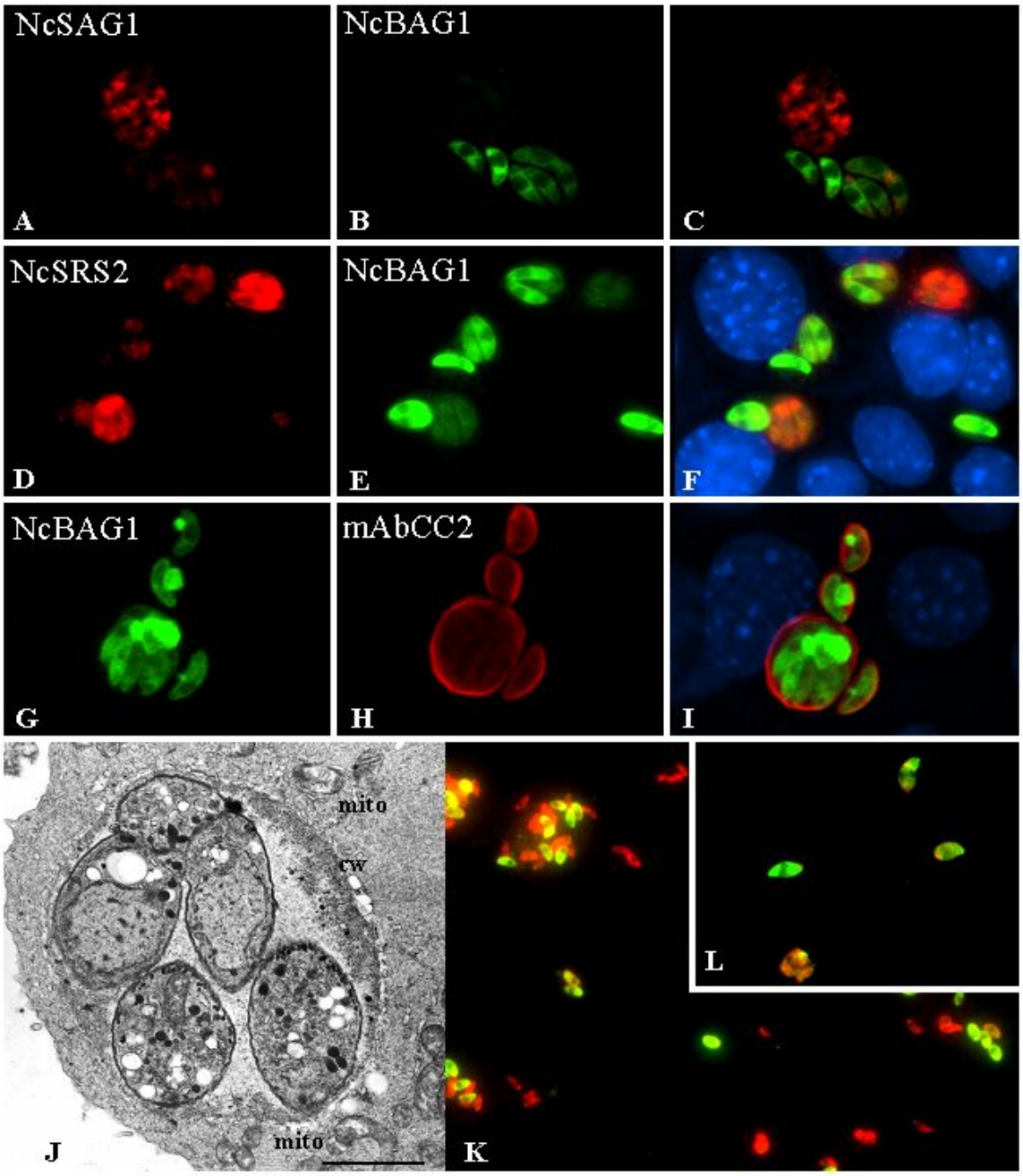

Figure 23: In vitro stage conversion in Vero cells. Vero cells were infected with Nc-Liverpool tachyzoites and treated with 17 µM sodium nitroprusside for 8 days. Note the down regulation of NcSAG1- (A-C) and NcSRS2-expression (D-F) in those parasites expressing NcBAG1. Parasites within vacuoles expressing NcBAG1 also exhibit peripheral labelling with mAbCC2 (G-I). (J) TEM of a tissue cyst with bradyzoites shows peripheral accumulation of electron-dense material reminiscent of a cyst wall (cw), and the presence of host cell mitochondria (mito) surrounding the cyst. Bar = 0.85 µm. (K, L) Purified parasites labelled with anti-BAG1 (green) and anti-SAG1 (red) antibodies.

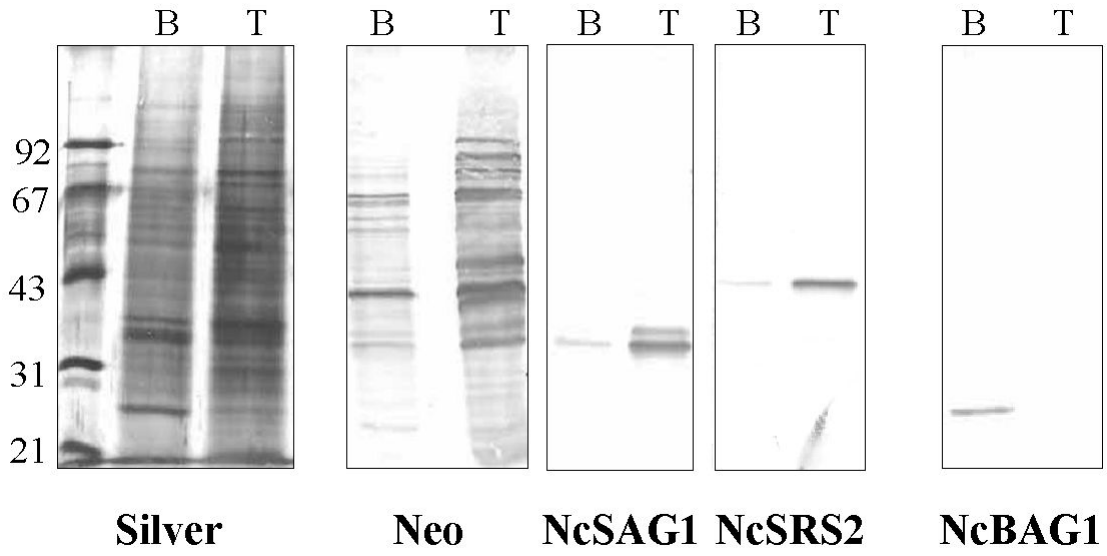

Figure 24: SDS-PAGE (silver stain) and corresponding immunoblots of tachyzoite (T) and bradyzoite (B) extracts. Note differential banding patterns obtained in bradyzoite and tachyzoite extracts by silver staining and immunoblotting using an anti-*N. caninum* antiserum (Neo), and the down regulation of NcSAG1- and NcSRS2-expression and the appearance of NcBAG1-expression in bradyzoites.

(Figure 25J-L), which has largely shifted towards the periphery of the vacuole, and has become incorporated into the tissue cyst wall. For NcGRA2 (Figure 25G-I), cyst wall-associated labelling was not as pronounced, but clearly evident as well, and NcGRA2 could also be detected within the parasite cytoplasm.

These findings were confirmed by immunogold labelling on sections of LR-White-embedded in vitro generated bradyzoites. Figure 26 shows a parasitophorous vacuole of *N. caninum* tachyzoites stained with anti-NcGRA1 antibodies and a secondary anti-rabbit antibody conjugated to 10 nm gold particles. Most of the immunogold labelling is localised at a high density within the tachyzoite dense granules, with fewer gold particles also labelling the matrix of the parasitophorous vacuole. Similar results were obtained using anti-NcGRA2 and anti-NcGRA7 antibodies (data not shown). Figure 27 shows immunogold labelled, in vitro generated *N. caninum* bradyzoites using antibodies directed against NcGRA1 (Figure 27A, B), NcGRA2 (Figure 27C) and NcGRA7 (Figure 27D). For NcGRA1 and NcGRA7 antibodies, the intensity of dense granule labelling was clearly reduced compared to tachyzoites, and for all three

dense granule antibodies, distinct staining of the cyst periphery could be observed.

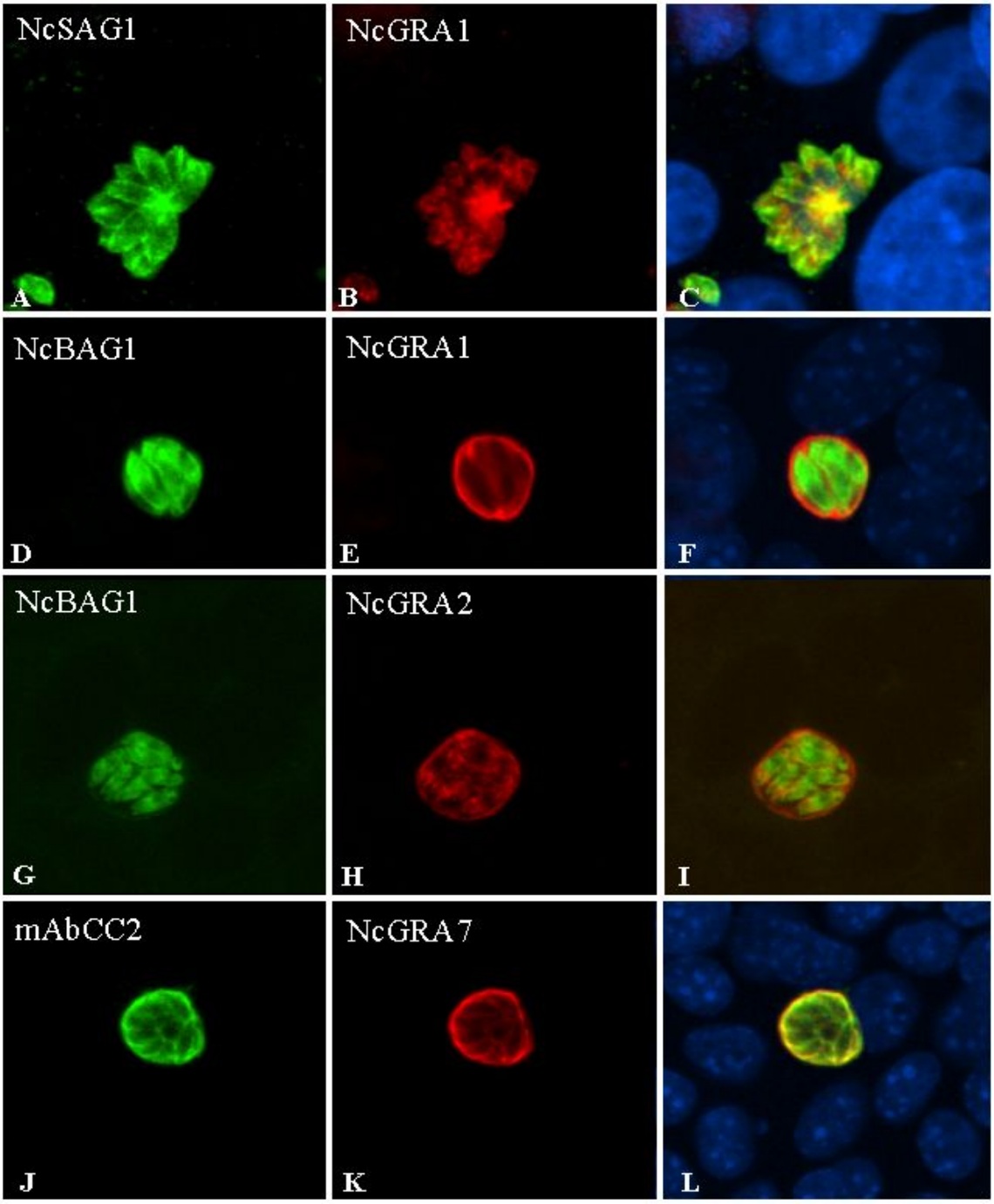

Figure 25: Differential localisation of dense granule antigens in tachyzoites and bradyzoites during in vitro culture. Localisation of NcGRA1, NcGRA2 and NcGRA7 in tachyzoite cultures were identical as exemplified for NcGRA1 (A-C), with a distinct granular staining at the anterior and posterior end of parasites. During in vitro stage conversion, a strong shift of labelling towards the vacuole periphery was noted for NcGRA1 (D-F) and NcGRA7 (J-L), and to a lesser extent also for NcGRA2 (G-I).

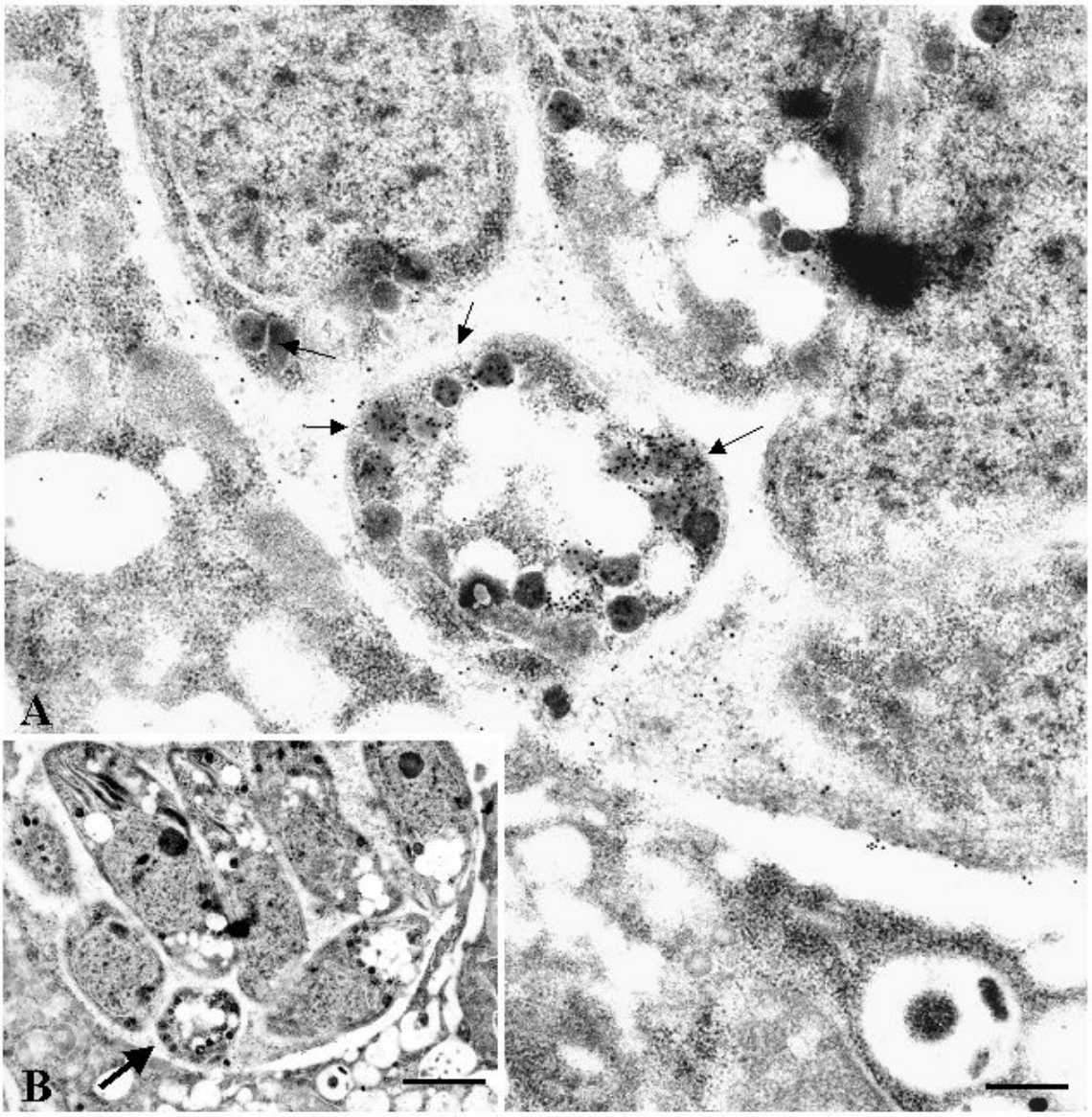

Figure 26: Immunogold localisation of dense granule antigens in *N. caninum* tachyzoites. NcGRA1, NcGRA2 and NcGRA7 showed an identical pattern to the one exemplified here for NcGRA1 which allows to visualise strong association of gold particles with the parasite dense granules (small arrows), and to a lesser extent with the vacuolar matrix. Bar in (A) = 0.23 µm. (B) Smaller magnification view of (A), showing the parasitophorous vacuole with numerous tachyzoites. The large arrow depicts the area magnified in (A). Bar in (B) = 0.9 µm.

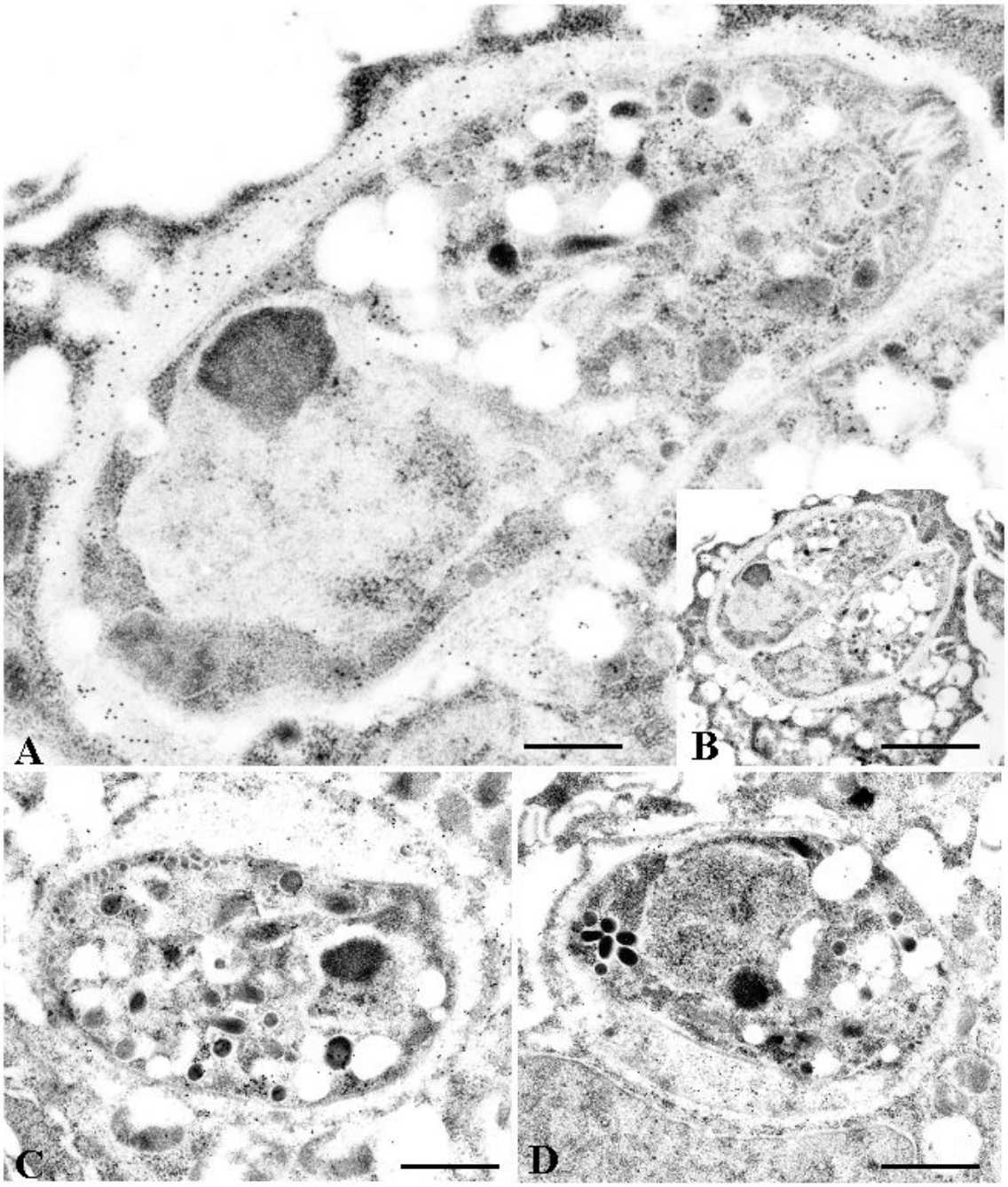

Figure 27: Immunogold localisation of dense granule antigens in *N. caninum* bradyzoites following induction of stage conversion by sodium nitroprusside during 8 days. (A) Labelling with anti-NcGRA1 antibodies, mainly at the cyst periphery. Bar = 0.25 µm. (B) Smaller magnification view of (A), bar = 1.25 µm. (C) Staining with NcGRA2 antibodies, bar = 0.42 µm. (D) Staining with anti-NcGRA7, bar = 0.51 µm. Note the decrease in number of gold particles within the parasite dense granules, and the increased labelling of the periphery.

3.4.1.4 Adhesive and invasive properties of Neospora caninum tachyzoites and bradyzoites

Adhesion and invasion of Vero cells by *N. caninum* tachyzoites and bradyzoites was comparatively assessed using a recently developed adhesion / invasion assay (Naguleswaran *et al*., 2003). Equal numbers of tachyzoites and bradyzoites were allowed to interact with Vero cell monolayers for 30 min either directly following isolation (Figure 28A, B), after treatment of Vero cells with neuraminidase at 37°C for 2h (Figure 28A), or after treatment of parasites with neuraminidase at 37°C for 30 min (Figure 28B). We found that the number of tachyzoites actually capable of either adhering or invading Vero cells was consistently several fold higher compared to bradyzoites (Figure 28A, B). In addition, tachyzoites also exhibited a pronounced higher invasion rate compared to bradyzoites. The situation changed after enzymatic removal of terminal sialic acid residues from the Vero host cell surface (Figure 28A). The absence of sialic acid residues did not markedly affect *N. caninum* tachyzoites, neither with regard to adhesion nor with respect to invasion. In contrast, the invasive capacities of bradyzoites were significantly increased upon removal of terminal sialic acid residues from the Vero cell surface from 25% to 46% (Figure 28A).The invasion of bradyzoites was also increased significantly from 15% to 36% when parasites were treated with neuraminidase prior to host cell interaction. In contrast, tachyzoite invasion was not affected at all (Figure 28B). While only one representative result of one experiment is shown in Figure 28, these assays were repeated twice and resulted in essentially identical results in all three experiments (data not shown). The findings show that the two in vitro generated stages exhibit different properties with regard to host cell interaction, and our results indicate that the presence of host cell surface sialic acid residues could influence host cell invasion by *N. caninum* bradyzoites.

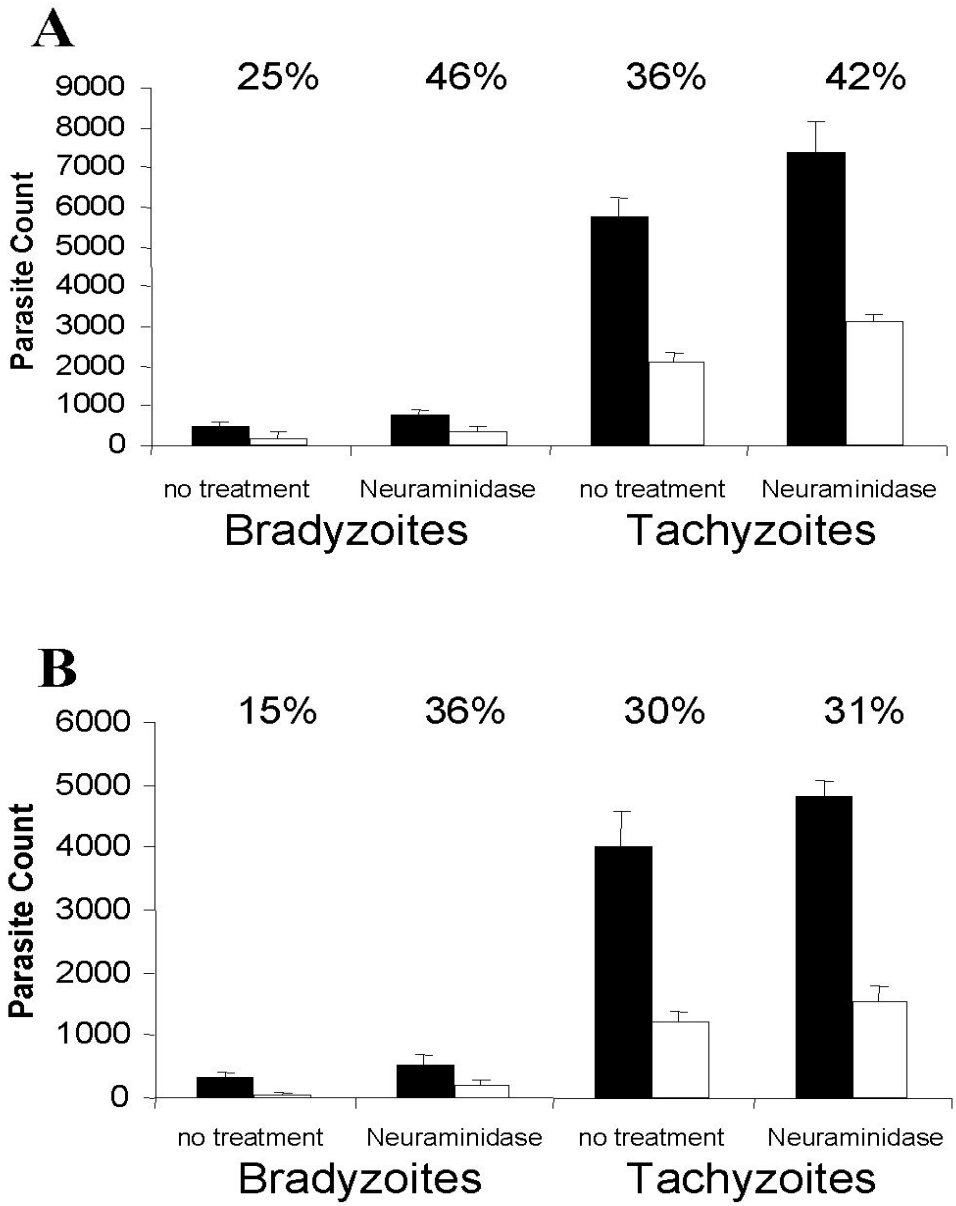

Figure 28: Adhesion and invasion of Vero cells by in vitro cultivated *N. caninum* tachyzoites and bradyzoites. Black columns indicate the overall number of parasites interacting with Vero cells (adherent and invaded), while white columns indicate the number of intracellular parasites only. (A) Identical numbers of parasites were allowed to interact with either untreated Vero cells, or with Vero cells which had been treated with neuraminidase. Note that in general, bradyzoites exhibit much lower adhesive as well as invasive capacities for Vero cells. Removal of sialic acid residues increased bradyzoite invasion but did not markedly affect tachyzoites. (B) Parasites were treated with neuraminidase prior to Vero cell interaction. Note again, that neuraminidase-treatment of bradyzoites increased their invasive capacity, in contrast to tachyzoites which remained unaffected. Data are displayed as means ± standard deviation, and a representative experiment of three independent experiments is shown.

3.4.2 Discussion

In the present study, we introduce a protocol for the induction of *N. caninum* tachyzoite-to-bradyzoite stage conversion in Vero cells. The use of Vero host cells allows to generate and purify large amounts of bradyzoite-enriched parasite populations. This enabled us to study the expression of NcSAG1, NcSRS2 and NcBAG1 antigens in both stages not only by means of immunofluorescence, but also by immunoblotting, and we also investigated the differential localisation of several dense granule proteins in tachyzoites and bradyzoite-containing cysts by immunofluorescence and TEM. In addition, we demonstrated that tachyzoites and bradyzoites differ with regard to host cell adhesion and invasion, and in particular sialic acid residues were found to be implicated in bradyzoite-host cell invasion, but not in tachyzoite-host cell interactions.

3.4.2.1 Neospora caninum in vitro bradyzoite culture in murine epidermal keratinocytes

We had previously reported on the development of an in vitro culture technique for generating *N. caninum* bradyzoites in vitro using murine epidermal keratinocytes by addition of exogenous NO (Vonlaufen *et al*., 2002b), and this protocol had proven to be suitable for immunofluorescence and TEM studies (Hemphill *et al*., 2003). However, in order to study the bradyzoite stage in more detail, a protocol is required to produce larger amounts of parasites. Treatment of Nc-Liverpool infected keratinocytes with continuously lower concentrations of SNP from 70 down to 17 µM resulted in a dose-dependent weaker suppression of parasite growth, while the percentage of NcBAG1-positive parasites remained unchanged, independently of the SNP concentration. Although this resulted in a higher yield in terms of actual bradyzoites, our attempts to purify in vitro-induced

parasites out of keratinocyte cultures consistently failed due to the high density and the physical stability of keratin filaments surrounding the cysts. Similar observations with regard to the overcoating of *T. gondii* tissue cysts with intermediate filaments in various host cells have been reported by others. Halonen *et al.* (1998) have shown that host cell intermediate filaments were associated with the cytoplasmic side of *T. gondii* tissue cysts within in vitro cultured murine astrocytes. Layers of glial filaments had also been observed around young *T. gondii* tissue cysts developing in astrocytes of human brain (Powell *et al.*, 1978). Finally, infection of astrocytes with *N. caninum* tachyzoites also resulted in an association of glial filaments with the outer surface of the parasitophorous vacuole membrane (Vonlaufen *et al.*, 2002a). Thus, host cells with a high intermediate filament content are not suitable for parasite purification.

3.4.2.2 Neospora caninum in vitro bradyzoite culture in Vero host cells

Since treatment of infected keratinocytes with 17 µM SNP allowed us to generate an overall larger number *of N. caninum* bradyzoites, but purification of bradyzoites was not possible, the method was adapted to Vero cells. 20-70 µM SNP consistently lead to detachment of the monolayers within few days, but treatment with 17 µM SNP did not, and resulted only in partial inhibition of Vero cell proliferation (data not shown). Immunofluorescence labelling of infected Vero cells treated with 17 µM SNP showed that expression of the major surface antigens of tachyzoites, NcSAG1 and NcSRS2 was down regulated in NcBAG1-positive vacuoles (see Figure 23). This was confirmed by immunoblotting (see Figure 24), and corresponds to earlier findings which had shown that NcSAG1 antigen was stage specifically down regulated in *N. caninum* bradyzoite cysts generated in mice (Fuchs *et al.*, 1998). The same authors had found that NcSRS2 (or Nc-p43) was still expressed by those bradyzoites. In contrast,

Schares *et al*. (1999) had demonstrated that the mAb5.2.1.5 directed against NcSRS2 did not label tissue cysts of the brain of an infected dog. Our experiments confirmed these findings, demonstrating inhibition of NcSRS2-expression also under in vitro conditions. While NcSAG1 and NcSRS2 antigens were shown to be involved in adhesion and invasion of tachyzoites into the host cells (Hemphill *et al*., 1996; Nishikawa *et al*., 2000), the down regulation of these surface antigens in bradyzoites suggests that they probably play a minor role in the biology of bradyzoites.

However, NcSRS2 or Ncp38, purified through monoclonal antibody affinity chromatography, exhibits a high diagnostic potential (Schares *et al*., 2000). On the other hand, bradyzoite proteins such as NcBAG1 could serve as tools for diagnostic purposes, in order to discern acute and chronic infection in animals. In this respect, our purification protocol allows to harvest the parasites out of Vero host cells (see Figure 23K), and these purified bradyzoites are now accessible to studies on altered gene expression during stage conversion by construction of cDNA libraries and expressed sequence tags (EST) sequencing, as it is currently done for a number of other apicomplexan parasites including the *N. caninum* tachyzoite stage (Li *et al*., 2003). This information would provide better understanding of the events occurring during the stage conversion process, which represents a crucial event in the pathogenesis of *Neospora* infection, influencing both the formation and reactivation of tissue cysts.

Soon after the invasion of host cells by apicomplexan parasites, dense granule proteins are released in order to modify the parasitophorous vacuole (Carruthers and Sibley, 1997). Our studies have shown that during in vitro stage conversion, NcGRA1, NcGRA2 and NcGRA7 also follow this pattern. However, all three proteins are most abundant within the tachyzoite dense granules (see Figure 25, Figure 26), but less abundant in bradyzoite dense granules. Instead, they are secreted and continuously integrated into the cyst wall, as assessed by immunofluorescence and immunogold TEM (see Figure 26, Figure 27), which indicates that they are functionally involved in the modification of the cyst wall. However, NcGRA2 appears to be less actively secreted in bradyzoites compared to NcGRA1 and NcGRA7, which argues for a different functional relevance of

this molecule. NcGRA1 and NcGRA2 antigens were recognised by sera from chronically infected mice and naturally infected cows (Atkinson *et al*., 2001; Ellis *et al*., 2000), indicating that these proteins elicit an immune response during chronic infection and could be used as a marker to identify chronically infected animals by serological means. Additionally, dense granule proteins are likely vaccine candidates, since they are expressed and secreted in both tachyzoites and bradyzoites. In *T. gondii*, protective immunity has been achieved in mice, using TgGRA1, TgGRA7 and TgROP2 recombinant proteins and DNA vaccines (Vercammen *et al*., 2000). For *N. caninum*, recombinant NcMIC3, and recombinant NcSAG1 and NcSRS2 combined with the corresponding DNA vaccines, exhibit the potential to prevent cerebral *N. caninum* infection in mice (Cannas *et al*., 2003a, b).

3.4.2.3 Neospora caninum tachyzoites and bradyzoites differ in host cell interaction

The adhesion to and invasion of Vero cells by in vitro generated and isolated tachyzoites and bradyzoites were investigated (see Figure 28). Our results suggest that *N. caninum* tachyzoites and bradyzoites exhibit distinctly different adhesive and invasive capacities. Tachyzoite-host cell interaction is several fold more efficient than host cell recognition by bradyzoites, and invasion rates for tachyzoites were consistently higher than for bradyzoites (see Figure 28). Differences in host cell invasion between tachyzoites and bradyzoites have also been described earlier for *T. gondii*, albeit at the ultrastructural level (Sasono and Smith, 1998), and respective receptor-ligand interactions have not been elucidated so far.

It seems likely that during natural infection, bradyzoites invade epithelial cells of the dog gut to induce the sexual cycle that leads to formation of oocysts (Dubey and Lindsay, 1996; Dubey *et al*., 2002). Epithelial cells of the gut are covered

with mucin glycoproteins, whose carbohydrates are mainly attached through o-glycosylation to serine and threonine in repeating regions of the polypeptide core. These carbohydrate chains are usually terminally modified by charged residues such as sialic acids (Hicks *et al*., 2000). Mucins might act as a barrier for invasion by intestinal pathogens. It was suggested by Pellegrin *et al*. (1993) that invasion of epithelial cells by *Eimeria* might be facilitated by the desialylation of caecal mucin by sialidase expressed in sporozoites and merozoites of *Eimeria*. For *T. gondii* tachyzoites it had also been shown earlier that removal of sialic acid residues from the macrophage surface has lead to increased invasion of macrophages (De Carvalho *et al*., 1993).

In our experiments (see Figure 28A), removal of sialic acid from the Vero cell surface lead to enhanced invasion of bradyzoites, while for tachyzoites this treatment had no effect on invasion. In addition, treatment of parasites with neuraminidase prior to host cell interaction also lead to an increase in bradyzoite invasion, and did not affect tachyzoites (see Figure 28B). This suggests that the two stages employ different mechanisms for invading their host cells, and the fact that neuraminidase-treatment of parasites contributes to bradyzoite invasion implies that bradyzoites express sialic acid residues, and possibly mucin-like molecules, on their surface. This has been previously demonstrated for other invasive protozoan parasites such as *Trypanosoma cruzi* and it was also shown that removal of sialic acid residues from the surface of metacyclic trypomastigotes enhanced host cell invasion (Yoshida *et al*., 1997). With regard to apicomplexan parasites, it is interesting to note that Cleary *et al.* (2002) used microarray analysis to study changes in transcript levels during *T. gondii* tachyzoite-to-bradyzoite conversion, and besides other developmentally regulated genes, they identified a gene coding for a putative, mucin domain containing bradyzoite surface molecule. Given the role of a close homologue in host cell invasion by another apicomplexan parasite, *Cryptosporidium parvum* (Barnes *et al*., 1998), it is likely that mucin-like bradyzoite proteins are also functionally implicated in host cell invasion by *N. caninum* upon oral ingestion of tissue cysts. In addition, it is possible that the highly glycosylated mucin-like

domains provide protection from degradative enzymes in the gut. Thus, the role of sialic acid in *N. caninum* host cell interactions is worthy of further studies.

4. References

Alexander J., Scharton-Kersten T.M., Yap G., Roberts C.W., Liew F.Y. and Sher A. (1997). Mechanisms of innate resistance to *Toxoplasma gondii* infection. Phil. Trans. R. Soc. Lond. B 352: 1355-1359.

Atkinson R., Harper, P.A., Ryce, C., Morrison, D.A., Ellis, J.T. (1999). Comparison of the biological characteristics of two isolates of *Neospora caninum.* Parasitology 118: 363-370.

Atkinson R.A., Ryce C., Miller C. M., Balu S., Harper P. A. and Ellis J. T. (2001). Isolation of *Neospora caninum* genes detected during a chronic murine infection. Int. J. Parasitol. 31: 67-71.

Barber J.S., Holmdahl O.J., Owen, M.R., Guy F., Uggla A., Trees A.J. (1995). Characterization of the first European isolate of *Neospora caninum*. (Dubey, Carpenter, Speer, Topper and Uggla). Parasitology 111: 563-568.

Barnes D.A., Bonnin A., Huang J. X., Gousset L., Wu J., Gut J., Doyle P., Dubremetz J.F, Ward H. and Petersen C. (1998). A novel multi-domain mucin-like glycoprotein of *Cryptosporidium parvum* mediates invasion. Mol. Biochem. Parasitol. 96: 93-110.

Bazler T.V., Long M.T., McElwain T.F., Mathison B.A. (1999). Interferon-γ and Interleukin-12 mediate protection to acute *Neospora caninum* infection in BALB/c mice. Int. J. Parasitol. 29: 1635-1648.

Beckers C.J., Wakefield T., Joiner K.A. (1997). The expression of *Toxoplasma* proteins in *Neospora caninum* and the identification of a gene encoding a novel rhoptry protein. Mol. Biochem. Parasitol. 89: 209-223.

Björkman C., Hemphill A. (1998). Characterization of *Neospora caninum* iscom antigens using monoclonal antibodies. Parasite Immunol. 20: 73-80.

Bohne W., Heesemann J., Gross U. (1993). Induction of bradyzoite-*specific Toxoplasma gondii* antigens in gamma interferon-treated mouse macrophages. Infect. Immun. 61: 1141-1145.

Bohne W., Heesemann J., Gross U. (1993). Coexistence of heterogeneous populations of *Toxoplasma gondii* parasites within parasitophorous vacuoles of murine macrophages as revealed by a bradyzoite-specific monoclonal antibody. Parasitol. Res. 79: 485-487.

Bohne W., Heesemann J., Gross U. (1994). Reduced replication of *Toxoplasma gondii* is necessary for induction of bradyzoite-specific antigens: A possible role for nitric oxide in triggering stage conversion. Infect. Immun. 62: 1761-1767.

Bohne W., Gross U., Ferguson D.J., Heesemann J. (1995). Cloning and characterization of a bradyzoite-specifically expressed gene (hsp30/bag1) of *Toxoplasma gondii*, related to genes encoding small heat-shock proteins of plants. Mol. Microbiol. 16: 1221-1230.

Bohne W., Hunter C.A., White M.W., Ferguson D.J., Gross, U., Roos D.S. (1998). Targeted disruption of the bradyzoite-specific gene BAG1 does not prevent tissue cyst formation in *Toxoplasma gondii*. Mol. Biochem. Parasitol. 92: 291-301.

Bohne W., Holpert M. and Gross U. (1999). Stage differentiation of the protozoan parasite *Toxoplasma gondii.* Immunobiology 201: 248-254.

Boothroyd J.C., Black M., Bonnefoy S., Hehl A., Knoll L.J., Manger I.D., Ortega-Barria E., Tomavo S. (1997). Genetic and biochemical analyses of development in *Toxoplasma gondii*. Philos. Trans. R. Soc. Lond. B. Biol. Sci. 352: 1347-1354.

Brown G.C. (2001). Regulation of mitochondrial respiration by nitric oxide inhibition of cytochrome c oxidase. Biochim. Biophys. Acta. 1504: 46-57.

Burney S., Tamir S., Gal A., Tannenbaum S.R. (1997). A mechanistic analysis of nitric oxide induced cellular toxicity. Nitric oxide: Biology and Chemistry: 1: 130-144.

Buxton D., McAllister, M.M., Dubey J.P. (2002). The comparative pathogenesis of neosporosis. Trends Parasitol. 18: 546-551.

Caldelari R., Suter M.M., Bauman D., DeBruin A., Müller E. (2000). Long term culture of murine epidermal keratinocytes. J. Inv. Dermatol. 114: 1064-1065.

Cannas A., Naguleswaran A., Müller N., Gottstein B., Hemphill A. (2003). Reduced cerebral infection of *Neospora caninum*-infected mice after vaccination with recombinant microneme protein NcMIC3 and ribi adjuvant. J. Parasitol. 89: 44-50.

Cannas A., Naguleswaran A., Müller N., Eperon S., Gottstein B., Hemphill A. (2003). Vaccination of mice against experimental *Neospora caninum* infection using NcSAG1- and NcSRS2-based recombinant antigens and DNA vaccines. Parasitology 126: 303-312.

Carruthers V.B., Sibley L.D. (1997). Sequential protein secretion from three distinct organelles of *Toxoplasma gondii* accompanies invasion of human fibroblasts. Eur. J. Cell Biol. 73: 114-123.

Carruthers V.B., Hakansson S., Giddings O. K., Sibley L.D. (2000). *Toxoplasma gondii* uses sulfated proteoglycans for substrate and host cell attachment. Infect. Immun. 68: 4005-4011.

Chao C.C., Hu S., Gekker G., Novick W.J., Remington J.S. and Peterson P.K. (1993). Effects of cytokine on multiplication of *Toxoplasma gondii* in microglial cells. J. Immunol. 150: 3404-3410.

Chao C.C., Gekker G., Hu S. and Peterson P.K. (1994). Human microglial cell defence against *Toxoplasma gondii*: The role of cytokines. J. Immunol. 152: 1246-1252.

Cleary M.D., Singh U., Blader I.J., Brewer J.L. and Boothroyd J.C. (2002). *Toxoplasma gondii* asexual development: Identification of developmentally regulated genes and distinct patterns of gene expression. Eukaryot. Cell 1: 329-340.

Coombs G.H., Denton H., Brown S.M.A. and Thong K. (1997) Biochemistry of the Coccidia. Adv. Parasitol. 39: 142-226.

Coombs G.H., Müller S. (2002). Recent advances in the search for new anti-coccidial drugs. Int. J. Parasitol. 32: 497-508.

Cooper C.E. (1999). Nitric oxide and iron proteins. Biochim. Biophys. Acta 1411: 290-309.

Creuzet C., Robert F., Roisin M.P., Van Tan H., Benes C., Dupouy-Camet J., Fagard R. (1998). Neurons in primary culture are less efficiently infected by *Toxoplasma gondii* than glial cells. Parasitol. Res. 84: 25-30.

Däubener W.C., Remscheid L., Nockemann S., Pilz K., Seghrouchni S., Mackenzi C. and Hadding U. (1996). Anti- parasitic effect or mechanism in human brain tumor cells: Role of interferon-γ and tumor necrosis factor-α. Eur. J. Immunol. 26: 487-492.

De Carvalho L., Yan C. Y., de Souza W. (1993). Effect of various digestive enzymes on the interaction of *Toxoplasma gondii* with macrophages. Parasitol. Res. 79: 114-118.

Denninger J.V., Marletta M.A. (1999). Guanylate cyclase and the NO/cGMP signalling pathway. Biochim. Biophys. Acta. 1411: 334-350.

Denton H., Roberts C.V., Alexander J., Thong K., Coombs G.H. (1996). Enzymes of energy metabolism in the bradyzoites and tachyzoites of *Toxoplasma gondii*. FEMS Microbiol. Letters 137: 103-108.

Dimer I.H. and Bout D.T. (1998). Interferon-γ activated primary enterocytes inhibit *Toxoplasma gondii* replication: A role for intracellular iron. Immunol. 94: 488-495.

Dubey J.P., Hattel A.L., Lindsay D.S., Topper M.J. (1988). Neonatal *Neospora caninum* infection in dogs: Isolation of the causative agent and experimental transmission. J. Am. Vet. Med. Assoc. 193: 1259-1263.

Dubey J.P., De Lahunta A. (1993). Neosporosis associated congenital limb deformities in a calf. Appl. Parasitol. 34: 229-233.

Dubey J.P., Lindsay D.S. (1996). A review of *Neospora caninum* and neosporosis. Vet. Parasitol. 67: 1-59.

Dubey J.P., Dorough K.R., Jenkins M.C., Liddell S., Speer C.A., Kwok O.C.H., Shen S.K. (1998). Canine neosporosis: Clinical signs, diagnosis, treatment and isolation of *Neospora caninum* in mice and cell culture. Int. J. Parasitol. 28: 1293-1304.

Dubey J.P. (1999). Neosporosis-the first decade of research. Int. J. Parasitol. 29: 1485-1488.

Dubey J.P. (1999). Recent advances in *Neospor*a and neosporosis. Vet. Parasitol. 84: 349-367.

Dubey J.P., Barr B.C., Barta J. R., Bjerkas I., Björkman C., Blagburn B.L., Bowman D.D., Buxton D., Ellis J. T., Gottstein B., Hemphill A., Hill D.E., Howe D.K., Jenkins M.C., Kobayashi Y., Koudela B., Marsh A. E., Mattsson J.G., McAllister M.M., Modry D., Omata Y., Sibley L.D., Speer C.A., Trees A.J., Uggla A., Upton S.J., Williams D.J., Lindsay D.S. (2002). Redescription of *Neospora caninum* and its differentiation from related coccidia. Int. J. Parasitol. 32: 929-946.

Dubey J.P., Hill D. E., Lindsay D. S., Jenkins M. C., Uggla A., Speer C.A. (2002). *Neospora caninum* and *Hammondia heydorni* are separate species. Trends Parasitol. 18: 66-69.

Dzierszinski F., Popescu O., Toursel C., Slomianny C., Yahiaoui B., Tomavo S. (1999). The protozoan parasite *Toxoplasma gondii* expresses two functional plant-like glycolytic enzymes. Implications for evolutionary origin of apicomplexans. J. Biol. Chem. 274: 24888-24895.

Dzierszinski F., Mortuaire M., Dendouga N., Popescu O., Tomavo S. (2002). Differential expression of two plant-like enolases with distinct enzymatic and antigenic properties during stage conversion of the protozoan parasite *Toxoplasma gondii*. J. Mol. Biol. 309: 1017-1027.

Ellis J.T. (1998). Polymerase chain reaction approaches for the detection of *Neospora caninum* and *Toxoplasma gondii*. Int. J. Parasitol. 28: 1053-1106.

Ellis J.T., Ryce C., Atkinson R., Balu S., Jones P., and Harper P.A. (2000). Isolation, characterization and expression of a GRA2 homologue from *Neospora caninum*. Parasitology 120: 383-390.

Eperon S., Brönnimann K., Hemphill A., Gottstein B. (1999). Susceptibility of B-cell deficient C57BL/6 (μMT) mice to *Neospora caninum* infection. Parasit. Immunol. 21: 225-236.

Fagard R., Van Tan H., Creuzet C., Pelloux H. (1999). Differential development of *Toxoplasma gondii* in neural cells. Parasitol. Today 15: 504-507.

Frenkel J.K, Dubey J.P., Hoff R.L. (1976). Loss of stages after continuous passage of *Toxoplasma gondii* and *Besnoitia jellisoni.* J. Protozool. 23: 421-424.

Fuchs N., Sonda S., Gottstein B., Hemphill A. (1998). Differential expression of cell surface- and dense granule-associated *Neospora caninum* proteins in tachyzoites and bradyzoites. J. Parasitol. 84: 753-758.

Gazzinelli R.T., Wysocka M., Hieny S., Scharton-Kersten T., Cheever A., Kuhn R., Müller W., Trinchieri G., Sher A. (1996). In the absence of endogenous IL-10 mice acutely infected with *Toxoplasma gondii* succumb to lethal immune response dependent on $CD4^+$-T cells and accompanied by overproduction of IL-12, IFN-γ and TNF-α. J. Immunol. 157: 798-805.

Gondim L.F., Pinheiro A.M., Santos P.O., Jesus E.E., Ribeiro M.B., Fernandes H.S., Almeida M.A., Freire S.M., Meyer R., McAllister M.M. (2001). Isolation of *Neospora caninum* from the brain of a naturally infected dog, and production of encysted bradyzoites in gerbils. Vet. Parasitol. 101: 1-7.

Gondim L.F.,Gao L., McAllister M.M. (2002). Improved production of *Neospora caninum* oocysts, cyclical oral transmission between dogs and cattle, and in vitro isolation from oocysts. J. Parasitol. 88: 1159-1163.

Gross U., Bormuth H., Gaissmaier C., Dittrich C., Krenn V., Bohne W., Ferguson D.J. (1995). Monoclonal rat antibodies directed against *Toxoplasma gondii* suitable for studying tachyzoite-bradyzoite interconversion in vivo. Clin. Diagn. Lab. Immunol. 2: 542-548.

Gross U., Bohne W., Luder C.G., Lugert R., Seber F., Dittrich C., Pohl F., Ferguson D.J. (1996) Regulation of developmental differentiation in the protozoan parasite *Toxoplasma gondii*. J. Eukariot. Microbiol. 43: 114-116.

Halonen S.K., Weidner E. (1994). Overcoating of *Toxoplasma* parasitophorous vacuoles with host cell vimentin-type intermediate filaments. J. Eukariot. Microbiol. 41: 65-71.

Halonen S.K., Chiu F.C, Weiss L.M. (1998). Effect of cytokines on growth of *Toxoplasma gondii* in murine astrocytes. Infect. Immun. 66: 4989-4993.

Halonen S.K., Weiss L.M., Chiu F.C. (1998). Association of host cell intermediate filaments with *Toxoplasma gondii* cysts in murine astrocytes in vitro. Int. J. Parasitol. 28: 815-823.

Halonen S.K., Weiss L.M. (2000). Investigation into the mechanism of gamma interferon-metiated inhibition of *Toxoplasma gondii* in murine astrocytes. Infect. Immun. 68: 3426-3430.

Halonen S.K., Taylor G.A. and Weiss L.M. (2001). Gamma Interferon- induced inhibition of *Toxoplasma gondii* in astrocytes is mediated by IGTP. Infect. Immun. 69: 5573-5576.

Hemphill A. (1996). Subcellular localization and functional characterization of Nc-p43, a major *Neospora caninum* tachyzoite surface protein. Infect. Immun. 64: 4279-4287.

Hemphill A., Gottstein B., Kaufmann H. (1996). Adhesion and invasion of bovine endothelial cells by *Neospora caninum* tachyzoites. Parasitology 112: 183-197.

Hemphill A., Croft S.L. (1997). Electron microscopy in Parasitology, p 227-268. *In*: M. Rogan (ed.), Analytical Parasitology. Springer Verlag, Heidelberg.

Hemphill A., Felleisen R., Connolly B., Gottstein B., Hentrich B., Müller N. (1997). Characterisation of a cDNA clone encoding Nc-p43, a major *Neospora caninum* surface protein. Parasitology 115: 581-590.

Hemphill A., Gajendran N., Sonda S., Fuchs N., Gottstein B., Hentrich B., Jenkins M. (1998). Identification and characterization of a dense granule-associated protein in *Neospora caninum* tachyzoites. Int. J. Parasitol. 28: 429-438.

Hemphill A. (1999). The host-parasite relationship in neosporosis. Adv. Parasitol. 43: 48-105.

Hemphill A., Gottstein B. (2000). A European perspective on *Neospora caninum*. Int. J. Parasitol. 30: 877-924.

Hemphill A., Vonlaufen N., Naguleswaran A., Guetg N., Srinivsan S., Alaeddine F. (2003). Tissue culture and explant approaches to study and visualise *Neospora caninum* and its interactions with the host cell. Microscopy and Microanalyses: in press.

Hennings H., Michael D., Cheng C., Steinert P., Holbrook K., Yuspa S.H. (1980). Calcium regulation of growth and differentiation of mouse epidermal cells in culture. Cell 19: 245-254.

Hicks S.J., Theodoropoulos G., Carrington S.D., Corfield A. P. (2000). The role of mucins in host-parasite interactions. Part I-protozoan parasites. Parasitol. Today 16: 476-481.

Howe D.K., Sibley L.D. (1997). Development of molecular genetics for *Neospora caninum:* A complementary system to *Toxoplasma gondii*. Methods 13: 123-133.

Howe D.K., Mercier C., Messina M., Sibley L.D. (1997). Expression of *Toxoplasma gondii* genes in the closely related apicomplexan parasite *Neospora caninum*. Mol. Biochem. Parasitol. 86: 29-36.

Howe D.K., Sibley L.D. (1999). Comparison of the major antigens of *Neospora caninum* and *Toxoplasma gondii*. Int. J. Parasitol. 29: 1489-1496.

Innes E.A., Buxton D., Eperon S., Gottstein B. (2000). Immunology of *Neospora caninum* infection in cattle and mice. *In*: A. Hemphill, B. Gottstein (eds.) A European perspective on *Neospora caninum*. Int. J. Parasitol. 30: 877-924.

Innes E.A., Wright S.E., Maley S., Rae A., Schock A., Kirvar E., Bartley P., Hamilton C., Carey I.M., Buxton D. (2001). Protection against vertical transmission in bovine neosporosis. Int. J. Parasitol. 31: 1523-1534.

Innes E.A., Andrianarivo A.G., Björkman C., Williams D.J., Conrad P.A. (2002). Immune responses to *Neospora caninum* and prospects for vaccination. Trends Parasitol. 18: 497-504.

Jardine J.E. (1996). The ultrastructure of bradyzoites and tissue cysts of *Neospora caninum* in dogs: Absence of distinguishing morphological features between parasites of canine and bovine origin. Vet. Parasitol. 62: 231-240.

Jensen P.K.A., Norgard J.O.R, Knudsen C., Nielsen V., Bolund L. (1990). Effects of extra- and intracellular calcium concentration on DNA replication, lateral growth, and differentiation of human epidermal cells in culture. Virchows Arch. B. 59: 17-25.

Kasper L.H. (1989). Identification of stage-specific antigens of *Toxoplasma gondii*. Infect. Immun. 57: 668-672.

Keller N., Naguleswaran A., Cannas A., Vonlaufen N., Bienz M., Björkman C., Bohne W., Hemphill A. (2002). Identification of a *Neospora caninum* microneme protein (NcMIC1) which interacts with sulfated host cell surface glycosaminoglycans. Infect. Immun. 70: 3187-3198.

Khan I.A., Schwartzman J.D., Fonseka S., Kasper L.H. (1997). *Neospora caninum*: Role for immune cytokines in host immunity. Exp. Parasitol. 85: 24-34.

Kirkman L.A., Weiss L.M., Kim K. (2001). Cyclic nucleotide signaling in *Toxoplasma gondii* bradyzoite differentiation. Infect. Immun. 69: 148-153.

Lally N., Jenkins M., Liddell S., Dubey J.P. (1997). A dense granule protein (NCDG1) gene from *Neospora caninum*. Mol. Biochem. Parasitol. 87: 239-243.

Li L., Brunk B.P., Kissinger J.C., Pape D., Tang K., Cole R.H., Martin J., Wylie T., Dante M., Fogarty S.J., Howe D.K., Liberator P., Diaz C., Anderson J., White M., Jerome M.E., Johnson E.A., Radke J.A., Stoeckert Jr C.J., Waterston R.H., Clifton S.W., Roos D.S., Sibley L.D. (2003). Gene discovery in the apicomplexa as revealed by EST sequencing and assembly of a comparative gene database. Genome Res. 13: 443-454.

Lindsay D.S., Dubey J.P. (1989). *Neospora caninum* (Protozoa: apicomplexa) infections in mice. J. Parasitol. 75: 772-779.

Lindsay D.S., Dubey J.P. (1989). Evaluation of anti-coccidial drugs' inhibition of *Neospora caninum* development in cell cultures. J. Parasitol. 75: 990-992.

Lindsay D.S., Speer C.A., Toivio-Kinnucan M.A., Dubey J.P., Blagburn B.L. (1993). Use of infected cultured cells to compare ultrastructural features of *Neopsora caninum* and *Toxoplasma gondii.* Am. J. Vet. Res. 54: 1103-1106.

Lindsay D.S., Rippey N.S., Cole R.A., Parsons L.C., Dubey J.P., Tidwell R.R., Blagburn B. L. (1994). Examination of the activities of 43 chemotherapeutic agents against *Neospora caninum* tachyzoites in cultured cells. Am. J. Vet. Res. 55: 976-981.

Lindsay D.S., Butler J.M., Rippey N.S., Blagburn B.L. (1996). Demonstration of synergistic effects of sulfonamides and dihydrofolate reductase/thymidylate synthase inhibitors against *Neospora caninum* tachyzoites in cultured cells, and characterization of mutants resistant to pyrimethamine. Am. J. Vet. Res. 57: 68-72.

Lindsay D.S., Butler J.M., Blagburn B.L. (1997). Efficacy of decoquinate against *Neospora caninum* tachyzoites in cell culture. Vet. Parasitol. 68: 35-40.

Lindsay D.S., Dubey J.P., Duncan R.B. (1999). Confirmation that the dog is a definitive host for *Neospora caninum*. Vet. Parasitol. 82: 327-333.

Lovett J.L., Howe D.K., Silbey L.D. (2000). Molecular characterization of a thrombospondin-related anonymous protein homologue in *Neospora caninum.* Mol. Biochem. Parasitol. 107: 33-43.

Luft J.H. (1971). Ruthenium red and violet. I. Chemistry, purification, methods of use for electron microscopy and mechanism of action. Anat. Rec. 171: 347-68.

Lunden A., Marks J., Maley S.W., Innes E.A. (1998). Cellular immune responses in cattle experimentally infected with *Neospora caninum*. Parasit. Immunol. 20: 519-526.

Lyons R.E., McLeod R., Roberts C.W. (2002). *Toxoplasma gondii* tachyzoite-bradyzoite interconversion. Trends Parasitol. 18: 198-201.

Mayhew I.G., Smith K.C., Dubey J.P., Gatward L K., McGlennon N.J. (1991). Treatment of encephalomyelitis due to *Neospora caninum* in a litter of puppies. J. Small Animal Pract. 32: 609-612.

McAllister M.M., Parmley S.F., Weiss L.M., Welch V.J., McGuire A.M. (1996). An immunohistochemical method for detecting bradyzoite antigen (BAG5) in *Toxoplasma gondii*-infected tissues crossreacts with a *Neospora caninum* bradyzoite antigen. J. Parasitol. 82: 354-355.

McAllister M.M., Dubey J.P., Lindsay D.S., Jolley W.R., Wills R.A., McGuire A.M. (1998). Dogs are definitive hosts of *Neospora caninum*. Int. J. Parasitol. 28: 1473-1478.

McGuire A.M., McAllister M.M., Jolley W.R., Anderson-Sprecher R.C. (1997a). A protocol for the production of *Neospora caninum* tissue cysts in mice. J. Parasitol. 83: 647-651.

McGuire A.M., McAllister M.M., Jolley W.R. (1997b). Separation and cryopresevarion of *Neospora caninum* tissue cysts from murine brains. J. Parasitol. 83: 319-321.

McHugh T.D., Holliman R.E., Butcher P.D. (1994). The in vitro model of tissue cyst formation in *Toxoplasma gondii*. Parasitol. Today 10: 281-285.

Mehlhorn H., Heydorn A.O. (2000). *Neospora caninum*: Is it really different from *Hammondia heydorni* or is it a strain of *Toxoplasma gondii*? An opinion. Parasitol. Res. 86: 169-178.

Morsomme P., Boutry M. (2000). The plant plasma membrane H(+)-ATPase: Structure, function and regulation. Biochim. Biophys. Acta. 1465: 1-16.

Müller N., Zimmermann V., Hentrich B., Gottstein B. (1996). Diagnosis of *Neospora caninum* and *Toxoplasma gondii* infection by PCR and DNA hybridization immunoassay. J. Clin. Microbiol. 34: 2850-2852.

Müller N., Sager H., Hemphill A., Gottstein B. (2001). Comparative molecular investigation of Nc5-PCR amplicons from *Neospora caninum* NC-1 and *Hammondia heydorni*-Berlin-1996. Parasitol. Res. 87: 883-885.

Müller N., Vonlaufen N., Gianinazzi C., Leib S.L., Hemphill A. (2002). Application of real-time fluorescent PCR for quantitative assessment of *Neospora caninum* infections in organotypic slice cultures of rat central nervous system tissue. J. Clin. Microbiol. 40: 252-255.

Murray H.W., Rubens B.Y, Carriero S.M., Harris A.M., and Jaffee E.A.(1985). Human mononuclear phagocyte antiprotozoal mechanisms: Oxygen-dependent vs oxygen-independent activity against intracellular *Toxoplasma gondii*. J. Immunol.134: 1982-1888.

Naguleswaran A., Cannas A., Keller N., Vonlaufen N., Schares G., Conraths F. J., Björkman C., Hemphill A. (2001). *Neospora caninum* microneme protein NcMIC3: Secretion, subcellular localization and functional involvement in host cell interaction. Infect. Immun. 69: 6483-6494.

Naguleswaran A., Cannas A., Keller N., Vonlaufen N., Björkman C., Hemphill A. (2002). Vero cell surface proteoglycan interaction with the microneme protein NcMIC3 mediates adhesion of *Neospora caninum* tachyzoites to host cells unlike that in *Toxoplasma gondii.* Int. J. Parasitol. 32: 695-704.

Naguleswaran A., Müller N., Hemphill A. (2003). *Neospora caniunum* and *Toxoplasma gondii*: A novel adhesion/invasion assay reveals distinct differences in tachyzoite-host cell interactions. Exp. Parasitol. In press.

Nasmyth K. (1996). Viewpoint: Putting the cell cycle in order. Science 274: 1643-1645.

Nishikawa Y., Xuan X., Nagasawa H., Igarashi I., Fujisaki K., Otsuka H., Mikami T. (2000). Monoclonal antibody inhibition of *Neospora caninum* tachyzoite invasion into host cells. Int. J. Parasitol. 30: 51-58.

Nishikawa Y., Makala L., Haruki O., Mikami T., Nasawa H. (2002). Mechanisms of apoptosis in murine fibroblasts by two intracellular protozoan parasites, Toxoplasma gondii and *Neospora caninum*. Parasit. Immunol. 24: 347-354.

Ortega-Barria E., Boothroyd J.C. (1999). Toxoplasma-lectin like activity for sulphated polysaccharide is involved in host cell infection. J. Biol. Chem. 274: 1267-1276.

Parmley S.F., Weiss L.M., Yang L. (1995). Cloning of a bradyzoite-specific gene of *Toxoplasma gondii* encoding a cytoplasmic antigen. Mol. Biochem. Parasitol. 73: 253-257.

Pellegrin J.L., Ortega-Barria E., Prioli R.P., Buerger M., Strout R.G., Alroy J., Pereira M.E. (1993). Identification of a developmentally regulated sialidase in *Eimeria tenella* that is immunologically related to the *Trypanosoma cruzi* enzyme. Glycoconj. J. 10: 57-63.

Peters M., Lütkefels E., Heckeroth A.R., Schares G. (2001). Immunohistochemical and ultrastructural evidence for *Neospora caninu*m tissue cysts in skeletal muscles of naturally infected dogs and cattle. Int. J. Parasitol. 31: 1144-1148.

Powell H.C., Gibbs C.J., Lorenzo A.M., Lambert P.W., Gadjusek D.C. (1978). Toxoplasmosis of the central nervous system in the adult. Electron microscopic observations. Acta Neuropathol. 41: 211-216.

Quinn H.E., Ellis J.T., Smith N.C. (2002). *Neospora caninum*: A cause of immune-mediated failure of pregnancy? Trends Parasitol. 18: 391-394.

Sahm M., Fischer H.G., Gross U., Reiter-Owona I., Seitz H.M. (1997). Cyst formation by *Toxoplasma gondii* in vivo and in brain-cell culture: A comparative morphology and immunocytochemistry study. Parasitol. Res. 83: 659-665.

Sager H., Fischer I., Furrer K., Strasser M., Waldvogel A., Boerlin P., Audigé L. and Gottstein B. (2001). A Swiss case-control study to assess *Neospora caninum*-associated bovine abortions by PCR, histopathology and serology. Vet. Parasitol. 102: 1-15.

Sasono P.M., Smith J.E. (1998). *Toxoplasma gondii*: An ultrastructural study of host-cell invasion by the bradyzoite stage. Parasitol. Res. 84: 640-645.

Schares G., Dubremetz J.F., Dubey J.P., Barwald A., Loyens A., Conraths F.J. (1999). *Neospora caninum:* Identification of 19-, 38-, and 40-kDa surface antigens and a 33-kDa dense granule antigen using monoclonal antibodies. Exp. Parasitol. 92: 109-119.

Schares G., Rauser M., Sondgen P., Rehberg P., Barwald A., Dubey J.P., Edelhofer R., Conraths F.J. (2000). Use of purified tachyzoite surface antigen p38 in an ELISA to diagnose bovine neosporosis. Int. J. Parasitol. 30: 1123-1130.

Schock A., Innes E.A., Yamane I., Latham S.M., Wastling J.M. (2001). Genetic and biological diversity among isolates of *Neospora caninum*. Parasitology 123: 13-23.

Serrano R. (1988). Structure and function of proton translocatin ATP-ase in plasma membranes of plants and fungi. Biochim. Biophys Acta 947: 1-28.

Scharton-Kersten T.M., Yap G., Magram J., Sher A. (1997). Inducible nitric oxide is essential for host control of persistent but not acute infection with intracellular pathogen *Toxoplasma gondii*. J. Exp. Med. 185: 1261-1273.

Shaw M.K., Roos D.S., Tilney L.G. (2002). Cysteine and serine protease inhibitors block intracellular development and disrupt the secretory pathway of *Toxoplasma gondii*. Microbes and Infection 4: 119-132.

Sims T.A., Talbot I.C. (1988). Host-parasite relationship in the brains of mice with congenital toxoplasmosis. J. Path. 156: 255-261.

Silva N.M., Wagner L.T., Alvarez-Leite J.I., Mineo J.R., Gazinelli R.T. (2002). *Toxoplasma gondii*: In vivo expression of BAG5 and cyst formation is independent of TNFp55 receptor and inducible nitric oxide synthase functions. Microbes and Infections 4: 261-270.

Smith J.E. (1995). A ubiquitous intracellular parasite: The cellular biology of *Toxoplasma gondii.* Int. J. Parasitol. 25: 1301-1309.

Soete M., Camus D., Dubremetz J.F. (1994). Experimental induction of bradyzoite-specific antigen expression and cyst formation by the RH strain of *Toxoplasma gondii* in vitro. Exp. Parasitol. 78: 361-370.

Sonda S., Fuchs N., Gottstein B., Hemphill A. (2000). Molecular characterization of a novel microneme antigen in *Neospora caninum*. Mol. Biochem. Parasitol. 108: 39-51.

Speer C.A., Dubey J.P. (1989). Ultrastructure of tachyzoites, bradyzoites and tissue cysts of *Neospora caninum*. J. Protozol. 36: 458-463.

Speer C.A., Dubey J.P., McAllister M.M., Blixt J.A. (1999). Comparative ultrastructure of tachyzoites, bradyzoites, and tissue cysts of *Neospora caninum* and *Toxoplasma gondii*. Int. J. Parasitol 29: 1509-1520.

Stenlund S., Björkman C., Holmdahl O.J., Kindahl H., Uggla A. (1997). Characterization of a Swedish bovine isolate of *Neospora caninum.* Parasitol. Res. 83: 214-219.

Stoppini L., Buchs P.A., Müller D. (1991). A simple method for organotypic cultures of nervous tissue. J. Neurosci. Methods 37: 173-182.

Stoppini L., Buchs P.A, Brun R., Müller D., Duport S., Parisi L., Seebeck T. (2000). Infection of organotypic slice cultures from rat central nervous tissue with *Trypanosoma brucei*. Int. J. Med. Microbiol. 290: 105-113.

Suzuki Y., Yang Q., Yang S., Nguyen N., Lim S., Lierenfeld O., Kozima T and Remington J.S. (1996). IL-4 is protective against development of toxoplasmic encephalitis. J. Immunol. 15: 2564-2569.

Swanson R.A. (1992). Physiologic coupling of glial glycogen metabolism to neuronal activity in brain. Can. J. Physiol. Pharmacol. 70: S138-S144.

Swanson R.A., Choi D.W. (1993). Glial glycogen stores affect neuronal survival during glucose deprivation in vitro. J. Cereb. Blood Flow Metab. 13: 162-169.

Tanaka H., Nagasawa H., Fujisaki K., Suzuki N., Mikami T. (2000). Growth inhibitor effect of interferon-γ on *Neospora caninum* in murine macrophages by a nitric oxide mechanism. Parasitol. Res. 86: 768-771.

Tomavo S., Boothroyd J.C. (1995). Interconnection between organellar function development and drug resistance in the protozoan parasite *Toxoplasma gondii*. Int. J. Parasitol. 25: 1293-1299.

Tomavo S. (2001). The differential expression of multiple isoenzymes forms during stage conversion of *Toxoplasma gondii*: an adaptive developmental strategy. Int. J. Parasitol. 31: 1023-1031.

Torpier G., Charif H., Darcy F., Liu J., Darde M.L., Capron A. (1993). *Toxoplasma gondii:* Differential location of antigens secreted from encysted bradyzoites. Exp. Parasitol. 77: 13-22.

Trees A.J., Davison H.C., Innes E.A., Wastling J.M. (1999). Towards evaluating the economic impact of bovine Neosporosis. Int. J. Parasitol. 29: 1195-1200.

Tunev S.S., McAlilster M.M., Anderson-Sprecher R.C., Weiss L.M. (2002). *Neospora caninum in vitro*: Evidence that the destiny of a parasitophorous vacuole depends on the phenotype of the progenitor zoite. J. Parasitol. 88: 1095-1099.

Vercammen M, Scorza T., Huygen K., De Braekeleer J., Diet R., Jacobs D., Saman E., Verschueren H. (2000). DNA vaccination with genes encoding *Toxoplasma gondii* antigens GRA1, GRA7, and ROP2 induces partially protective immunity against lethal challenge in mice. Infect. Immun. 68: 38-45.

Vonlaufen N., Gianinazzi C., Müller N., Simon F., Björkman C., Jungi T.W., Leib S.L., Hemphill A. (2002a). Infection of organotypic slice cultures from rat central nervous tissue with *Neospora caninum:* An alternative approach to study host-parasite interactions. Int. J. Parasitol. 32: 533-542.

Vonlaufen N., Müller N., Keller N., Naguleswaran A., Bohne W., McAllister M.M., Björkman C., Müller E., Caldelari R., Hemphill A. (2002b). Exogenous nitric oxide triggers *Neospora caninum* tachyzoite-to-bradyzoite stage conversion in murine epidermal keratinocyte cell cultures. Int. J. Parasitol. 32: 1253-1265.

Weiss L.M., LaPlace D., Tanowitz H.B., Wittner H.B. (1992). Identification of *Toxoplasma gondii* bradyzoite-specific monoclonal antibodies. J. Infect. Dis. 166: 213-215.

Weiss L.M., Ma Y.F., Takvorian P.M., Tanowitz H.B., Wittner M. (1998). Bradyzoite development in *Toxoplasma gondii* and the hsp70 stress response. Infect. Immun. 66: 3295-3302.

Weiss L.M., Ma Y.F., Halonen S., McAllister M.M, Zhang Y.W. (1999). The in vitro development of *Neospora caninum* bradyzoites. Int. J. Parasitol. 29: 1713-1723.

Yang S., Parmley S.F. (1997). *Toxoplasma gondii* expresses two distinct lactate dehydrogenase homologous genes during its life cycle in intermediate hosts. Gene. 184: 1-12.

Yoshida N., Dorta M. L., Rerreira A.T., Oshiro M.E.M., Mortara R.A., Acosta-Serrano A., Favoreto S. Jr. (1997). Removal of sialic acid from mucin-like surface molecules of *Trypanosoma cruzi* metacyclic trypomastigotes enhances parasite-host cell interaction. Mol. Biochem. Parasitol. 84: 57-67.

Zhang Y.W., Kim K., Ma Y.F., Wittner M., Tanowitz H.B., Weiss L.M. (1999). Disruption of the *Toxoplasma gondii* bradyzoite-specific gene BAG1 decreases in vivo cyst formation. Mol. Microbiol. 31: 691-701.

Zhang, Y.W., Halonen, S.K., Ma, Y.F., Wittner, M., Weiss, L.M. (2001). Initial characterization of CST1, a *Toxoplasma gondii* cyst wall glycoprotein. Infect. Immun. 69: 501-517.

List of publications

Naguleswaran A., Cannas A., Keller N., **Vonlaufen N**., Schares G., Conraths F.J., Björkman C., Hemphill A. (2001). *Neospora caninum* microneme protein NcMIC3: secretion, subcellular localization, and functional involvement in host cell interaction. Infect. Immun. 69: 6483-6494.

Müller N., **Vonlaufen N**., Gianinazzi C., Leib S.L., Hemphill A. (2002). Application of real-time fluorescent PCR for quantitative assessment of *Neospora caninum* infections in organotypic slice cultures of rat central nervous system tissue. J. Clin. Microbiol. 40: 252-255.

Vonlaufen N., Gianinazzi C., Müller N., Simon F., Björkman C., Jungi T.W., Leib S.L., Hemphill A. (2002). Infection of organotypic slice cultures from rat central nervous tissue with *Neospora caninum*: an alternative approach to study host-parasite interactions. Int. J. Parasitol. 32: 533-542.

Keller N., Naguleswaran A., Cannas A., **Vonlaufen N**., Bienz M., Björkman C., Bohne W., Hemphill A. (2002). Identification of a *Neospora caninum* microneme protein (NcMIC1) which interacts with sulfated host cell surface glycosaminoglycans. Infect. Immun. 70: 3187-3198.

Naguleswaran A., Cannas A., Keller N., **Vonlaufen N**., Björkman C., Hemphill A. (2002). Vero cell surface proteoglycan interaction with the microneme protein NcMIC3 mediates adhesion of *Neospora caninum* tachyzoites to host cells unlike that in *Toxoplasma gondii*. Int. J. Parasitol. 32: 695-704.

Vonlaufen N., Müller N., Keller N., Naguleswaran A., Bohne W., McAllister M.M., Björkman C., Müller E., Caldelari R., Hemphill A. (2002). Exogenous nitric oxide triggers *Neospora caninum* tachyzoite-to-bradyzoite stage conversion in murine epidermal keratinocyte cell cultures. Int. J. Parasitol. 32: 1253-1265.

Hemphill A., **Vonlaufen N**., Naguleswaran A., Guetg N., Srinivasan S., Alaeddine F. Tissue culture and explant approaches to study and visualize *Neospora caninum* and its interaction with the host cell. Microscopy and Microanalyses: in press.

Vonlaufen N., Guetg N., Naguleswaran A., Müller N., Björkman C., Shares G., von Blumroeder D., Ellis J., Hemphill A. In vitro induction of *Neospora caninum* bradyzoites in Vero cells reveals differential antigen expression of tachyzoites and bradyzoites. Infect. Immun.: in press.

Scheidegger A., **Vonlaufen N**., Naguelswaran A., Gianinazzi C., Müller N., Hemphill A., Leib S.L. Differential effects of IFN-γ and TNF-α on *Toxoplasma gondii* proliferation in organotypic rat brain slice cultures. Submitted.

Congresses

Vonlaufen N., Gianinazzi C., Müller E., Leib S.L., Hemphill A. *Neospora caninum* infection of organotypic slice cultures from rat central nervous tissue. Meeting for PhD students in Parasitology and Tropical Medicine. Münchenwiler 13.8.-14.8.01. **Oral presentation**.

Vonlaufen N., Keller N., Bohne W., Müller E., Caldelari R., Hemphill A. *Neospora caninum* in vitro tachyzoite-bradyzoite stage conversion in naturally immortalized epidermal keratinocytes. International Congress of Parasitology (ICOPA) V. Vancouver, 4.8.-9.8.2002. **Oral presentation**.

Vonlaufen N., Guetg N., Caldelari R., Müller E., Hemphill A. *Neospora caninum* tachyzoite-bradyzoite stage conversion in murine epidermal keratinocytes. Joint Annual Meeting of the Swiss Society for Microbiology, Infectious Disease and Tropical Medicine and Parasitology. Basel, 6.3.-7.3. 2003. **Poster presentation**.

Lectures and courses

Müller N., Hemphill A., Sager H., Gottstein B.: Medizinische Parasitologie und tropische Parasitosen

PhD-Course: Müller N., Hemphill A.: Applied molecular biology

Acknowledgments

I am grateful to Professor Andrew Hemphill for his excellent supervision, critical scientific advice and encouragement during my thesis work.
I would like to thank Professor Stephan Krähenbühl for accepting to be my doctor father and for his interest in this work and Professor Jürgen Drewe for taking over the coreferat. Furthermore, I thank Professor Niklaus Weiss for taking the chair in the exam.
My special thanks are addressed to Nagul who contributed to this work by his helpfulness, valuable suggestions and interesting and fruitful discussions. I also would like to thank him for his friendship.
Thanks are due to Professor Bruno Gottstein for providing an enjoyable working environment, Professor Norbert Müller for his help and suggestions during the LightCycler PCR work and Dr. Christian Gianinazzi and Professor Stephen Leib for introducing me into the cultivation technique of organotypic brain slices.
I would like to express my warmest thanks to my parents for their continuous presence and encouragement and to my sister Karin and my brother Alain for their moral support.
Finally, and more deeply, I wish to thank Adrian for his tireless help and for supporting me at any time.
This study was financed by the Foundation Research 3R.